Real Impact of CO_2 Utilization:

A Dynamic LCA Approach

by

Majd Tabbara

A thesis

presented to the University of Waterloo

in fulfillment of the

thesis requirement for the degree of

Master of Applied Science

in

Chemical Engineering

Waterloo, Ontario, Canada, 2019

Author's Declaration

I hereby declare that I am the sole author of this thesis. This is a true copy of the thesis, including any required final revisions, as accepted by my examiners.

I understand that my thesis may be made electronically available to the public.

Abstract

Global warming has received widespread attention in recent years due to increasing levels of carbon dioxide (CO_2) and other pertinent greenhouse gases in the atmosphere. Various solutions have been proposed to reduce the net CO_2 emissions, including switching to renewable energy and CO_2 capture and sequestration. A probable and attractive alternative to CO_2 storage could be CO_2 utilization which is defined as the conversion of already-captured CO_2 into final chemicals or energy products. Customarily, a static life cycle analysis (LCA) has been employed to comprehend the environmental costs and benefits associated with CO_2 utilization processes. Essentially, the LCA procedure retains a crucial aspect in understanding the extent to which CO_2 is truly being mitigated within a CO_2 utilization process. However, the scope and extent of the LCA procedure requires careful attention. Although ultimately all of the CO_2 utilized will likely end up in the atmosphere, a comprehensive dynamic LCA needs to be conducted in order to encompass a time scale to represent the time that CO_2 is being displaced by within a proposed CO_2 utilization process.

The research presented within this thesis primarily focused on assessing two products, methanol (MeOH) and dimethyl carbonate (DMC), through the application of the dynamic LCA procedure. Initially, a model schematic, inclusive to the necessary equations, was established so as to compute the net CO_2 emissions within a given system. This included the use of a 620 MW natural gas combined cycle power plant, that accounted for de-rating, to produce the required amount of CO_2 necessary for the utilization process. Additionally, the conventional process and the so-called CO_2 utilization process for manufacturing MeOH, were developed and simulated in Aspen Plus™. Normalizing the values to 1 $\frac{tonne\ MeoH}{hr}$, the cumulative amount of CO_2 emitted within both the conventional and utilization processes is 1.878 $\frac{tonne\ CO_2}{hr}$ and 1.703 $\frac{tonne\ CO_2}{hr}$ respectively. These results were then utilized so as to compute the net CO_2 emissions within each respective approach. Subsequently, the values attained were then used as an input to the dynamic LCA framework yielding in the necessary environmental results. After an in-depth comparison, the utilization approach proved superior, from an environmental perspective, when contrasted against the conventional route of manufacturing MeOH. This is seen as the cumulative impact on

radiative forcing, at year 100, was computed for both routes yielding in $4.328 * 10^{-5} \frac{W}{m^2}$ for the conventional approach and $3.613 * 10^{-5} \frac{W}{m^2}$ for the utilization approach. Notably, implementing the utilization approach would result in a 16.51 % percent reduction in the cumulative impact of radiative forcing at year 100. Furthermore, a sensitivity analysis was also conducted on the utilization route and this showed that an increase in the CO_2 storage duration within the MeOH product results in a diminished environmental impact.

Similarly, an environmental comparison-based assessment was conducted to analyze both a conventional and CO_2 utilization approach of manufacturing DMC. The conventional approach analyzed the partial carbonylation route, whilst the utilization approach assessed the urea route through reactive distillation. Subsequent to the cradle-to-grave computations, the obtained CO_2 emissions within both approaches were further inputted into the dynamic LCA framework. Overall, the cumulative impact on radiative forcing, at year 100, was calculated for both routes resulting in $5.118 * 10^{-5} \frac{W}{m^2}$ for the conventional approach and $5.859 * 10^{-5} \frac{W}{m^2}$ for the utilization approach. From an environmental standpoint, employing this utilization approach to manufacture DMC results in a 14.46 % increase in the cumulative impact of radiative forcing at year 100. A sensitivity analysis was also performed to study the effect of increasing the CO_2 storage duration, in the DMC product, on the cumulative impact on radiative forcing. An inverse relationship was observed showing that an increase in the CO_2 storage duration yields a relative decrease in the cumulative impact on radiative forcing.

Acknowledgments

I would like to acknowledge certain individuals that aided me in the preparation of this thesis and further extend my sincere appreciation to those individuals to which the completion of this thesis would not have been made probable without.

Firstly, I would like to relay my utmost appreciation to my supervisors Dr. Eric Croiset and Dr. Peter Douglas for providing me with their inspiring mentorship throughout my graduate career in the master's program, and for the fruitful propositions and recommendations they have aided me with.

Adding to that, I would like to extend my appreciation and gratitude to my committee members, Dr. Ali Elkamel and Dr. Ting Tsui, for their time and insightful remarks serving as my committee members. I also would like to thank Mrs. Judy Caron for her support and assistance throughout my graduate career.

Furthermore, I would like to express my thankfulness to my friends and colleagues at the university for their insightful knowledge, support, and memorable time we spent altogether.

Finally, I would like to illustrate my sincere appreciation to my family for their continuous encouragement, unwavering support, and positivity throughout the course of my graduate degree.

To Mom and Dad

Table of Contents

List of Figures ..... **ix**

List of Tables ..... **xi**

Acronyms and Abbreviations ..... **xii**

Chapter 1: Introduction **1**

1.1 Carbon Dioxide and Climate Change 1

1.2 Carbon Dioxide Capture and Utilization (CCU) 3

1.3 Traditional Life Cycle Analysis (LCA): An Environmental Assessment Tool for CCU 5

1.4 Dynamic LCA: A Proposed Evaluation Tool for CCU 9

1.5 Research Objectives, Motivations, and Contributions 11

1.6 Thesis Outline 12

Chapter 2: Literature Review **13**

2.1 Applications of Traditional LCA on CCU Products 13

2.2 Dynamic LCA Applications and Implementations 19

2.3 Conventional Processes 23

2.4 Carbon Dioxide Capture and Utilization Processes 27

Chapter 3: Model Development **30**

3.1 Dynamic LCA 30

3.2 Conventional Processes and Base Case 36

3.3 Utilization Processes and Integrated Case 43

3.4 Conventional MeOH Production in Aspen Plus 55

3.5 CO_2 Utilization Approach for MeOH Production in Aspen Plus 60

Chapter 4: Model Implementation and Dynamic LCA Results **63**

4.1 Results for MeOH Production 65

4.2 Results for DMC Production 73

4.3 Sensitivity Analysis for MeOH Production 82

4.4 Sensitivity Analysis for DMC Production 84

Chapter 5: Conclusions and Recommendations **86**

5.1 Conclusions 86

5.2 Recommendations 88

References **89**
Appendix A: Stream Results for Conventional Approach (MeOH Production) **100**
Appendix B: Stream Results for CO_2 Utilization Approach (MeOH Production) **105**

List of Figures

Figure 1.1 Canadian GHG emission trend from 2005 to 2016 (excluding LULUCF). Adopted from: Environment and Climate Change Canada (Giammario et al., 2018) 2
Figure 1.2 Cumulative web diagram incorporating all the various pathways for CO_2. Adopted from Jarvis and Samsatli (2018) 4
Figure 1.3 LCA assessment framework pertaining to the standards by ISO 14040 and ISO 14044. Adopted from Von der Assen et al. (2015) 8
Figure 3.1 BCCC model utilizing a background CO_2 concentration of 378 ppm depicted over 1000 years 32
Figure 3.2 General model framework 37
Figure 3.3 Base case model encapsulating system 1 37
Figure 3.4 Base case model encapsulating system 2 37
Figure 3.5 Base case model encapsulating system 3 38
Figure 3.6 Integrated case model encapsulating system 4 44
Figure 3.7 Integrated case model encapsulating system 5 45
Figure 3.8 Integrated case model encapsulating system 6 45
Figure 3.9 Linear interpolation of D versus % CO_2 capture for an integrated 633.5 MW NGCC PP and CC unit 47
Figure 3.10 Conventional SMR flowsheet for MeOH production 56
Figure 3.11 MeOH production flowsheet 59
Figure 3.12 Conventional SMR flowsheet incorporating CO_2 utilization for MeOH production 61
Figure 3.13 MeOH production flowsheet 62
Figure 4.1 Avoided burden for both a 100 MW NGCT and 300 MW NGCC PP unit 64
Figure 4.2 Gate-to-grave impact for the MeOH utilization approach 70
Figure 4.3 Gate-to-grave impact for the MeOH conventional approach 71
Figure 4.4 Cradle-to-grave impacts for MeOH production 72
Figure 4.5 Cradle-to-grave assessment for the conventional approach 75
Figure 4.6 Cradle-to-grave assessment for the utilization approach 76
Figure 4.7 Gate-to-grave impact for the DMC utilization approach 79

Figure 4.8 Gate-to-grave impact for the DMC conventional approach 80
Figure 4.9 Cradle-to-grave impacts for DMC production 81
Figure 4.10 Sensitivity analysis for the MeOH utilization approach..... 83
Figure 4.11 Sensitivity analysis for the DMC utilization approach..... 85

List of Tables

Table 2.1 Summary of LCA applications for DMC synthesis 17
Table 2.2 Summary of LCA applications for MeOH synthesis 18
Table 2.3 List of conventional process routes and reaction mechanisms for DMC production .. 26
Table 2.4 List of utilization process routes and reaction mechanisms for DMC production..... 29
Table 2.5 List of utilization process routes and reaction mechanisms for MeOH production..... 29
Table 3.1 Summary of variables and their descriptions for the base case scenario 42
Table 3.2 Summary of variables and their descriptions for the integrated case scenario 54
Table 4.1 Detailed summary of the thermal and electrical duties..... 66
Table 4.2 Summary of CO_2 emissions for MeOH production 68
Table 4.3 Summary of CO_2 emissions for DMC production 78
Table A.1 Stream summary for SMR section 101
Table A.2 Stream summary for MeOH section..... 103
Table B.1 Stream summary for SMR section 106
Table B.2 Stream summary for MeOH section..... 108

Acronyms and Abbreviations

AGWP	Absolute Global Warming Potential
AP	Acidification Potential
ASU	Air Separation Unit
BCCC	Bern Carbon Cycle-Climate
CC	Carbon Capture
CCS	Carbon Dioxide Capture and Sequestration
CCU	Carbon Dioxide Capture and Utilization
CEQR-NY	The City Environmental Quality Review of the City of New York
Cetesb	Companhia Ambiental do Estado de S$\tilde{a}$o Paulo
CH_4	Methane
CO	Carbon Monoxide
CO_2	Carbon Dioxide
CuCl	Copper Chloride (I)
DCF	Dynamic Characterization Factor
DHW	Domestic Hot Water
DLCI	Dynamic Life Cycle Inventory
DMC	Dimethyl Carbonate
DME	Dimethyl Ether
EC	Ethylene Carbonate
EG	Ethylene Glycol
EIA	Energy Information Administration
EO	Ethylene Oxide

EP	European Patent
GHG	Greenhouse Gas
GW	Global Warming
GWI	Global Warming Impact
GWI_{cum}	Cumulative Impact
GWI_{inst}	Instantaneous Impact
GWI_{rel}	Relative Impact
GWP	Global Warming Potential
H_2	Hydrogen
ILCD	International reference Life Cycle Data system
IPCC	Intergovernmental Panel on Climate Change
ISO	International Standard for Organization
LCA	Life Cycle Analysis
LCI	Life Cycle Inventory
LCIA	Life Cycle Impact Assessment
LU	land Use
LUC	Land-Use Change
LULUCF	Land Use, Land-Use Change, and Forestry
MeOH	Methanol
N_2	Nitrogen
NG	Natural Gas
NGCC	Natural Gas Combined Cycle
NGCT	Natural Gas Combustion Turbine
NGSR	Natural Gas Steam Reforming

NH_3	Ammonia
N_2O	Nitrous Oxide
Pc	Polycarbonate
PC	Propylene Carbonate
PEI	Potential Environmental Impact
PG	Propylene Glycol
PP	Power Plant
RF	Radiative Forcing
RWGS	Reverse Water-Gas Shift
SMR	Steam-Methane Reforming
Syngas	Synthesis Gas
td	Time Delay
TH	Time Horizon
US-EPA	The United States Environmental Protection Agency
WAR	Generalized Waste Reduction Algorithm

Chapter 1: Introduction

1.1 Carbon Dioxide and Climate Change

The industrial revolution, dating back to the mid-eighteenth century, marked a transitional age in humanity where the manifestation of technological advancements played a pivotal role in altering the course of mankind (Chu & Majumdar, 2012). Further technological developments and enhancements pursued carrying the revolution onwards to the nineteenth and twentieth centuries. Significantly, the immense power utilized within this era was largely derived from exploiting depletable fossil sources. As a consequence, even greater amounts of greenhouse gas (GHG) emissions were released into the atmosphere posing perilous climate change hazards.

The greenhouse effect is the process within which the gases in the upper atmosphere absorb a share of heat radiation emitted from the surface. Climate change, usually stated in conjunction with the greenhouse effect, refers to a long-term shift in climate conditions (Giammario et al., 2018). Progressively, the side-effects of the post-industrial revolution are strengthening the greenhouse effect triggering and consolidating climate change risks.

GHG emissions primarily comprise of 72% carbon dioxide (CO_2), 19% methane (CH_4), 6% nitrous oxide (N_2O), and 3% fluorinated gases (Olivier, Schure, & Peters, 2017). Carbon dioxide, contributing approximately 60% to global warming (GW), witnessed a rapid increase in concentration from the pre-industrial level of below 300ppm leveling off at 411 ppm in 2019 (Albo, Luis, & Irabien, 2010; NASA, 2019; Oh, 2010). Consequently, a temperature increase is evident across the globe and is vividly depicted within Canada's national average temperature for 2016 which was 2.1°C above normal (Giammario et al., 2018). Moreover, treaties such as the Kyoto Protocol and the Paris Agreement clearly depict that we are on the verge of recognizing the disastrous effects caused by GW (Cook et al., 2016; Protocol, 1997). In an effort to resolve this dilemma, the Paris Agreement aspiringly sets a temperature goal of $2°C$ increase above pre-industrial levels. Nevertheless, it is crucial for additional mitigation efforts to be put forward in order to truncate the net GHG emissions present in the atmosphere and hinder the perilous effects associated with GW.

The Canadian GHG emission trend, excluding land use, land-use change, and forestry (LULUCF), is presented in Figure 1.1 depicting a decrease in the net GHG emissions relative to 2005. Remarkably, a fluctuation occurs between 2005 and 2008 where a net decrease in GHG emissions is evident in 2009 accomplishing an all-time low. Currently, further efforts are required to decrease the net GHG emissions to lower levels in order to cope with the menacing effects of GW.

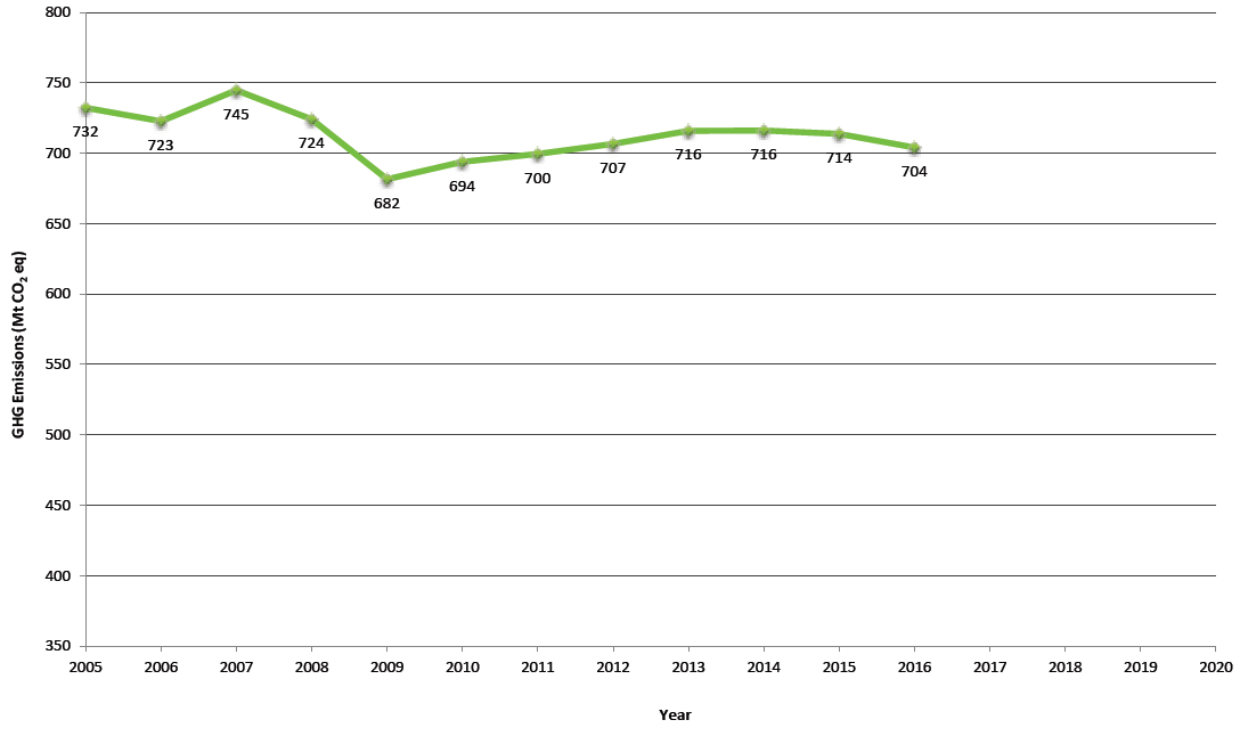

Figure 1.1 Canadian GHG emission trend from 2005 to 2016 (excluding LULUCF). Adopted from: Environment and Climate Change Canada (Giammario et al., 2018)

1.2 Carbon Dioxide Capture and Utilization (CCU)

In an ambitious effort to subdue GW, various carbon dioxide capture and sequestration (CCS) technologies have been developed to mitigate the net global carbon dioxide present in the atmosphere (Thambimuthu, Gupta, & Davison, 2003). However, public concern dealing with underground and ocean storage regarding several safety issues persist and are still being addressed (Huang & Tan, 2014). Alternatively, the captured CO_2 can undertake a diverging route where CO_2 is converted into a commercial product through CO_2 utilization techniques. Hence, researchers have embarked into the domain of carbon dioxide capture and utilization (CCU) in order to incorporate strategies to convert the captured CO_2 into final profitable products.

CO_2 utilization offers the advantage of eradicating the undesired CO_2 located in the atmosphere while generating a beneficial product. For example, dimethyl carbonate (DMC), one of the many valuable products of CCU, has been researched extensively with the integration and optimization of many routes. The principal motivation behind this, is the discovery of a sustainable route which lies in overcoming the energy barrier in order to activate the inert CO_2 molecule and further reduce any CO_2 generated in the domain of the utilization process (Huang & Tan, 2014; Jarvis & Samsatli, 2018; Keller, Rebmann, & Keller, 2010; Tan et al., 2018). In addition, CO_2 has some innate drawbacks as a chemical reactant due to its non-reactivity and low Gibbs free energy properties (Huang & Tan, 2014; Jarvis & Samsatli, 2018). Consequently, it is anticipated that a singular solution to GW is implausible, requiring the need for multiple CO_2 utilization and sequestration systems as a probable resolution.

Generally, CO_2 utilization can be broken down into two groups where direct utilization of CO_2 takes place in the former and conversion of CO_2 into chemicals and energy products in the latter (Huang & Tan, 2014). For example, the former depicts a scenario where CO_2 can directly be utilized to cultivate microalgae, whereas the latter converts the already captured CO_2 into chemicals and energy products such as DMC and dimethyl ether (DME) which have a substantial market scale. Moreover, the vast domain of industrial applications for CO_2 demands an in-depth expedition to allocate a sustainable route for its utilization. Figure 1.2 portrays the majority of routes for CO_2 utilization and sequestration displaying a wide array of possibilities that could claim the ultimate fate of CO_2.

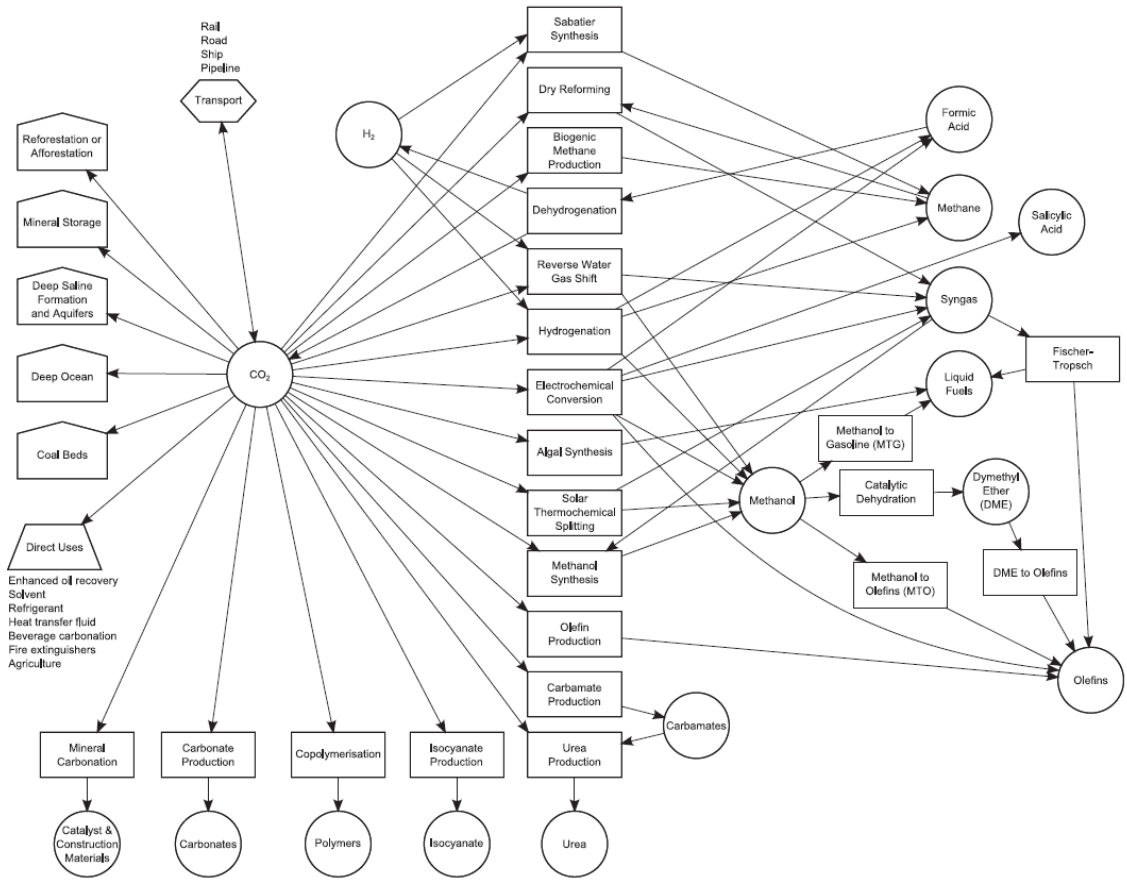

Figure 1.2 Cumulative web diagram incorporating all the various pathways for CO_2. Adopted from Jarvis and Samsatli (2018)

1.3 Traditional Life Cycle Analysis (LCA): An Environmental Assessment Tool for CCU

Utilization of CO_2, seemingly sustainable and environmentally appealing, maintains several drawbacks forming questions about its feasibility. The viability of CCU, a frequent and controversial topic disputed among scientific and climate-political entities, spurs the debates and discussions necessary for allocating a feasible assessment to CCU (N. V. von der Assen, Lafuente, Peters, & Bardow, 2015). Hence, evaluating the innate benefits arising from CCU requires a systematic and quantitative environmental assessment in order to appropriately evaluate its associated environmental impacts. A renowned holistic evaluation methodology suitable for this purpose is the life cycle analysis (LCA) (Peters et al., 2011; Quadrelli, Centi, Duplan, & Perathoner, 2011). LCA is a systematic and consistent approach concerned with the environmental aspects and potential environmental impacts throughout a product's life cycle from raw material procurement through manufacture, utilization, end-of-life treatment, recycling and final disposal (International Organization for Standardization, 2006b, 2006a).

David Novick was the first to address the life cycle concept, dating back to 1959, where the LCA of cost was analyzed by the RAND Corporation (Curran, 2012). It was until the Eighties, when environmental policies became a major issue in society, that environmental LCA began to emerge with it becoming official in the Nineties through the Society of Environmental Toxicology and Chemistry and the standardization in the 14040 Series of International Standard for Organization (ISO) (International Organization for Standardization, 2006a, 2006b; Klöpffer, 2006). The updated standards from the ISO 14040 and 14044 state that the major sections of the LCA should consist of the goal and scope definition, life cycle inventory (LCI), life cycle impact assessment (LCIA), and interpretation. Initially, a proper goal, functional unit, and system boundary should be designated. A functional unit quantifies the related function of a product through consideration of its performance characteristics. In addition, the system boundaries define which processes are included in the study. For instance, cradle-to-gate ranges from raw material extraction to the factory gate, while cradle-to-grave encompasses everything from raw material extraction, including all processes, until its end-of-life treatment. Thereafter, the collection of data occurs in the LCI section and this is most commonly undertaken through the use of LCA databases

such as Ecoinvent and PlasticsEurope's Eco-profiles (PlasticsEurope Eco-profiles, 2013; Swiss Centre for Life Cycle Inventories, 2013). Ensuing this, LCIA accumulates all the inventory into an appropriate number of comprehensible environmental impact categories that are quantitative in nature. Lastly, interpretation of the results occurs where an immense emphasis should be placed on transparency since it plays a key role in determining certain outcomes. Notably, LCA is an iterative methodology necessitating consistent updates along its successive phases. Thus, an imperative aspect of utilizing LCA is that the segments should be conducted in conjunction rather than in segregation. This is vividly portrayed in Figure 1.3 which depicts the LCA framework adopted from the updated standards by the ISO 14040 and 14044 (International Organization for Standardization, 2006a, 2006b).

The general concept of LCA, when applied to CCU, entails that all inputs and outputs of material and energy for each individual process should be quantified (N. V. von der Assen et al., 2015; N. von der Assen, Voll, Peters, & Bardow, 2014). The streams connecting processes together are termed economic flows while processes exchanging with the natural environment are termed elementary flows. In addition, these elementary flows are aggregated along the life cycle with the accumulation terminating in various environmental impacts. For example, these impacts could be related to various impact categories such as global warming, cumulative (fossil) energy demand/fossil resource depletion, resource depletion, stratospheric ozone depletion, photochemical ozone creation/summer smog, particulate matter formation/respiratory inorganics, acidification, eutrophication, eco and human toxicity, and water consumption (N. V. von der Assen et al., 2015). Generally, CCU is primarily concerned with decreasing the effects of the first two impact categories (Peters et al., 2011; Quadrelli et al., 2011).

In the LCIA segment, metrics termed as category indicators are utilized to quantify a specific impact category. This is typically undertaken by multiplying each GHG, intrinsic within the inventory list, by its corresponding global warming potential ($GWP_{TH=Time\ Horizon}$) value. GWP is defined as the infrared radiation absorbed by a given GHG, in a time horizon, relative to the infrared radiation absorbed by CO_2. Specifically, it describes the relative GW strength of a GHG emission and exemplifies the radiation absorption of an individual GHG emission independently from any product life cycle (Von Der Assen, Jung, & Bardow, 2013). Furthermore, a midpoint category indicator is generally utilized for CCU since it assesses the environmental

impact associated at the "midpoint" of the environmental cause-and-effect chain (N. V. von der Assen et al., 2015). The midpoint category indicator assesses the environmental impact terminating at the absorbed radiation. However, an endpoint category indicator proceeds to analyze and quantify the loss of species, changes in climate, ecosystems, and human activities as a result of a temperature increase due to the absorbed radiation.

In general, LCA maintains numerous advantages suitable for assessing the environmental impacts associated with CCU. Nonetheless, Von Der Assen et al. (2013) states that there exists three methodological pitfalls commonly encountered when conducting a LCA on CCU processes and products. These pitfalls consist of the improper consideration of utilized CO_2 as a negative GHG emission, incorrect allocation procedures related to product-specific LCA results involving multiple companies, and exclusion of the CO_2 storage duration within the traditional LCA. Moreover, Von Der Assen et al. (2013) presents a methodical framework, which strives to steer clear of these pitfalls, where the utilized CO_2 is appropriately accounted for as a regular feedstock with its own emissions, proposed recommendations for obtaining reliable product-specific LCA results for CCU processes are depicted, and the integration and implementation of the CO_2 storage duration within the LCA results is undertaken. Significantly, the third pitfall, depicting a lack of mandatory time (temporal) information, represents a major disadvantage attributed to the application of the traditional LCA approach to CCU (Levasseur, Lesage, Margni, Deschenes, & Samson, 2010; Schwietzke, Griffin, & Matthews, 2011). It is crucial that delayed GHG emissions are accounted for since they are environmentally beneficial when compared to early GHG emissions (Brandão et al., 2013; Schwietzke et al., 2011). Therefore, it is vital that this commonly encountered pitfall is dealt with so as to circumvent the resultant bias which undesirably influences the LCA results and conclusions.

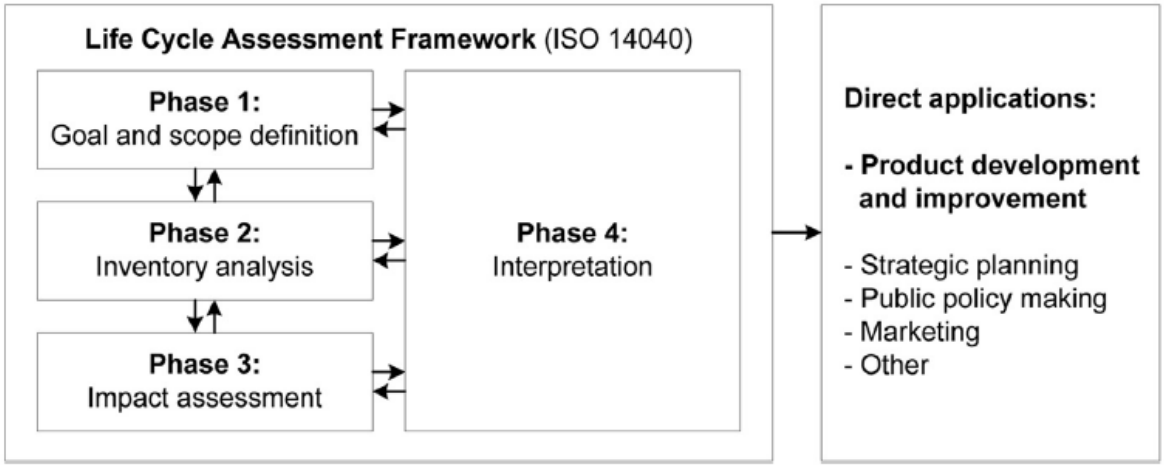

Figure 1.3 LCA assessment framework pertaining to the standards by ISO 14040 and ISO 14044. Adopted from Von der Assen et al. (2015)

1.4 Dynamic LCA: A Proposed Evaluation Tool for CCU

LCA was primarily designed to be a steady state tool, neglecting time varying emissions within its scope of analysis (Udo de Haes, 2006). Numerous problems occur when utilizing LCA to evaluate CCU processes and products, as mentioned in section 1.3, due to the omission of time-related conditions intrinsic within its segments (Reap, Roman, Duncan, & Bras, 2008a). The dynamic LCA approach addresses this crucial limitation and enhances the accuracy of the LCA methodology by implementing a temporal-based framework (Levasseur et al., 2010). Originally, Levasseur et al. (2010) developed the dynamic LCA procedure, based on the radiative forcing (RF) concept, to assess GW. The Intergovernmental Panel on Climate Change (IPCC) defines RF as an externally imposed perturbation in the balance between the energy absorbed by the earth and that emitted by it in the form of longwave infrared radiation (Ramaswamy et al., 2001). Explicitly, the procedure consists of initially calculating a dynamic life cycle inventory (DLCI) followed by the computation of dynamic characterization factors (DCFs) (Levasseur et al., 2010). Thereafter, these factors are utilized to assess the DLCI in real-time impact scores for any time period. Precisely, the LCIA characterization model is now solved dynamically and the time-dependent global warming impact (GWI) is attained by combining the dynamic inventory with the DCFs. Typically, the time frame is set as 100 years, and this is commonly adopted as an ideal choice, as it is the reference time frame implemented for the Kyoto Protocol (UNFCCC, 1998).

DynCO_2 version 2.0 implements the dynamic LCA model in Excel and is further utilized as the calculation tool to enable the application of the dynamic LCA methodology (Levasseur et al., 2010). Moreover, three different types of GWI results are acquired for every simulation and these are termed the instantaneous impact (GWI_{inst}), cumulative impact (GWI_{cum}), and relative impact (GWI_{rel}). The instantaneous impact is the RF caused by the life cycle GHG emissions at any time ensuing the moment when the initial emission occurs. A positive value indicates an increase in RF which also indirectly implies a detrimental effect on GW. Summing up the instantaneous impacts over the entire time period of consideration yields in the cumulative impact. Fundamentally, this impact permits the comparison of scenarios and illustrates which scenario will have a higher impact on RF for any given time period. Lastly, the relative impact is the ratio of the life cycle cumulative impact over the cumulative impact of a 1 kg CO_2 pulse-emission at time zero.

Essentially, the relative impact converts the dynamic LCA results into the same units as the traditional LCA whilst accounting for the timing of emissions.

The dynamic LCA approach possesses countless advantages as an environmental assessment tool due to the consistency it delivers within its temporal assessment. Consequently, this allows for enhanced accuracy within the concluding results when compared to the generic LCA. Adding to that, another advantage of the dynamic LCA approach is its relevance to any type of LCA study and temporal profile of emissions. Furthermore, afforestation, reforestation, and any other temporary carbon sequestration application, necessitating a temporal profile of emissions, benefits immensely from the dynamic LCA approach (Levasseur, Lesage, Margni, Brandão, & Samson, 2012). The dynamic LCA approach also circumvents the obligation of artificially tagging carbon flows, associated with biogenic and fossil carbon emissions in origin, within any type of biogenic carbon application (Levasseur, Lesage, Margni, & Samson, 2013). Therefore, the dynamic LCA conserves an immense amount of time typically attributed to allocating the source of the emissions in biogenic carbon scenarios. In addition, the dynamic LCA approach also permits sensitivity testing of the results, in any application, by means of altering the given time period.

1.5 Research Objectives, Motivations, and Contributions

Thus far, the quantitative environmental assessment of CCU has relied appreciably upon the static traditional LCA. This should come as no surprise given that LCA retains commendable superiority in offering paramount feedback as a holistic methodology. However, the absence of dynamics within the traditional LCA presents a substantial limitation paving the route to prejudiced results. Therefore, the chief objective of this thesis is to portray the application of the dynamic LCA approach to various CCU processes and products so as to acquire a feasible and justifiable environmental assessment. In addition to, resolving a major shortcoming by integrating and implementing the CO_2 storage duration into the environmental assessment (Von Der Assen et al., 2013). To our knowledge, no dynamic LCA application on CCU processes and products exists. Therefore, this thesis examines the implications of utilizing the dynamic LCA approach on various CCU processes and products.

In order to accomplish these objectives, an integrated model of several CCU processes and products is generated. The integrated model consists of a power plant (PP) utilizing natural gas (NG), that accounts for de-rating, integrated with CCU to manufacture the desired product. Adding to that, the scope of the analysis will principally revolve around a generic 620 MW natural gas combined cycle (NGCC) PP. Two commercial products, methanol (MeOH) and DMC, are also comprehensively analyzed within the vicinity of their respective production process. Essentially, both DMC production flowsheets, employing either the conventional or the CO_2 utilization approach, are adopted from simulations by Kongpanna et al. (2015, 2016). Both MeOH production flowsheets are developed and simulated in Aspen Plus™ V10 (Aspen Plus™, 2017). Then an environmental comparison between the conventional and utilization approaches is conducted. Notably, the comparison is imperative so as to justify the shrouded benefits of employing various CCU methodologies to manufacture these products. The environmental analysis will primarily consist of utilizing the dynamic LCA approach, employing both CCU and the conventional method, to scrutinize the underlying system through a CO_2 balance.

1.6 Thesis Outline

In order to develop a well-grounded environmental assessment for CCU, a variable number of interconnected activities were undertaken. An overview of the intrinsic segments and tasks discussed within this thesis is provided within each chapter:

Chapter 1 includes a discussion of tackling and subduing climate change through CCU methodologies. Moreover, the environmental assessment approaches, traditional LCA and dynamic LCA, are introduced and presented in detail. In addition, the contributions towards this thesis are also depicted**.**

Chapter 2 discusses a literature review on dynamic and traditional LCA applications. Furthermore, the conventional and utilization methodologies of manufacturing various products are also deliberated.

Chapter 3 entails the development of both the base case and integrated case models utilized in the environmental assessment. Additionally, schematics are established alongside the obligatory equations which portray the focal systems within the generated framework. The intrinsic equations employed within the dynamic LCA framework are also deliberated in detail. The development of both the conventional and utilization approaches of manufacturing MeOH in Aspen Plus^{TM} is also discussed.

Chapter 4 presents the application of the models developed in the preceding chapter in conjunction with the dynamic LCA framework. Moreover, various products are scrutinized within the underlying models with environmental results being generated for each individual model. Sensitivity analysis of the developed model results is also depicted.

Chapter 5 illustrates the conclusions attained from conducting this research together with the provision of laudable recommendations for future work that could be undertaken to progress research within this field.

Chapter 2: Literature Review

2.1 Applications of Traditional LCA on CCU Products

LCA is a valuable tool allowing for continuous improvements to be made to a process. Hence, it comes as no surprise that its exceptional ability is utilized in evaluating CCU processes. Presently, there exists a limited amount of conducted LCA studies exploring the environmental impacts of utilizing CO_2 based routes to manufacture DMC. Moreover, none of the current assessment methodologies have utilized the dynamic LCA procedure. The scant accessibility to reliable sources of data pertaining to industrial processes plays a major role in impeding assessments to CO_2-based DMC production routes (Aresta & Galatola, 1999). Nevertheless, there exists some LCA studies that have been conducted on CCU within the literature domain. A supplementary overview of the discussed LCA literature on CCU products is tabulated in Tables 2.1 and 2.2, and a detailed analysis is deliberated in the ensuing domain of this chapter. Tables 2.1 and 2.2 do not have identical columns and this is as a result of the lack of data presented within the analyzed studies.

Thus far, five LCA studies have been conducted with the first LCA study presented by Aresta & Galatola (1999) who undertook an LCA comparison between the conventional phosgene route and a CO_2-based urea route to manufacture 1 kilogram of DMC (Heijungs et al., 1992). The authors utilized a cradle-to-gate system boundary in their analysis stating that their sole intention is to assess the "green chemistry" aspects as opposed to the analysis of mitigating anthropogenic CO_2. Furthermore, the LCA analysis was attributed as a "preliminary" study due to the lack of appropriate field data and reliable databases. In conclusion, Aresta & Galatola (1999) found the GWI of the conventional phosgene route to be greater than the CO_2-based urea route with a grand total of $\frac{116\ \text{kg CO2 eq.}}{kg\ of\ DMC}$ obtained versus $\frac{29.45\ \text{kg CO2 eq.}}{kg\ of\ DMC}$ respectively. In addition, they stated that utilizing the LCA procedure to peruse two processes that manufacture DMC aided with the identification of core areas for improvement within each process. Thus, this stressed the effectiveness of utilizing LCA as a strategic management tool which could be augmented with more reliable sources of data.

Monteiro et al. (2009) conducts an optimization LCA study considering a sustainability analysis which assesses two different CO_2-based routes for the production of DMC. Specifically, the author analyzed the transesterification route using ethylene carbonate (EC) with methanol and the CO_2-based urea route. The LCA analysis utilized a sustainability function which was defined as a 2D indicator that involved both an environmental and economic aspect (Monteiro et al., 2009). The author concluded his analysis obtaining a GWI of $\frac{0.86 \text{ kg CO2 eq.}}{kg\ of\ DMC}$ for the transesterification route using EC with methanol and a GWI of $\frac{0.34 \text{ kg CO2 eq.}}{kg\ of\ DMC}$ for the CO_2-based urea route. In essence, the CO_2-based urea route was more sustainable than the transesterification route and was shown to decrease the emissions by a factor of 2.5 relative to the transesterification route. However, when the author employed an identical analysis utilizing a gate-to-gate system boundary, assessing everything from one factory gate to another, the perceived result obtained was now reversed. Under these circumstances, the CO_2-based urea route is now less sustainable in comparison to the transesterification route. Hence, the result attained stressed the impact of the initial requirement of a rational system boundary which plays a crucial role in influencing the final conclusions.

In contrast to the route comparison-based studies, Souza et al. (2014) conducts a technical, economical, and environmental assessment of an individual DMC synthesis route. The indirect route of consideration was the transesterification route utilizing EC with methanol. The author's principal objective was to address the energetic hinderance existing in the separation of the azeotropic pair DMC-MeOH. Two entrainers, EG and methyl-isobutyl-ketone, are evaluated for extractive distillation and the formation of the azeotropic pair. Thereafter, the two entrainers are evaluated for their environmental impacts via the LCA, exergy analysis, the generalized waste reduction algorithm (WAR) database for the LCI portion, and the methodology based on the potential environmental impact (PEI) balances (Cabezas, Bare, & Mallick, 1999). The analysis culminated obtaining a GWI of $\frac{0.77 \text{ kg CO2 eq.}}{kg\ of\ DMC}$ for the indirect route of transesterification utilizing EC with methanol. Both entrainers utilized in the extractive distillation were simulated with identical processes, PEI indexes, GWPs, and acidification potentials (APs). Regardless, notable advantages were in favor of the EG entrainer due to its superior sustainability, economic indexes, chemical reduction of 92% versus 85% of the emitted CO_2, health, safety, and environment issues.

However, both entrainer routes were found to emit amounts of CO_2 greater than they sequester yielding negative indexes of chemical sequestration of CO_2.

Identical to Monteiro et al. (2009), Kongpanna et al. (2015) simulated the same CO_2-based routes for the production of DMC and also added the conventional BAYER process (Kalakul, Malakul, Siemanond, & Gani, 2014). Moreover, Garcia-Herrero et al. (2016) employed a LCA comparison of the conventional oxidative carbonylation of methanol versus the electrochemical reaction of CO_2 and methanol in the presence of potassium methoxide and the ionic liquid 1-butyl-3-methylimidazolium bromide (Garcia-Herrero, Alvarez-Guerra, & Irabien, 2016). The intrinsic information regarding the aforementioned articles can be obtained within the cited references and a supplementary overview is depicted within Table 2.1.

In contrast to DMC, MeOH possesses a variety of LCA studies, assessing several chemical routes, within the literature domain. Three different LCA studies assessing the environmental impact of numerous routes and processes that synthesize commercial MeOH are explored in this literature review.

In one particular study, Aresta et al. (2002) considers four different synthetic routes within which MeOH is being produced. Furthermore, Aresta et al. (2002) proceeds to also compare these routes utilizing the LCA approach. The routes he considered consisted of synthesis gas (Syngas) produced from steam reforming with and without heat recovery in the MeOH synthesis step, natural gas steam reforming (NGSR) syngas and recovered CO_2 without heat recovery, natural gas dry reforming and NGSR with heat recovery in the MeOH synthesis step, and recovered CO_2 reacted with hydrogen (H_2) from water electrolysis. To summarize, the results presented by the fourth option, with recovered CO_2 and H_2 produced by electrolysis, yielded the most environmentally appealing route when contrasted against the other three synthetic routes (Aresta et al., 2002).

More recently, Al-Kalbani et al. (2016) contrasted two CO_2-to-MeOH conversion processes, MeOH production by CO_2 hydrogenation and MeOH production based on high-temperature CO_2 electrolysis, with the conventional approach of manufacturing MeOH utilizing Aspen HYSYS. In conclusion, both processes, heavily depending on renewable energies, surpassed the conventional fossil-fuel based MeOH process yielding in inferior net CO_2 emissions

(Al-Kalbani et al., 2016). However, if these processes implemented petroleum-based fuels as opposed to utilizing renewable sources of energy, the perceived results obtained are now reversed.

In another study, Matzen & Demirel (2016) conducted an LCA regarding the synthesis of renewable MeOH and DME. The process routes utilized optimum feedstocks of wind-based electrolytic H_2 and considered CO_2 captured from an ethanol fermentation process. Adding to that, the emissions were also further compared to the emissions by conventional petroleum-based fuels through means of assessing the total environmental impacts, from well-to-wheel, of a given production process. To conclude, the processes involved with the manufacture of renewable MeOH and DME proved to be a better environmental alternative than the conventional fossil fuels (Matzen & Demirel, 2016). Adding to that, GHG emissions were reduced by approximately 82 – 86 % and fossil fuel depletion was also reduced by 82 – 91 % when compared to the conventional fossil-fuel sources.

Table 2.1 Summary of LCA applications for DMC synthesis

Literature Reference and Date	Process Route Analyzed	System Boundary	Life Cycle Inventory (LCI)	Assessment Methodology Data	GWI ($\frac{\text{kg CO2 eq.}}{kg\ of\ DMC}$)
Aresta & Galatola (1999)	Phosgene	Cradle-to-gate	Not mentioned	CML 2001[a]	116
	Urea Transesterification				29.45
Monteiro et al. (2009)	Transesterification (EC with methanol)	Cradle-to-gate	WAR database[b]	Cetesb[c]	0.86
	Urea Transesterification			EPAA[d]	0.34
Souza et al. (2014)	Transesterification (EC with methanol)	Gate-to-gate	WAR database[b]	CERQ-NY[e]	0.77
Kongpanna et al. (2015)	BAYER process	Gate-to-gate	thermal energy from stoichiometric CH_4 combustion	US-EPA[f]	0.52
	Transesterification (EC with methanol)			IPCC[g]	0.45
	Urea Transesterification				2.93
Garcia-Herrero et al. (2016)	Enichem process	Cradle-to-gate	Ecoinvent [h]	CML 2001[a]	3.18
	Electrochemical reaction of CO_2 and methanol				78.90

[a] CML 2001 impact assessment method (Heijungs et al., 1992).

[b] The generalized Waste Reduction Algorithm (WAR) database (Cabezas et al., 1999).

[c] Companhia Ambiental do Estado de São Paulo (Cetesb) is a Brazilian environmental agency (Cetesb, 2009).

[d] Environmental Protection Authority of Australia (EPAA) (Environmental Protection Authority of Australia, 2002).

[e] The City Environmental Quality Review of the City of New York (CEQR-NY) (CEQR, 2012).

[f] The United States Environmental Protection Agency (US-EPA).

[g] The Intergovernmental Panel on Climate Change (IPCC).

[h] The Ecoinvent database (Swiss Centre for Life Cycle Inventories, 2013).

Table 2.2 Summary of LCA applications for MeOH synthesis

Literature Reference and Date	Metrics	CO_2 source	H_2 Source	Assessment Methodology Data
Aresta et al. (2002)	Single Indicator[a]	Power Plant	Electrolyzer using photovoltaic and nuclear electricity	SimaPro SP4[b] EcoIndicator 95[c]
Al-Kalbani et al. (2016)	Global Warming Impact	Power Plant	Alkaline electrolyzer using wind, photovoltaic, NG, and coal electricity	US-EPA[d]
Matzen & Demirel (2016)	Global Warming Impact, Acidification Potential, Photochemical Oxidant Formation, Human Toxicity, Particulate Matter Formation	Ethanol fermentation	Electrolyzer using wind electricity	GREET[e] ReCiPe[f]

[a] The single indicator is defined as the weighted sum of the greenhouse effect, ozone layer depletion, acidification, nitrification, and photochemical oxidant formation (Aresta et al., 2002).

[b] The SimaPro SP4 database (SimaPro SP4, 2000).

[c] The EcoIndicator 95 database (Heijungs et al., 1992).

[d] The United States Environmental Protection Agency (US-EPA).

[e] The Greenhouse gases, Regulated Emissions, and Energy use in Transportation software (GREET) (M. Wang, Wu, & Huo, 2007).

[f] The ReCiPe database (Goedkoop et al., 2009).

2.2 Dynamic LCA Applications and Implementations

Dynamic LCA was developed in order to alleviate proposed limitations inherent within the generic LCA by addressing several key issues (Reap, Roman, Duncan, & Bras, 2008b). Explicitly, these issues pertained to the lack of temporal information intrinsic to the segments within the traditional LCA methodology (Levasseur et al., 2010). Consideration of the temporal aspects in carbon accounting has widely attracted attention from researchers with various resolutions recently being developed (Kendall, Chang, & Sharpe, 2009; O'Hare et al., 2009). Initially, Levasseur et al. (2010) developed the dynamic LCA specifically for the global warming impact category, for CO_2 and non-CO_2 GHGs, and ensured its applicability to any type of temporal profile. Therefore, promoting both its versatility and feasibility as an assessment tool for CCU products and resolving the aforementioned dilemma. Nevertheless, to my knowledge there subsists no application within the literature that utilizes the dynamic LCA as an assessment methodology for CCU products. However, there exists dynamic LCA applications conducted on renewable fuels, afforestation projects, land use (LU) and land-use change (LUC) projects, LCI databases, systems producing domestic hot water (DHW), and a fictious case study evaluating the life cycle of a wooden chair.

In her first publication, Levasseur et al. (2010) developed the dynamic LCA and applied it to the US EPA LCA on renewable fuels comparing the life cycle GHG emissions from different biofuels with fossil fuels inclusive to LUC emissions (U.S. Environmental Protection Agency, 2009). Specifically, the dynamic LCA was applied by utilizing the life cycle emissions per unit energy for three GHGs CO_2, CH_4, and N_2O considered for gasoline, corn ethanol, and corn stover cellulosic ethanol. Principally, the case study was conducted to demonstrate that utilizing GWPs for a given time horizon to characterize GHG emissions will result in a discrepancy between the time frames selected for the analysis and the time period covered by the LCA results. Furthermore, the time horizons were chosen in harmony with the US EPA data, as 30, 50, and 100 years, in order to maintain a reasonably comparative analysis. To conclude, the analysis brought about several substantial findings regarding the effects associated with lacking a temporal profile of emissions in a traditional LCA. Primarily, these consisted of underestimating LUC emissions, reduced accuracy, and the addition of bias due to the omission of variable time horizons, within the characterization factors, which account for the residence time of each GHG emission.

Moreover, the comparison between the generic and dynamic LCA approaches vividly depicted that the difference arising from neglecting temporal information of emissions can be significant enough to influence conclusions.

In another publication, Levasseur et al. (2012) showcases the dynamic LCA approach with a temporary carbon sequestration project, by afforestation, and includes a comparison with two principal ton-year methods. These approaches comprised of the renowned Lashof and Moura-Costa methodologies, typically known for their use in determining credits due to LULUCF projects (Costa & Wilson, 1999; Lashof & Hare, 1999). The analysis conducted covered six different scenarios with five out of the six taking place towards the final limit of the sequestration period. Specifically, these consisted of the baseline, fire, exploitation, fire multi-gas, neutral, and landfill scenarios. To sum up, the analysis culminated finding that the curves of the cumulative impact for the neutral scenario tend to zero with time since the total amount of carbon stored is assumed to be sequestered indefinitely as opposed to the other scenarios. In addition, the fire-multi gas scenario had the highest cumulative impact, following the baseline non-sequestration scenario, after the 70-year mark where sequestration is assumed to occur. Moreover, the methodology comparison depicted that the "static" Moura-Costa and Lashof approaches result in higher values for the calculated credit when compared to their dynamic counterpart. Overall, the dynamic LCA approach showcased greater versatility by outperforming its counterparts and by allowing decision makers to perform a sensitivity test of the results to various time horizons.

Ensuing this, Levasseur et al. (2013) performs a fictious case study evaluating the life cycle of a wooden chair, with five different approaches inclusive to the dynamic LCA, for four different end-of-life scenarios. Explicitly, the four other approaches consisted of the PAS 2050, international reference life cycle data system (ILCD) handbook method, and the traditional LCA with and without taking into account biogenic carbon (BSI, 2008; European Commission, 2010). In addition, the four end-of-life scenarios that are analyzed within this study consist of incineration, landfill, refurbishment, and energy recovery. To summarize, the analysis yielded the cumulative radiative forcing to be the highest for the incineration scenario within any time horizon. Identical to the dynamic LCA, the PAS 2050 and the ILCD handbook methodologies concluded that the landfill scenario is optimal. Adding to that, a comparison between the traditional LCA addressing and omitting biogenic carbon illustrated that omitting biogenic carbon will lead to biased

conclusions. This is evident within the results where omitting biogenic carbon leads to a different conclusion than the landfill scenario obtained by the four other approaches. Furthermore, this study concluded that the dynamic LCA is superior to the other approaches analyzed since it consistently assesses the impact on global warming for any product. In addition, the conclusions regarding the relevant scenarios are entirely dependent on the chosen time horizon. This is typically the case pertaining to LCA applications since transparency is crucial when dictating outcomes and conclusions. Moreover, the primary goal within the case study was not to analyze the various end-of-life scenarios but to depict how dynamic LCA simultaneously addresses both timing issues of GHG flows and biogenic CO_2.

In a further implementation, Pinsonnault et al. (2014) utilizes the DCFs, intrinsic within the dynamic LCA, to assess the real significance associated with the temporal distribution of the background system inventory; as opposed to, the foreground processes of product systems. Explicitly, the principal focal point was the GWI category where the development of DCFs were implemented in the Ecoinvent V2.2 database to be further utilized as both an exemplary database and a foundation of product systems to test the significance of considering temporal information in the background system. Furthermore, the methodology considered the addition of temporal information to 22% of the unit processes, inclusive to elementary and intermediate interactions, in the database. Thereafter, potential impacts were then calculated for 4,034 product systems within the Ecoinvent database resulting in 8.6% of the database product systems being affected by GWI impact scores of greater than 10%. In addition, the results depicted that the sectors that showed the greatest sensitivity to the temporal differentiation of the background processes were primarily associated with the wood, infrastructure, electricity, processing, chemical, and biofuel sectors. Pinsonnault et al. (2014) culminates the study claiming that the implementation of the temporal information to the processes in LCI databases augments some LCA studies but not every single one.

In a more recent publication, Beloin-Saint-Pierre et al. (2017) presents an enhanced dynamic LCA approach by integrating the enhanced structural path analysis method with the dynamic LCA (Beloin-Saint-Pierre, Heijungs, & Blanc, 2014; Levasseur et al., 2010). This integration permitted the characterization of potential impacts from each GHG emission over a time scale. Ensuing this, the integrated dynamic LCA methodology was further implemented on

two types of DHW production systems, with a comparative analysis, over an 80-year time period. Specifically, electricity is utilized in heating the water within the first system; however, a mixture of solar energy and gas is utilized to heat an identical amount of DHW within the second system. The results obtained showed that accounting for timing of GHG emissions diminishes the absolute values of the carbon footprint within the short term in contrast to the traditional static LCA. In addition, scenario 1 presented worse results for both the generic and annual dynamic LCA approaches, whereas scenario 2 showed inferior results for the monthly differentiated dynamic LCA scenario. Therefore, this realization portrayed the significance of temporal variability considerations by depicting a reversal of conclusions when modeling the energy consumption of the DHW production systems.

2.3 Conventional Processes

DMC, renowned for its versatility and environmental friendliness within the industrial sector, displayed a rapid increase in its utilization within recent decades. The annual production of DMC also showed a persistent increase throughout the years amounting to 90,000 tonnes/day DMC consumed universally in 2016 (Garcia-Herrero, Cuéllar-Franca, et al., 2016). There exist many promising large-scale applications within which DMC plays an essential role. Its exclusive intermediate allows for versatile chemical reactivity, leading to its immense application in many fields, such as the reagent for carbonylation, methylation, and methoxylation reactions (Cao, Cheng, Ma, Liu, & Liu, 2012; Tundo & Selva, 2002). Moreover, its eco-friendliness, low persistence, low toxicity, and low bioaccumulation has made it prominent in the field of "Green Chemistry". For example, polycarbonate (Pc), which is widely used in the automotive, building, and electronics industries, can be synthesized from DMC which acts as a carbonylation agent substituting the need for the perilous phosgene (Cao et al., 2012). DMC is also utilized as an electrolyte solvent in lithium batteries to augment the conductivity and enhance the overall efficiency of the electrochemical cycles (Naejus, Coudert, Willmann, & Lemordant, 1998; Park et al., 2007). In addition, DMC, having a high oxygen content, plays a significant role as a fuel additive to enhance the octane number in fuel (Pacheco & Marshall, 1997; Shukla & Srivastava, 2017). Furthermore, utilizing appropriate portions of DMC is beneficial in alleviating soot, smoke, and particulate emissions from hydrocarbon fuels (United States Patent No. US4891049A, 1990). DMC, having a strong solvation force, also poses as an alternative to ketones and esters in adhesives and paints (Keller et al., 2010).

Prior to 1980, DMC and more unambiguously dialkylcarbonates, were primarily manufactured by the Bayer company (Germany) and the Société Nationale des Poudres et Explosifs (SNPE, France), through the reaction of methanol on phosgene (Babad & Zeiler, 1973; Keller et al., 2010). However, the toxicity of the phosgene reactant together with the requirement to neutralize large amounts of pyridine and to remove NaCl salts, both requiring strongly obstructive and costly post-synthesis purification processes, resulted in the industrial shift towards enhanced processes (Huang & Tan, 2014; Keller et al., 2010). Post 1980, several phosgene-free processes for DMC synthesis began to emerge and these consisted of the Liquid-phase methanol oxidative carbonylation route (the Enichem process), Urea alcoholysis route, and Partial Carbonylation route (BAYER process).

In 1983, the liquid-phase methanol oxidative carbonylation Enichem process was industrialized by the Enichem Company located in Italy (United States Patent No. US4218391A, 1980). The process entailed a two-step mechanism involving the reaction of methanol with carbon monoxide (CO) and oxygen in the presence of a metal salt catalyst, generally a copper salt, yielding in esters of carbonic acid (Pacheco & Marshall, 1997; Tan et al., 2018). Specifically, the process exploited the use of copper chloride (I) (CuCl) within the reaction to produce DMC (Keller et al., 2010; Romano, Tesel, Mauri, & Rebora, 1980). Late in the Nineties, the development of the urea alcoholysis route to produce DMC was accomplished (United States Patent No. US4436668A, 1984; World Intellectual Property Organization Patent No. WO1995017369A1, 1995). The process undertaken encompassed a two-step reaction mechanism with a methyl carbamate intermediate produced in the first step through the reaction of urea and methanol, and DMC with ammonia (NH_3) generated in the second step (Keller et al., 2010; Tan et al., 2018). Researchers at BASF and Exxon patented two different processes with the former utilizing a stripping gas such as N_2 and the latter utilizing a dialkyl isocyanate alkoxy tin in the addition of a second alkoxy group to the carbamate (United States Patent No. US4436668A, 1984; World Intellectual Property Organization Patent No. WO1995017369A1, 1995).

In 1993, researchers at Bayer founded the Partial Carbonylation route (BAYER process) and patented it in the European Patent office (EP) (United States Patent No. US5233072A, 1993). This process built upon the already well-established Liquid-phase methanol oxidative carbonylation route through the addition of a molten salt mixture of CuCl and KCl (Pacheco & Marshall, 1997; Tundo & Selva, 2002). The process is a one-step reversible mechanism entailing the reaction of CO, oxygen, and methanol within the liquid phase to yield DMC and water (Kongpanna et al., 2015). A supplementary overview encompassing the reaction mechanisms of all the non-utilization processes that manufacture DMC is portrayed in Table 2.3.

The production of commercial MeOH, exhibiting a snowballing capacity globally, spans the whole globe generating $55 billion in economic activity per annum (Methanol Institute, 2015). Generating over 90,000 jobs across the globe, there exists over 90 operational MeOH plants yielding in a collective production capacity of approximately 110 million metric tons annually (Methanol Institute, 2015). This is to be expected as a result of the immense variety of applications within which MeOH plays a crucial role in. As a result, a large emphasis has been placed on

researching and optimizing diverse routes that could further enhance the contemporary approaches of synthesizing MeOH.

MeOH, as a final chemical product, has widely been utilized in pharmaceuticals, dyes, plastics, building activities, automobile production, panelboard substitution for solid wood, paints, and rubbers fibers (Huang & Tan, 2014). Serving as a testament to its versatility, MeOH can also be utilized as an energy product alleviating the current dependence on fossil fuels. Furthermore, its energetic efficiency is greater than that of its subsequent derivatives (Huang & Tan, 2014). Consequently, MeOH plays a pivotal role in serving as the feedstock for the commercial production of DMC and DME (Babad & Zeiler, 1973; Keller et al., 2010; Mbuyi, Scurrell, Hildebrandt, & Glasser, 2012). Moreover, the evolving energy applications for MeOH account for approximately 40% of the rising MeOH consumption (Methanol Institute, 2015).

Generally, MeOH is commercially manufactured through undertaking various routes involved with the reforming of fossil-derived syngas over metal based catalysts (Huang & Tan, 2014; Olah, 2013). Originally, Topsoe's conventional technology was utilized to manufacture syngas in MeOH plants. The processing path involved the two-step reforming approach to synthesize the necessary syngas. Moreover, the layout involved adiabatic prereforming, tubular reforming, and oxygen-blown secondary reforming (Dahl, Christensen, Winter-Madsen, & King, 2014). Notably, partial oxidation of CH_4 and additional steam reforming of CH_4 takes place simultaneously within the layout proposed by Dahl et al. (2014). Thereafter, the obtained syngas is sent forth to the methanol synthesis process where the hydrogenation of CO takes place so as to obtain commercial MeOH. Remarkably, the inherent processing path possesses the ability to integrate and utilize CO_2 as a raw material. In addition, numerous studies have been conducted, with variable alternatives being proposed, where the introduction of CO_2 is undertaken to manufacture high-grade MeOH.

Table 2.3 List of conventional process routes and reaction mechanisms for DMC production

Process route	Reaction	
Liquid-phase methanol oxidative carbonylation route (Enichem route)	$2CuCl + CH_3OH + \frac{1}{2}O_2 \rightarrow 2Cu(OCH_3)Cl + H_2O$	(R2.1)
	$2Cu(OCH_3)Cl + CO \rightarrow (CH_3O)_2CO + 2CuCl$	(R2.2)
Partial Carbonylation route (BAYER process)	$2CH_3OH + CO + \frac{1}{2}O_2 \rightarrow (CH_3O)_2CO + H_2O$	(R2.3)
Phosgene route (Phosgenation)	$COCl_2 + CH_3OH \rightarrow ClCOOCH_3 + HCl$	(R2.4)
	$ClCOOCH_3 + CH_3OH \rightarrow (CH_3O)_2CO + HCl$	(R2.5)
Urea Alcoholysis route	$NH_2CONH_2 + CH_3OH \rightarrow NH_2COOCH_3 + NH_3$	(R2.6)
	$NH_2COOCH_3 + CH_3OH \rightarrow (CH_3O)_2CO + NH_3$	(R2.7)

2.4 Carbon Dioxide Capture and Utilization Processes

In the 1990's, the two-step transesterification route of EC with methanol was industrialized by Texaco (America), Shell (Holland) and various other companies in China (Keller et al., 2010; United States Patent No. US4661609A, 1987; Tan et al., 2018). Utilization of CO_2 takes place in the reaction to synthesize EC and is undertaken by the cycloaddition of CO_2 to ethylene oxide (EO) (Kim, Kim, Koh, & Park, 2010; Watile, Deshmukh, Dhake, & Bhanage, 2012). Ensuing that, transesterification of the EC with methanol yields ethylene glycol (EG) and DMC (Jagtap, Bhor, & Bhanage, 2008; J.-Q. Wang et al., 2012; Yang, He, Dou, & Chanfreau, 2010). One advantage of manufacturing DMC through this route, is the production of the commercial byproduct EG which has many uses as a chemical raw material in the production of antifreeze, plasticizers, unsaturated polyester resins, polyester fibers, and surface active agents (Song, Jin, Kang, & Chen, 2013; Yue, Zhao, Ma, & Gong, 2012).

Identical to the two-step transesterification route of EC with methanol, the same procedure can be undertaken with the use of propylene carbonate (PC) to yield DMC (Keller et al., 2010; United States Patent No. US5436362A, 1995; Tan et al., 2018). However, in this approach the transesterification of the PC intermediate with methanol produces DMC and propylene glycol (PG) as opposed to EG (Jagtap, Raje, Samant, & Bhanage, 2007; Li, Xiao, Xia, & Hu, 2004; Watile et al., 2012). In general, both these transesterification routes suffer from high costs, adverse conditions dealing with the rate liming step, and the harmful source of propylene and ethylene oxide as a reactant source to the process (J.-Q. Wang et al., 2012; China Patent No. CN106957283A, 2017; China Patent No. CN206418062U, 2017).

Another approach of utilizing CO_2 to manufacture DMC is made possible by integrating the aforementioned urea alcoholysis route with the conventional approach of utilizing CO_2 to synthesize urea (Kongpanna et al., 2016, 2015). Kongpanna et al. (2016) depicts an optimal base case framework outlining this integration in two sections consisting of the CO_2 utilization section and the DMC synthesis section. The CO_2 utilization section embodies the conventional approach of manufacturing urea which occurs in the urea synthesizer. The first step, arising within the urea synthesizer, converts the CO_2 and NH_3 feed into the desired urea product with a water byproduct also being produced (United States Patent No. US4321410A, 1982; United States Patent No. US6632846B2, 2003). Subsequently, water, excess NH_3, and excess CO_2 are removed from the urea stream before reacting with the

additional methanol in order to synthesize DMC. Identical to the urea alcoholysis route, DMC is synthesized in a two-step reaction mechanism with a methyl carbamate intermediate produced in the first step, and DMC with an NH_3 byproduct generated in the second step (Lin, Yang, Sun, Wang, & Wang, 2004; Sun, Yang, Wang, Wang, & Lin, 2005). Table 2.4 vividly shows the reaction mechanisms of all the utilization processes mentioned above.

Utilizing CO_2 in the synthesis of MeOH is an environmentally appealing alternative to the use of CO as previously deliberated within the conventional approach. Initially, the first processing path consists of manufacturing syngas by converting CH_4, steam, and CO_2 to syngas (Roh, Lee, & Gani, 2016). Thereafter, the obtained syngas is fed to the MeOH synthesis reactor to manufacture the commercial MeOH product. In order to manufacture syngas, three chief approaches, involving multiple reforming steps, may be employed. These consist of steam-methane reforming (SMR), partial oxidation, and auto-thermal reforming (Dahl et al., 2014; Milani, Khalilpour, Zahedi, & Abbas, 2015). For example, the SMR approach proceeds in two steps with the prior step entailing the reforming reaction step. Initially, the reforming reaction step is strongly endothermic necessitating energy to be supplied for the reaction to proceed forward. Generally, the excess heat is typically supplied through means of an external source (Ott et al., 2012). Thereafter, the ensuing water-gas shift reaction step follows. Notably, the subsequent water-gas shift reaction step does not necessitate any energy and is slightly exothermic.

Thereafter, the obtained syngas product is syphoned to the MeOH synthesis reactor. Within the reactor, three overall reactions typically transpire so as to acquire the commercial MeOH product. These consist of the hydrogenation of CO, hydrogenation of CO_2, and the reverse water-gas shift (RWGS) reaction (Milani et al., 2015; Roh, Frauzem, Nguyen, Gani, & Lee, 2016). Typically, industrial reactors that manufacture MeOH vary in the reactor design (Milani et al., 2015). For instance, 60% of the worldwide MeOH production is undertaken within quench adiabatic reactors (Ott et al., 2012). Whereas, 30% of the global MeOH production is manufactured utilizing quasi-isothermal reactors (Ott et al., 2012). Furthermore, depending on the given process specifications and costing economics, there may exist an optimal reactor design.

Table 2.4 List of utilization process routes and reaction mechanisms for DMC production

Process route	Reaction	
Transesterification route (ethylene carbonate with methanol)	$C_2H_4O + CO_2 \rightarrow (CH_2O)_2CO$	(R2.8)
	$(CH_2O)_2CO + 2CH_3OH \rightarrow (CH_3O)_2CO + (CH_2OH)_2$	(R2.9)
Transesterification route (propylene carbonate with methanol)	$C_3H_6O + CO_2 \rightarrow CH_3(C_2H_3O_2)CO$	(R2.10)
	$CH_3(C_2H_3O_2)CO + 2CH_3OH \rightarrow (CH_3O)_2CO + C_3H_8O_2$	(R2.11)
Urea route (Integration approach)	$2NH_3 + CO_2 \rightarrow NH_2CONH_2 + H_2O$	(R2.12)
	$NH_2CONH_2 + CH_3OH \rightarrow CH_3OCONH_2 + NH_3$	(R2.13)
	$CH_3OCONH_2 + CH_3OH \rightarrow (CH_3O)_2CO + NH_3$	(R2.14)

Table 2.5 List of utilization process routes and reaction mechanisms for MeOH production

Process route	Reaction	
Hydrogenation of CO	$CO + 2H_2 \leftrightarrow CH_3OH$	(R2.15)
Hydrogenation of CO_2	$CO_2 + 3H_2 \leftrightarrow CH_3OH + H_2O$	(R2.16)
RWGS	$CO_2 + H_2 \leftrightarrow CO + H_2O$	(R2.17)

Chapter 3: Model Development

3.1 Dynamic LCA

Levasseur et al. (2010) developed the dynamic LCA framework, proceeding to analyze various renewable fuels. The general procedure entailing the developed dynamic LCA framework is discussed within this section. Adding to that, the methodology incorporating the dynamic LCA framework is embedded within the excel file termed DynCO_2 version 2.0. DynCO_2, being updated numerous times since originating in 2010, was last updated in May 2016. The final update permitted multiple variations to transpire within the excel file, from explicit values to naming schemes, all in accordance with the IPCC fifth assessment report (IPCC, 2013). Consequently, dynCO_2 is contemporary with the most recent IPCC report, allowing for superior accuracy to be attained within the environmental results being generated.

Initially, the first step of any given LCA approach is to define a coherent and comprehensible goal and scope definition as dictated by the updated standards from the ISO 14040 and 14044 (International Organization for Standardization, 2006b, 2006a). Additional information regarding the initial step, where an in-depth deliberation ensues, can be located within the Introduction section 1.3. Prominently, the LCI and LCIA segments will vary significantly from the traditional static LCA. This is largely attributed to the introduction and implementation of time-dependent factors within the quantitative analysis.

In general, the contemporary approach undertaken within the LCIA segment is to utilize the GWP as adopted by the IPCC (Ramaswamy et al., 2001). Thereafter, the GWP will be utilized as a characterization factor for the subsequent GWI assessment. As previously aforementioned, GWP is defined as the infrared radiation absorbed by a given GHG, in a time horizon, relative to the infrared radiation absorbed by a reference gas. The conventional reference gas is typically selected to be CO_2, and this is commonly employed by the IPCC and other environmental entities. Similarly, CO_2 was chosen and employed, within the dynamic LCA framework, as the reference gas for the GWP classification.

In order to obtain the mathematical expression of GWP, it is essential to initially define some of the intrinsic variables. These variables are defined as follows: a is given as the instantaneous radiative forcing per unit mass increase in the atmosphere (in $\frac{W}{kg*m^2}$), $C(t)$ is the time-dependent atmospheric load of the released gas, i depicts a given GHG present within the inventory, and r is the reference gas chosen to be CO_2 (Levasseur et al., 2010). Thereafter, absolute global warming potentials (AGWPs) are developed in equations (3.1) and (3.2). Taking the ratio of the AGWP developed in equation (3.1) by the AGWP generated in equation (3.2) yields in the required GWP of a specified GHG. Adding to that, the final mathematical expression of the required GWP is portrayed in equation (3.3) where TH is defined as the selected time horizon.

$$AGWP_i{}^{TH} = \int_0^{TH} a_i[C_i(t)dt] \tag{3.1}$$

$$AGWP_{CO_2}{}^{TH} = \int_0^{TH} a_r[C_r(t)dt] \tag{3.2}$$

$$GWP_i{}^{TH} = \frac{AGWP_i{}^{TH}}{AGWP_{CO_2}{}^{TH}} = \frac{\int_0^{TH} a_i[C_i(t)dt]}{\int_0^{TH} a_r[C_r(t)dt]} \tag{3.3}$$

Before proceeding to develop the mandatory DCFs, the atmospheric load must be defined for all given pulse emissions. Notably, the definition and mathematical formulation of the atmospheric load ensuing a pulse emission of CO_2 will differ from all the other GHGs under consideration. Furthermore, this is vividly depicted in equation (3.4) where the atmospheric load following a pulse emission of CO_2 ($C_{r=CO2}(t)$) is defined through the Bern Carbon Cycle-Climate (BCCC) model utilizing a background CO_2 concentration of 378 ppm (Forster et al., 2007). This model is primarily employed to predict the ultimate fate of the CO_2 emissions by accounting for carbon sink dynamics (Joos et al., 2001). Moreover, a visual representation of equation (3.4) is portrayed in Figure (3.1). As a testament to the hazards associated with CO_2, Figure (3.1) depicts the sluggish residual effects of CO_2 when emitted to the atmosphere.

$$C(t) = a_o + \sum_{i=1}^{3} a_i * e^{-\frac{t}{\tau_i}} \tag{3.4}$$

$$a_o = 0.217, a_1 = 0.259, a_2 = 0.338, a_3 = 0.186$$
$$\tau_1 = 172.9\ years, \tau_2 = 18.51\ years, \tau_3 = 1.186\ years$$

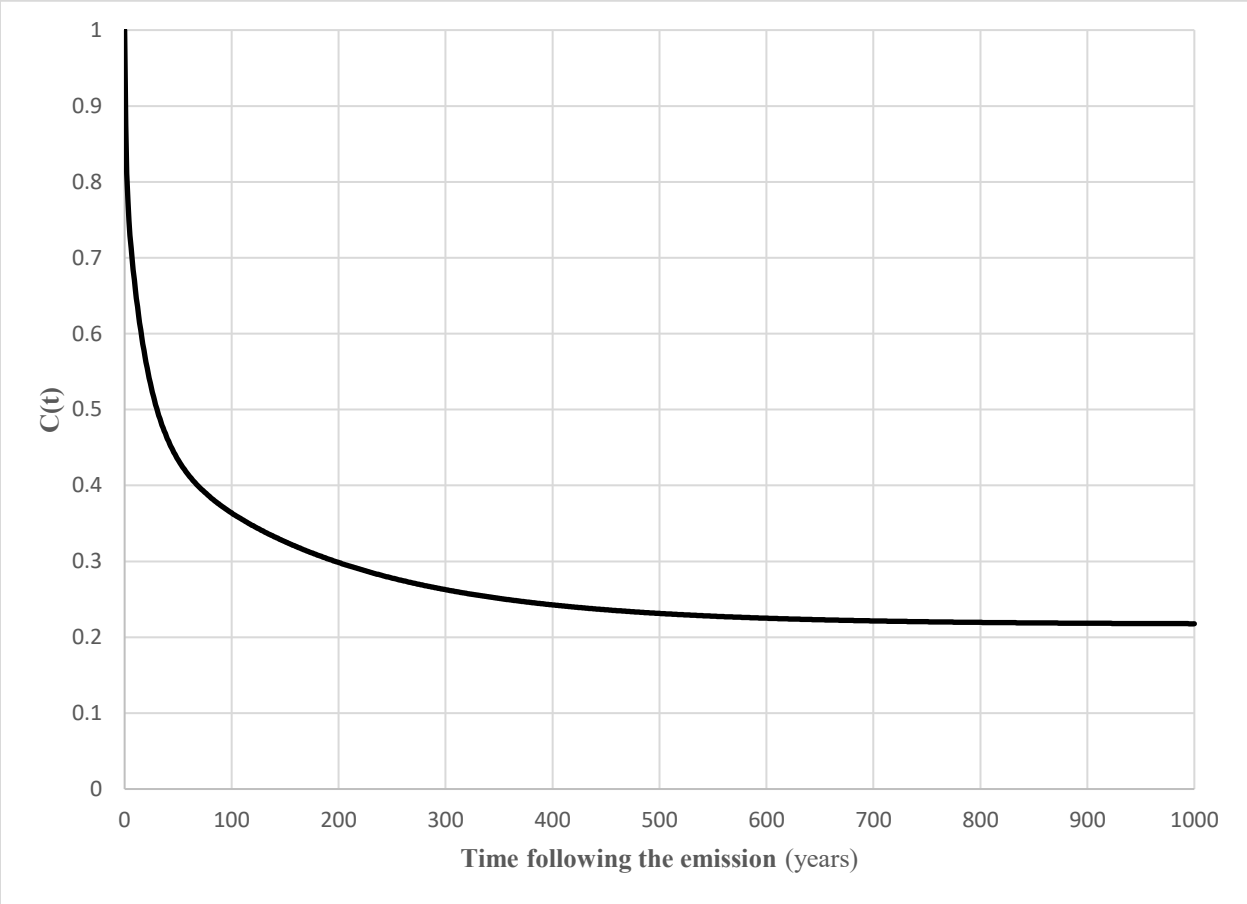

Figure 3.1 BCCC model utilizing a background CO_2 concentration of 378 ppm depicted over 1000 years

However, this equation will not suffice for all other GHGs analyzed within the domain of the dynamic LCA framework. Therefore, a first-order decay equation will be utilized to encompass the atmospheric load succeeding a given pulse emission. Significantly, the inverse of the kinetic constant will be utilized to signify the adjusted lifetime termed τ (Shine, Berntsen, Fuglestvedt, Skeie, & Stuber, 2007). The mathematical formulation for the time-dependent atmospheric load for all the other GHGs is portrayed in equation (3.5):

$$C(t) = e^{-\frac{t}{\tau}} \tag{3.5}$$

Forster et al. (2007) illustrates the intrinsic details regarding the adjusted lifetimes for various GHGs. Moreover, details related to the instantaneous radiative forcing per unit mass increase in the atmosphere for each gas is also depicted. In addition, Forster et al. (2007) also provides an in-depth report related to obtaining these values whilst taking into account any indirect effects.

A beneficial attribute of the dynamic LCA is that it assesses the impact of the life cycle GHG emissions on radiative forcing by taking into account the instance when a given emission transpires. Moreover, a dynamic inventory allows for a temporal distribution of the given emissions within the LCA framework. Possessing all the compulsory tools, one may now proceed to compute the imperative DCFs. Initially, the life cycle is divided into equal one-year time steps to acquire the instantaneous DCF. Adding to that, the amount of each pollutant emitted is obtained for each year and each GHG. Thereafter, the dynamic inventory is then evaluated with the DCFs, for each time step, embedded within the integral of the radiative forcing formulation given in equation (3.6). DCFs obtained through this methodology embody the cumulative radiative forcing per unit mass of GHG emitted in the atmosphere since the initial emission. Hence, equation (3.6) represents the atmospheric radiative forcing t years after the emission of 1 kg of GHG i (in $\frac{W}{kg*m^2}$).

$$DCF_i(t)_{instantaneous} = \int_{t-1}^{t} a_i[C_i(t)]\, dt \tag{3.6}$$

Ensuing this, the cumulative DCF is computed through equation (3.7). The chief principal here is to take the AGWP equation for each individual GHG and integrate it incessantly through time as depicted in equation (3.7). Notably, the cumulative DCF at time t can be obtained by adding the instantaneous DCFs of the preceding years.

$$DCF_i(t)_{cumulative} = \int_{0}^{t} a_i[C_i(t)]\, dt \tag{3.7}$$

Given the aforementioned DCF equations, it is now plausible to compute the time-dependent impact on global warming. Initially, the life cycle is split into one-year time intervals, and this is followed by the summation of all the given emissions for each GHG occurring at every time step. This results in the dynamic inventory for each given GHG. Thereafter, the essential GWIs are attained by combining the dynamic inventory for each GHG with the yearly computed DCFs. For example, the mathematical expression for the instantaneous impact on radiative forcing is shown below in equation (3.8):

$$GWI_{instantaneous}(t) = \sum_{i} GWI_i(t) = \sum_{i} \sum_{j=0}^{t} [g_i]_j * [DCF_i]_{t-j} \tag{3.8}$$

In equation (3.8), DCF represents the instantaneous dynamic characterization factor developed in equation (3.6), g is the inventory result (in kg), i depicts every given GHG present within the inventory, and t represents the time horizon under consideration. In order to attain the instantaneous impact on GW at time t instigated by a given GHG i, equation (3.8) indicates that the total dynamic inventory result transpiring at time t must be multiplied by the DCF computed at time zero. Thereafter, the instantaneous impact on GW at time t-1 is added and so on, until finally the impact on GW occurring at time zero is added on. The final result attained is the instantaneous impact on radiative forcing caused by the life cycle emissions from time zero to time t (in $\frac{W}{m^2}$). Remarkably, the result attained depicts the increase in radiative forcing at time t instigated by every discrete GHG emission over the course of all the life cycle processes from the beginning of the life cycle.

The two other impacts on global warming, both cumulative and relative, can be computed via the utilization of equation (3.8). Hence, the cumulative impact on radiative forcing can be computed at time t by summing up the instantaneous impacts on radiative forcing of the preceding years. Equation (3.9) depicts the mathematical formualtion for the cumulative impact on radiative forcing:

$$GWI_{cumulative}(t) = \sum_{j=0}^{t} GWI_{inst}(j) \tag{3.9}$$

As previously defined, the relative impact on radiative forcing is the ratio of the life cycle cumulative impact over the cumulative impact of a 1 kg CO_2 pulse-emission at time zero. Equation (3.10) represents the mathematical expression for the relative impact on radiative forcing:

$$GWI_{relative}(t) = \frac{GWI_{cum}(t)}{\int_0^{TH} a_r[C_r(t)dt]} \tag{3.10}$$

In equation (3.10), r is defined as the reference gas, which was previously selected as CO_2, and the denominator represents the cumulative DCF of CO_2. Additional information regarding the interpretation of the dynamic LCA framework GWI results can be located in the Introduction section 1.4 where a detailed deliberation ensues. The DynCO_2 excel file will always compute these three GWI for any given time period. Thus, the dynamic LCA framework provides a variety of tools that can be utilized appreciably in sensitivity testing assessments.

3.2 Conventional Processes and Base Case

Initiating the analysis, the base case scenario will encompass the model which encapsulates the various conventional processes. Furthermore, the base case scenario will entail the analysis of an isolated 620 MW NGCC PP unit, the conventional approach of manufacturing the desired product, and the final disposal of the manufactured product. Therefore, the scope of generating a well-grounded model will primarily revolve around three focal systems. Initially, the model generated will take into account a CO_2 balance around each system individually. Ensuing this, the net CO_2 emitted will be attained from a summation of the three principal systems. Notably, the addition of the PP unit and the final disposal of the generated product is primarily undertaken to represent a scenario that is identical to the one transpiring in reality. Moreover, the principal aim is to provide a vivid and comprehensible environmental assessment, one that hinders any underlying bias within the final results.

Primarily, a model schematic is developed to portray a vivid representation of the three focal systems. Figure 3.2 illustrates the general model framework within which the flow of CO_2 transpires. Moreover, every arrow within a given system represents a transitional flow of either an input or an output. The $Electricity$ arrow illustrates the net output of the product generated within system 1 on an annual basis. In general, this is typically the net electricity generated within the vicinity of the PP unit. Similarly, the $Product$ arrow represents the net output of the manufactured product on an annual basis within the vicinity of system 2. Generally, this is the mass flow rate of the commercial product manufactured via the conventional process.

Firstly, system 1 will consist of a generic 620 MW NGCC PP unit with two outputs being produced on an annual basis. Adding to that, system 2 will comprise the conventional process, manufacturing the commercial product, with two main outputs also being generated on an annual basis. Lastly, system 3 will entail the final disposal of the manufactured product with CO_2 being emitted into the atmosphere.

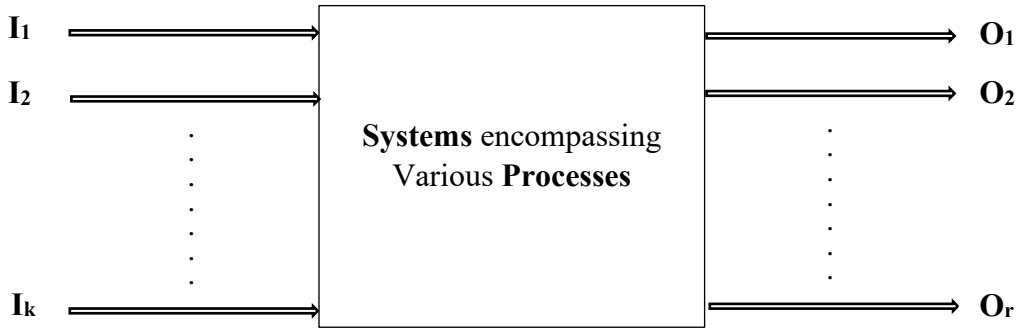

Figure 3.2 General model framework

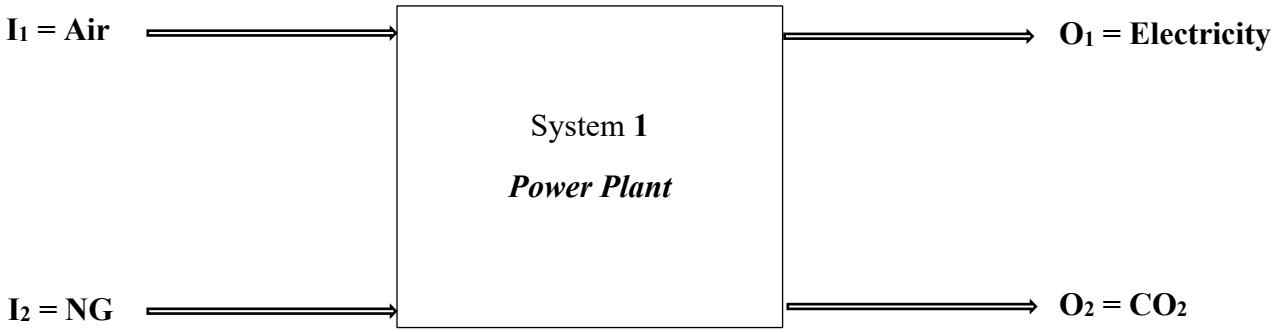

Figure 3.3 Base case model encapsulating system 1

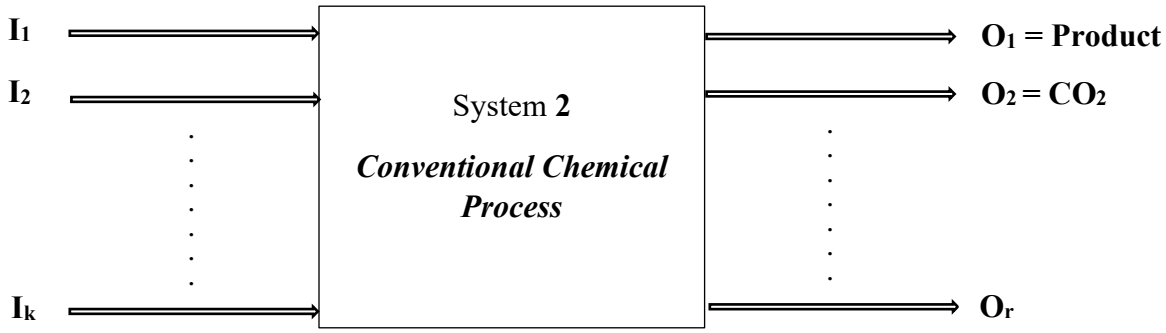

Figure 3.4 Base case model encapsulating system 2

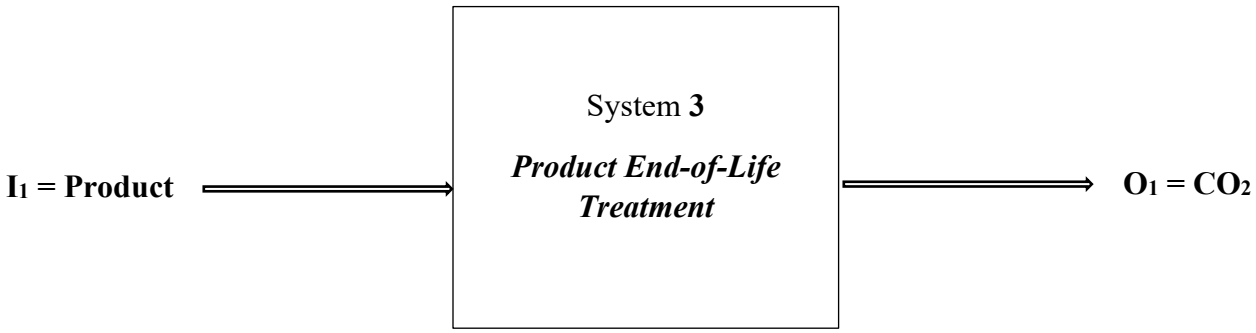

Figure 3.5 Base case model encapsulating system 3

Before proceeding to develop the obligatory equations, it will be essential to make several key assumptions related to the operating conditions within the base case model. Hence, we will assume that:

- The electricity production is constant at 620 MW, within the domain of system 1, for the NGCC PP unit.
- The PP unit produces a singular product of 620 MW of power.
- The amount of CO_2 emitted by burning NG is estimated via the US Energy Information Administration (EIA) guidelines (EIA, 2019).
- The net electricity produced by a conventional NGCC PP is adopted from the EIA's updated report on electricity generating plants (Wells, 2013).
- The production rate of the product manufactured within system 2 is constant.
- The manufactured product generated within the conventional process is singular in nature.
- The product is disposed of in consecutive and equal time steps within system 3.
- The time steps within which the final disposal of the product occurs in system 3 is identical to the integrated utilization scenario.
- The fractions representing the CO_2 emitted will be constant with respect to the time horizon.
- All CO_2 emissions generated are accounted for at the end of each life cycle year.
- The plants, intrinsic within systems 1 and 2, operate within a 20-year life time horizon.

Given these assumptions, it is now plausible to develop the mandatory equations for the base case scenario. Initially, each system is analyzed individually with an equation representing the segregated system. As previously aforementioned, system 1 consists of a 620 MW NGCC PP unit encompassing two outputs on an annual basis. Therefore, equation (3.11) is developed to represent n number of PP units operating within the domain of system 1. In addition, ω_i represents the emission intensity with respect to the given PP unit, $\dot{x}_i$ depicts the output of product x_i on an annual basis, χ_i portrays the fraction of carbon dioxide emitted within the domain of the given PP unit, and E_1 signifies the amount of carbon dioxide emitted on annual basis within system 1.

$$E_1(t) = \sum_{i=1}^{n} \omega_i(t)\dot{x}_i(t)\chi_i(t) \tag{3.11}$$

Thereafter, system 2 is scrutinized with equation (3.12) being developed to signify m conventional processes occurring within this domain. Moreover, α_i signifies the emission intensity with respect to the given conventional process, $\dot{y}_\iota$ portrays the output of the manufactured product y_i on an annual basis, and E_2 depicts the amount of carbon dioxide emitted on annual basis within system 2.

$$E_2(t) = \sum_{i=1}^{m} \alpha_i(t)\dot{y}_\iota(t) \tag{3.12}$$

Ensuing this, system 3 is analyzed and equation (3.13) is developed to represent the final disposal of the commercial product. In addition, d is defined as the number of times product y_i is disposed of, t is the current time being considered for the analysis, $t_{e_{ij}}$ is the exact time corresponding to the disposal of product y_i, β_{ij} is the amount of carbon dioxide (in kg) generated by disposing 1 kg of product y_i, and E_3 is the amount of carbon dioxide emitted on annual basis within system 3. The variable $\dot{y}_\iota * u\left(t - t_{e_{ij}}\right)$ depicts a discontinuous step function whose value is $\dot{y}_\iota$ for positive arguments and zero for all negative arguments. Specifically, the positive argument depicts a scenario where t is greater or equivalent to $t_{e_{ij}}$, and the negative argument represents all t less than $t_{e_{ij}}$. Therefore, the positive argument represents the time steps within which the

final disposal of product y_i occurs. Equation (3.14) illustrates the discontinuous step function defining the positive and negative arguments:

$$E_3(t) = \sum_{j=1}^{d} \sum_{i=1}^{m} \dot{y}_i * u\left(t - t_{e_{ij}}\right) \beta_{ij}(t) \tag{3.13}$$

$$\dot{y}_i * u\left(t - t_{e_{ij}}\right) = \begin{cases} 0, & t < t_{e_{ij}} \\ \dot{y}_i, & t \geq t_{e_{ij}} \end{cases} \tag{3.14}$$

In order to maintain consistency, the aforementioned assumption related to the third system proves to be essential when conducting the comparison-based analysis with the integrated utilization scenario. Furthermore, this will obstruct any resultant bias presented within the final results which could influence the generated conclusions. Additionally, we will assume that the scope of the analysis will encompass a rudimentary scenario entailing the incorporation of one PP unit and one conventional process. Overall, the work conducted within this thesis will revolve around this preliminary assumption. Hence, equations (3.11), (3.12), and (3.13) will be further simplified into equations (3.15), (3.16), and (3.17) respectively:

$$E_1(t) = \omega_1(t)\dot{x}_1(t)\chi_1(t) \tag{3.15}$$

$$E_2(t) = \alpha_1(t)\dot{y}_1(t) \tag{3.16}$$

$$E_3(t) = \sum_{j=1}^{d} \dot{y}_1 * u\left(t - t_{e_{1j}}\right) \beta_{1j}(t) \tag{3.17}$$

After analyzing the systems individually, we proceed to further compute the $Net\ E$ which signifies the net CO_2 emissions on an annual basis within the base case scenario. This will be undertaken by summing up equations (3.15), (3.16), and (3.17) to obtain equation (3.18):

$$Net\ E(t) = \omega_1(t)\dot{x}_1(t)\chi_1(t) + \alpha_1(t)\dot{y}_1(t) + \sum_{j=1}^{d} \dot{y}_1 * u\left(t - t_{e_{1j}}\right) \beta_{1j}(t) \tag{3.18}$$

In order to standardize the equation, all variables will be represented in terms of the current time being considered for the analysis. Therefore, a will be introduced and implemented into equation (3.18) to obtain a standardized equation as portrayed by equation (3.19). Moreover, variable a embodies the time steps within which the disposal of product y_1 will occur. Given the aforementioned assumptions, variable a will maintain a zero value when product y_1 is being disposed of. However, a negative value will be attained for any delay that occurs before finally disposing the product.

$$Net\ E(t) = \omega_1(t)\dot{x}_1(t)\chi_1(t) + \alpha_1(t)\dot{y}_1(t) + \sum_{j=1}^{d} \dot{y}_1 * u\big(a(t)\big)\,\beta_{1j}(t) \tag{3.19}$$

Taking into account the previous assumptions, further modifications will be allocated to equation (3.19). Therefore, all fractions presented within equation (3.19) are deemed constant with respect to the time horizon being analyzed:

$$Net\ E(t) = \omega_1(t)\dot{x}_1(t)\chi_1 + \alpha_1(t)\dot{y}_1(t) + \sum_{j=1}^{d} \dot{y}_1 * u\big(a(t)\big)\,\beta_{1j} \tag{3.20}$$

The final equation that will be utilized in the analysis of the base case scenario is portrayed above in equation (3.20). Consequently, the net emissions within a given base case scenario will be computed via equation (3.20). Thereafter, these values will be utilized as an input to the dynamic LCA framework so as attain the desired environmental assessment. Table 3.1 summarizes all the variables and their respective descriptions deliberated within the base case model development:

Table 3.1 Summary of variables and their descriptions for the base case scenario

Variables	Description
$\boldsymbol{a}$	The variable depicting the time steps within which the disposal of product y_i will occur
$\boldsymbol{d}$	The number of times product y_i is disposed of within system 3
$\boldsymbol{E_1}$	The amount of carbon dioxide emitted on an annual basis in system 1 (in kg CO_2)
$\boldsymbol{E_2}$	The amount of carbon dioxide emitted on an annual basis in system 2 (in kg CO_2)
$\boldsymbol{E_3}$	The amount of carbon dioxide emitted on an annual basis in system 3 (in kg CO_2)
$\boldsymbol{k}$	The number of inputs into a given system
$\boldsymbol{m}$	The number of conventional processes in the domain of system 2
$\boldsymbol{n}$	The number of power plant units in the domain of system 1
$\boldsymbol{Net\ E}$	The net carbon dioxide emission on an annual basis (in kg CO_2) in the overall system (systems 1, 2, and 3)
$\boldsymbol{r}$	The number of outputs from a given system
$\boldsymbol{t}$	The current time being considered for the analysis (in years)
$\boldsymbol{t_{e_{ij}}}$	The exact time corresponding to the disposal of product y_i (in years)
$\boldsymbol{\dot{x}_i}$	The output of product x_i on an annual basis in system 1 (in MWh)
$\boldsymbol{\dot{y}_\iota}$	The output of the manufactured product y_i on an annual basis in system 2 (in kg y_i)
$\boldsymbol{\alpha_i}$	An emission intensity with respect to the conventional process in system 2 (in $\frac{kg\ CO_2}{kg\ y_i}$)
$\boldsymbol{\beta_{ij}}$	The amount of carbon dioxide generated by disposing 1 kg of product y_i in the domain of system 3 (in $\frac{kg\ CO_2}{kg\ y_i}$)
$\boldsymbol{\chi_i}$	The fraction of carbon dioxide emitted within the domain of the power plant unit in system 1
$\boldsymbol{\omega_i}$	An emission intensity with respect to the power plant unit in system 1 (in $\frac{kg\ CO_2}{MWh}$)

3.3 Utilization Processes and Integrated Case

Following the base case model development, the integrated case, embodying the utilization process, will be generated. The integrated case, identical to the base case scenario, will incorporate the analysis of a 620 MW NGCC PP unit and the final disposal of the manufactured product. However, the analysis of a carbon capture (CC) unit and its implementation to the PP unit will also be undertaken. Additionally, a CO_2 utilization process will be integrated to the CC unit so as to manufacture the commercial product. Hence, the scope of developing a laudable model within the integrated scenario will also revolve around three core systems. Moreover, the approach employed is analogous to the base case scenario, where an initial CO_2 balance is undertaken for each system individually. Thereafter, the net CO_2 emitted is attained by summing up the individual system values. Remarkably, the addition of the integrated PP unit and the CO_2 storage duration before final disposal, facilitated through the Dynamic LCA, is primarily undertaken to represent a scenario that is identical to a viable utilization mechanism. Conveniently, the energy required to operate the CC unit will be obtained from the steam flowing through the turbines of the PP unit. Furthermore, the advantage of utilizing the steam from the steam cycle of the PP unit will also be accompanied by the disadvantage of a net reduction in electricity production. Consequently, the de-rating of the 620 MW NGCC PP unit will be accounted for so as to obtain the same net electricity production as the base case scenario.

Three principal schematics are established to portray the systems with all the obligatory inputs and outputs transpiring within the given systems. Figure 3.6 illustrates the integrated PP and CC unit with two inputs and three outputs flowing within the domain of system 4. Similar to the base case scenario, the $Electricity$ arrow exemplifies the net electrical output generated within system 4 on an annual basis. However, there also exists two diverse flows of CO_2 occurring within system 4. The O_1 arrow depicts the fraction of CO_2 emitted to the atmosphere, whilst the O_2 arrow depicts the fraction of CO_2 syphoned from system 4 to system 5. In addition, the $Product$ arrow represents the net output of the manufactured product on an annual basis within the vicinity of system 5. The major difference between the integrated and base case scenarios is depicted within system 5 where CO_2 is now being inputted and utilized to manufacture the commercial product.

Subsequently, it is critical to incorporate the CO_2 storage duration within the analysis so as to hinder any resultant bias within the concluding results.

System 4 will account for the integrated PP and CC unit with three outputs being generated on an annual basis. In addition, system 5 will comprise of the utilization process which administers CO_2, attained from the integrated PP and CC unit, as an input to the process to manufacture the desired product. Depending on the utilization process, several byproducts may also be generated within the vicinity of system 5. Lastly, system 6 will entail the CO_2 storage duration, facilitated through the Dynamic LCA, up until the generated product is finally disposed of and CO_2 is re-emitted back into the atmosphere.

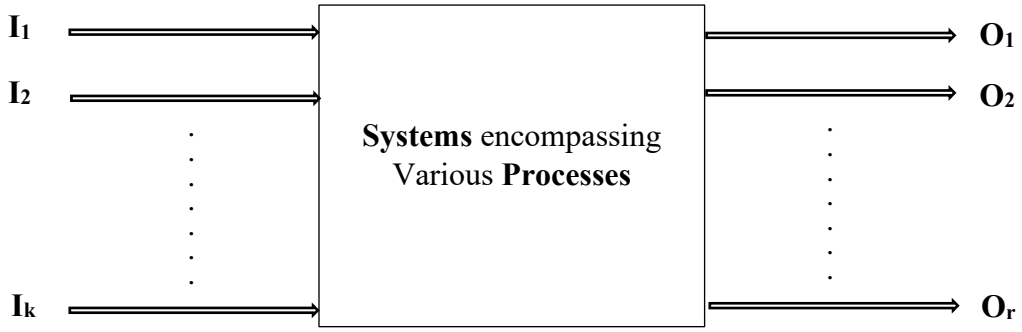

Figure 3.2 General model framework

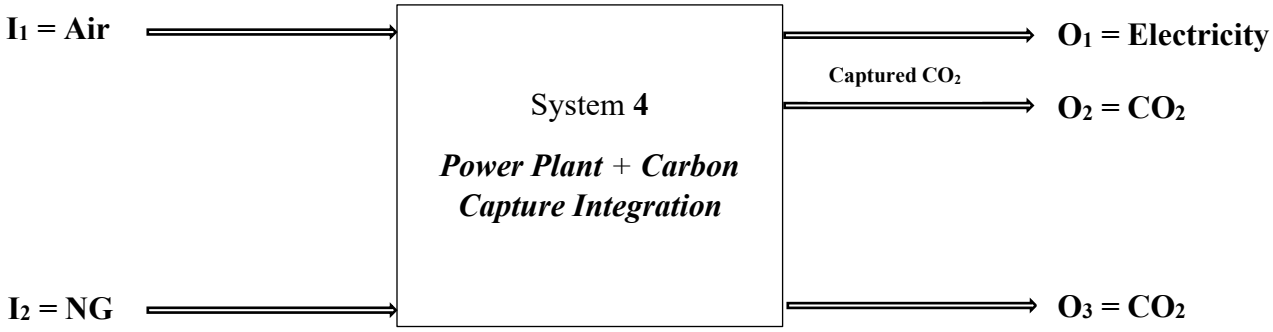

Figure 3.6 Integrated case model encapsulating system 4

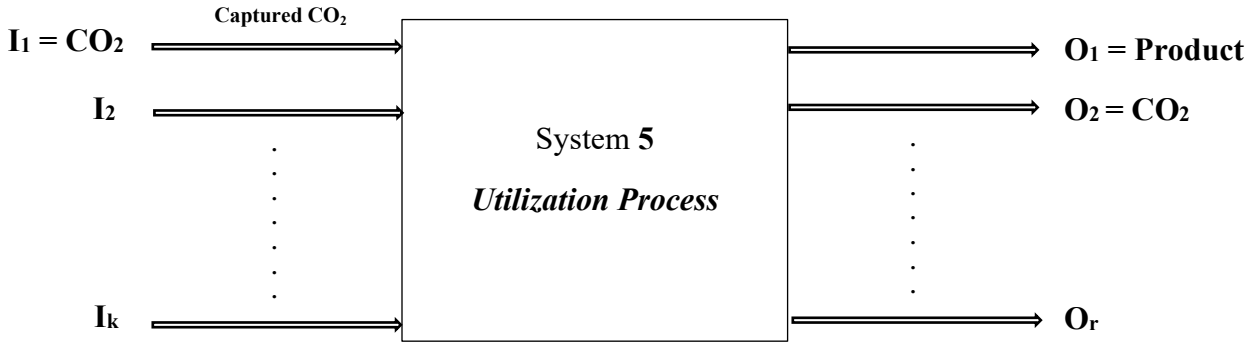

Figure 3.7 Integrated case model encapsulating system 5

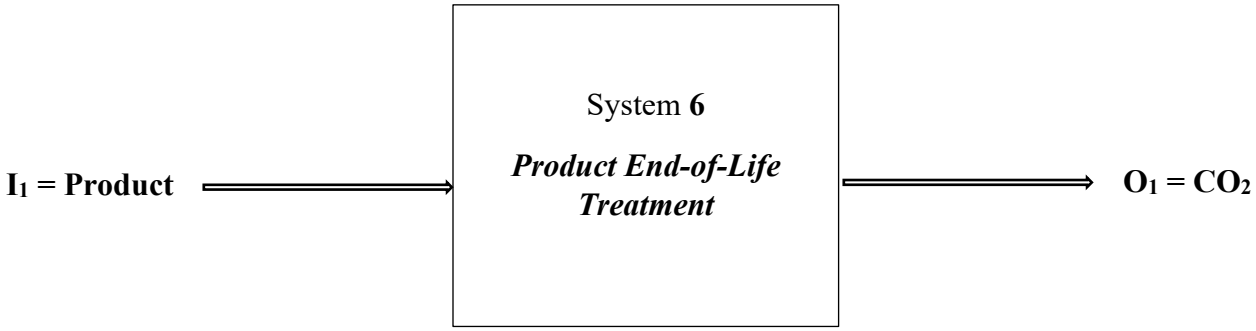

Figure 3.8 Integrated case model encapsulating system 6

As previously stated, a portion of the steam flowing within the turbines of the PP unit will be allocated to complement the energy needed to operate the CC unit. Accordingly, this results in the de-rating of the generic 620 MW NGCC PP unit. In order to attain an equivalent quantity of electricity generated in both the base and integrated cases, it is essential to account for this amount of de-rated power within the PP unit. Hence, this will be undertaken by increasing the net electricity production within the 620 MW NGCC PP unit by a specific amount so as to offset the consequences of de-rating.

The integrated 633.5 MW NGCC PP and CC unit, simulated by Rezazadeh et al. (2015), is employed to approximate the required values for the generic 620 MW NGCC PP. Therefore, the ensuing mathematical expression is formulated for the simulated 633.5 MW NGCC PP and CC

units. Initially, D, a ratio of the amount of de-rated power to the power generated by an identical stand-alone PP unit, is computed. Equation (3.21) illustrates the mathematical expression utilized in computing the aforementioned ratio for the integrated 633.5 MW NGCC PP and CC unit operating at 90% CO_2 capture. Significantly, $\dot{x}_i''$ depicts the output of product x_i , inclusive to de-rating, on an annual basis within system 4. In addition, as previously defined, $\dot{x}_i$ portrays the output of product x_i on an annual basis within system 1. Alternatively, $\dot{x}_i$ can also be defined as the net electrical output on an annual basis for a stand-alone PP unit.

$$D = \frac{\dot{x}_i - \dot{x}_i''}{\dot{x}_i} \tag{3.21}$$

Subsequently, two points, at 0% and 90% CO_2 capture, are selected so as to implement a linear interpolation plot for the integrated 633.5 MW NGCC PP and CC unit. Alongside their corresponding ratio D, these points are selected to span a wide array of various % CO_2 capture for the integrated 633.5 MW NGCC PP and CC unit. Moreover, the linear interpolation plot is employed to approximate the de-rated power for various % CO_2 capture within the generic 620 MW NGCC PP. Figure 3.9 portrays the graph utilized in obtaining the ratios for various % CO_2 capture:

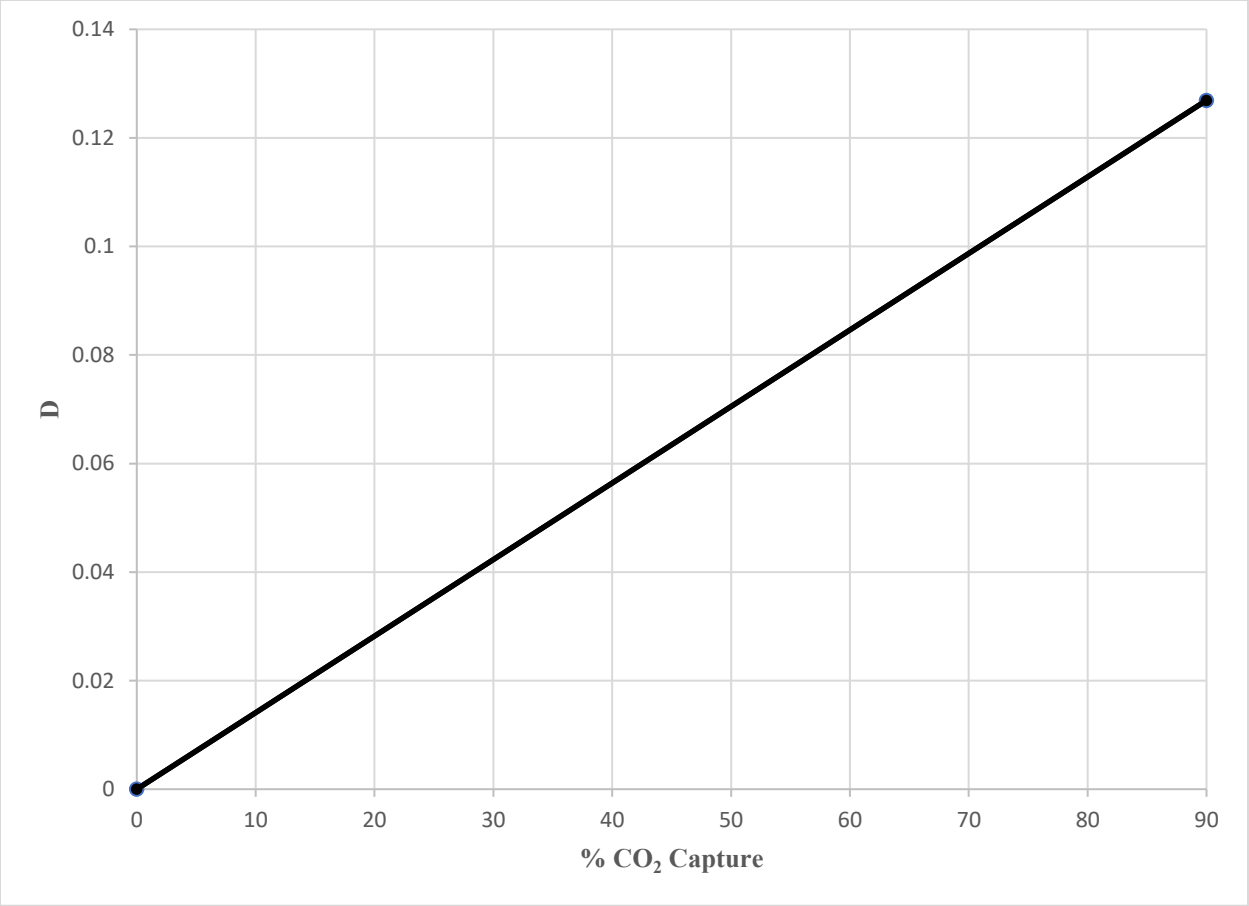

Figure 3.9 Linear interpolation of D versus % CO_2 capture for an integrated 633.5 MW NGCC PP and CC unit

Ensuing this, the obligatory de-rated power can now be computed. The amount of de-rated power, termed p, can be calculated by multiplying D by the net electrical output on an annual basis for a stand-alone PP. Equation (3.22) depicts the mathematical expression utilized in obtaining the de-rated power:

$$p = D * \dot{x}_i \tag{3.22}$$

Lastly, the output of product x_i , accounting for de-rating, within the vicinity of system 4 can be computed. Subsequently, the summation of the de-rated power with the net electrical output on an annual basis for a stand-alone PP yields in the net electrical output of product x_i , accounting

for de-rating, within the vicinity of system 4. Equation (3.23) illustrates the mathematical formulation employed to obtain $\dot{x}_i{}'$:

$$\dot{x}_i{}' = p + \dot{x}_i \tag{3.23}$$

Previously, several key assumptions, related to the operating conditions within the base case model, were implemented into the model development. Similarly, numerous identical assumptions will be made within the integrated scenario so as to acquire an impartial assessment. Hence, we will assume that:

- The electricity production is constant at 620 MW, within the domain of system 4, for the NGCC PP unit.
- The PP unit produces a singular product of 620 MW of power.
- The amount of CO_2 emitted by burning NG is estimated via the US EIA guidelines (EIA, 2019).
- The net electricity produced by a conventional NGCC PP is adopted from the EIA's updated report on electricity generating plants (Wells, 2013).
- Linear interpolation of an integrated 633.5 MW NGCC PP and CC unit, with 90% CO_2 capture rate, is utilized to approximate the de-rated power for any % CO_2 capture rate within the integrated 620 MW NGCC PP and CC unit (Rezazadeh et al., 2015).
- The exact amount of CO_2 necessary to produce the manufactured product is syphoned from system 4 to system 5.
- The production rate of the product manufactured within system 5 is constant.
- The manufactured product generated within the utilization process is singular in nature.
- The product is disposed of in consecutive and equal time steps within system 6.
- The time steps within which the final disposal of the product occurs in system 6 is identical to the conventional base case scenario.
- The temporary CO_2 storage within system 6 is initiated at year 1.
- The fractions representing the CO_2 emitted will be constant with respect to the time horizon.
- All CO_2 emissions generated are accounted for at the end of each life cycle year.

- The plants, intrinsic within systems 4 and 5, operate within a 20-year life time horizon.

Accounting for the additional assumptions, it is now plausible to advance with the development of the equations for the integrated scenario. The procedural setup is identical to the base case model development. Hence, the initial steps undertaken will scrutinize each system individually up until the concluding equations which encompass the cumulative CO_2 emissions within the overall system. System 4 incorporates an integrated 620 MW NGCC PP and CC unit generating three outputs on an annual basis. Equation 3.24 illustrates n' integrated PP and CC units operating within the vicinity of system 4. In addition, $\omega_i{}'$ represents the emission intensity with respect to the given PP unit, $\dot{x}_i{}'$ depicts the output of product x_i , accounting for de-rating, on an annual basis, $\emptyset_i$ is the fraction of carbon dioxide emitted within the domain of the given carbon capture unit, $\chi_i{}'$ portrays the fraction of carbon dioxide emitted within the domain of the given PP unit, and E_4 signifies the amount of carbon dioxide emitted on annual basis within system 4.

$$E_4(t) = \sum_{i=1}^{n'} \omega_i{}'(t)\dot{x}_i{}'(t)\chi_i{}'(t) + \omega_i{}'(t)\dot{x}_i{}'(t)(1 - \chi_i{}'(t))\emptyset_i(t) \tag{3.24}$$

Thereafter, system 5 is analyzed with equation (3.25) being established to signify m' utilization processes occurring within this domain. Additionally, $\alpha_i{}'$ signifies the emission intensity with respect to the given utilization process, $\dot{y}_i{}'$ portrays the output of the manufactured product y_i on an annual basis, and E_5 depicts the amount of carbon dioxide emitted on annual basis within system 5.

$$E_5(t) = \sum_{i=1}^{m'} \alpha_i{}'(t)\dot{y}_i{}'(t) \tag{3.25}$$

Subsequently, system 6 is analyzed and equation (3.26) is utilized to represent the final consumption of the commercial product. Furthermore, d' is defined as the number of times product y_i is disposed of, t is the current time being considered for the analysis, $t_{e_{ij}}$ is the exact time corresponding to the disposal of product y_i, $\beta_{ij}{}'$ is the amount of carbon dioxide (in kg)

generated by disposing 1 kg of product y_i, and E_6 depicts the amount of carbon dioxide emitted on annual basis within system 6. Correspondingly, equation (3.27) is defined in identical manner to the description presented within the base case scenario for equation (3.14).

$$E_6(t) = \sum_{j=1}^{d'} \sum_{i=1}^{m'} \dot{y_i}' * u\left(t - t_{e_{ij}}\right) \beta_{ij}'(t) \tag{3.26}$$

$$\dot{y_i}' * u\left(t - t_{e_{ij}}\right) = \begin{cases} 0, & t < t_{e_{ij}} \\ \dot{y_i}', & t \geq t_{e_{ij}} \end{cases} \tag{3.27}$$

Identical to the base case scenario, we will also assume that the scope of the analysis will incorporate one integrated PP and CC unit and one utilization process. Hence, equations (3.24), (3.25), and (3.26) will be further simplified into equations (3.28), (3.29), and (3.30) respectively:

$$E_4(t) = \omega_1'(t)\dot{x}_1'(t)\chi_1'(t) + \omega_1'(t)\dot{x}_1'(t)(1 - \chi_1'(t))\emptyset_1(t) \tag{3.28}$$

$$E_5(t) = \alpha_i'(t)\dot{y}_1'(t) \tag{3.29}$$

$$E_6(t) = \sum_{j=1}^{d'} \dot{y}_1' * u\left(t - t_{e_{1j}}\right) \beta_{1j}'(t) \tag{3.30}$$

Ensuing the segregated assessment, we progress to further compute the $Net\ E$ which is defined as the net CO_2 emissions on an annual basis within the overall system. This is accomplished by summing up the individual equations (3.28), (3.29), and (3.30) to acquire equation (3.31):

$$\begin{aligned} Net\ E(t) = {} & \omega_1'(t)\dot{x}_1'(t)\chi_1'(t) + \omega_1'(t)\dot{x}_1'(t)(1 - \chi_1'(t))\emptyset_1(t) + \alpha_1'(t)\dot{y}_1'(t) \\ & + \sum_{j=1}^{d'} \dot{y}_1' * u\left(t - t_{e_{1j}}\right) \beta_{1j}'(t) \end{aligned} \tag{3.31}$$

In an effort to standardize the above equation, all variables will be represented in terms of the current time being considered for the analysis. Consequently, a will be introduced and

implemented into equation (3.31) to obtain a standardized equation as portrayed by equation (3.32). Likewise, variable a symbolizes the time steps within which the disposal of product y_1 will occur. Correspondingly, the variable a is defined in a similar fashion to the description presented in the base case scenario.

$$Net\ E(t) = \omega_1'(t)\dot{x}_1'(t)\chi_1'(t) + \omega_1'(t)\dot{x}_1'(t)(1-\chi_1'(t))\emptyset_1(t) + \alpha_1'(t)\dot{y}_1'(t) + \sum_{j=1}^{d'} \dot{y}_1' * u(a(t))\,\beta_{1j}'(t) \quad (3.32)$$

Further modifications to equation (3.32) are presented within equation (3.33), where the expansion of the second term on the right-hand side transpires. This is undertaken so as to set up the equation for the mathematical procedures that will ensue. Moreover, the principal objective is to simplify the equation by grouping any identical variables intrinsic within the right-hand side of the equation.

$$Net\ E(t) = \omega_1'(t)\dot{x}_1'(t)\chi_1'(t) + [\omega_1'(t)\dot{x}_1'(t)\emptyset_1(t) - \chi_1'(t)\omega_1'(t)\dot{x}_1'(t)\emptyset_1(t)] + \alpha_1'(t)\dot{y}_1'(t) + \sum_{j=1}^{d'} \dot{y}_1' * u(a(t))\,\beta_{1j}'(t) \quad (3.33)$$

Thereafter, several steps, incorporating rudimentary mathematical procedures, succeed equation (3.33) and are illustrated in equations (3.34) and (3.35):

$$Net\ E(t) = \omega_1'(t)\dot{x}_1'(t)[\chi_1'(t) + \emptyset_1(t) - \chi_1'(t)\emptyset_1(t)] + \alpha_1'(t)\dot{y}_1'(t) + \sum_{j=1}^{d'} \dot{y}_1' * u(a(t))\,\beta_{1j}'(t) \quad (3.34)$$

$$Net\ E(t) = \left(\omega_1'(t)\dot{x}_1'(t)\left[\emptyset_1(t) + \chi_1'(t)\left(1-\emptyset_1(t)\right)\right]\right) + \alpha_1'(t)\dot{y}_1'(t) + \sum_{j=1}^{d'} \dot{y}_1' * u(a(t))\,\beta_{1j}'(t) \quad (3.35)$$

Accounting for the aforementioned assumptions, supplementary alterations will be allocated to equation (3.35). Consequently, all fractions presented within equation (3.35) are deemed constant with respect to the time horizon analyzed yielding equation (3.36):

$$Net\ E(t) = (\omega_1{}'(t)\dot{x}_1{}'(t)[\emptyset_1 + \chi_1{}'(1-\emptyset_1)]) + \alpha_1{}'(t)\dot{y}_1{}'(t) + \sum_{j=1}^{d'} \dot{y}_1{}' * u(a(t))\,\beta_{1j}{}' \quad (3.36)$$

Culminating the model development, equation (3.36) is generated and will be utilized in the analysis of the integrated case scenario. Consequently, the net emissions within a given integrated case scenario will be computed via equation (3.36).

Conspicuously, the stand-alone 620 MW NGCC PP unit plays a major role in contributing to immense amounts of CO_2 emissions emitted to the atmosphere annually. This is to be expected since fossil fuel-fired PPs are renowned as prime sources of anthropogenic CO_2 emissions (Karimi, Hillestad, & Svendsen, 2012). NGCC PPs typically have half the CO_2 production rate in comparison to a coal PP unit generating an equivalent amount of power (Meyer et al., 2005; Rubin, Chen, & Rao, 2007). Nevertheless, NGCC PPs still account for large quantities of CO_2 present within the atmosphere. As a result, it is vital to account for the environmental impact associated with the substituted PP and CC unit. This is undertaken through the implementation of the avoided burden methodology as explicated by the updated standards from the ISO 14040 and 14044 (International Organization for Standardization, 2006a, 2006b). Hence, the ensuing comparison amongst the integrated and base cases will entail the avoided burden approach. For comparison purposes, equation (3.20) is now altered by eliminating system 1 in order to acquire equation (3.37) which is utilized in computing the net emissions within the resultant base case scenario. Adding to that, equation (3.38) is also now established to calculate the net emissions generated within the utilization scenario whilst accounting for the avoided burden methodology. Thereafter, these values will be utilized as an input to the dynamic LCA framework to attain an impartial comparison between these two scenarios. Following the equations, Table 3.2 summarizes all the variables, exclusive to the variables stated in Table 3.1, and their respective descriptions deliberated within the integrated case scenario model development.

$$Net\ E(t) = \alpha_1(t)\dot{y}_1(t) + \sum_{j=1}^{d} \dot{y}_1 * u\big(a(t)\big)\,\beta_{1j} \tag{3.37}$$

$$Net\ E(t) = \{(\omega_1(t)\dot{x}_1(t)\chi_1) - (\omega_1{}'(t)\dot{x}_1{}'(t)[\emptyset_1 + \chi_1{}'(1-\emptyset_1)])\} + \alpha_1{}'(t)\dot{y}_1{}'(t) + \sum_{j=1}^{d'} \dot{y}_1{}' * u(a(t))\,\beta_{1j}{}' \tag{3.38}$$

Table 3.2 Summary of variables and their descriptions for the integrated case scenario

Variables	Description
$\boldsymbol{a}$	The variable depicting the time steps within which the disposal of product y_i will occur
$\boldsymbol{D}$	The ratio of the amount of de-rated power to the power generated by an identical stand-alone power plant unit
$\boldsymbol{d'}$	The number of times product y_i is disposed of within system 6
$\boldsymbol{E_4}$	The amount of carbon dioxide emitted on an annual basis in system 4 (in kg CO_2)
$\boldsymbol{E_5}$	The amount of carbon dioxide emitted on an annual basis in system 5 (in kg CO_2)
$\boldsymbol{E_6}$	The amount of carbon dioxide emitted on an annual basis in system 6 (in kg CO_2)
$\boldsymbol{k}$	The number of inputs into a given system
$\boldsymbol{m'}$	The number of utilization processes in the domain of system 5
$\boldsymbol{n'}$	The number of integrated power plant and carbon capture units in the domain of system 4
$\boldsymbol{Net\ E}$	The net carbon dioxide emission on an annual basis (in kg CO_2) in the overall system (systems 4, 5, and 6)
$\boldsymbol{p}$	The amount of de-rated power in the power plant unit (in MWh)
$\boldsymbol{r}$	The number of outputs from a given system
$\boldsymbol{t}$	The current time being considered for the analysis (in years)
$\boldsymbol{t_{eij}}$	The exact time corresponding to the disposal of product y_i (in years)
$\boldsymbol{\dot{x}_i'}$	The output of product x_i , accounting for de-rating, on an annual basis in system 4 (in MWh)
$\boldsymbol{\dot{x}_i''}$	The output of product x_i , inclusive to de-rating, on an annual basis in system 4 (in MWh)
$\boldsymbol{\dot{y}_i'}$	The output of the manufactured product y_i on an annual basis in system 5 (in kg y_i)
$\boldsymbol{\alpha_i'}$	An emission intensity with respect to the utilization process in system 5 (in $\frac{kg\ CO_2}{kg\ y_i}$)
$\boldsymbol{\beta_{ij}'}$	The amount of carbon dioxide generated by disposing 1 kg of product y_i in the domain of system 6 (in $\frac{kg\ CO_2}{kg\ y_i}$)
$\boldsymbol{\emptyset_i}$	The fraction of carbon dioxide emitted within the domain of the carbon capture unit in system 4
$\boldsymbol{\chi_i'}$	The fraction of carbon dioxide emitted within the domain of the power plant unit in system 4
$\boldsymbol{\omega_i'}$	An emission intensity with respect to the power plant unit in system 4 (in $\frac{kg\ CO_2}{MWh}$)

3.4 Conventional MeOH Production in Aspen Plus

The conventional MeOH flowsheet was simulated through the utilization of Aspen Plus^{TM} V10 (Aspen Plus^{TM}, 2017). Adding to that, a conventional SMR flowsheet was also developed and integrated to the conventional MeOH flowsheet so as to generate the necessary syngas required for MeOH production. Notably, the numerical values, related to temperature and pressure, present within the SMR section are attained from the simulation conducted by Milani et al. (2015). However, the conventional flowsheet employed within this study is slightly different as it utilizes the heater model as opposed to the Heat-X model chosen by Milani et al. (2015).

Figure 3.10 illustrates the conventional flowsheet employed to obtain the obligatory syngas that is further utilized within the domain of the MeOH production process. In this study, impurities present within the NG stream are assumed to be negligible. Moreover, the feed to the conventional SMR process consists of solely purified methane and steam entering at a mass flowrate of 5,000 $\frac{kg}{hr}$ and 5,620 $\frac{kg}{hr}$ respectively. Initially, the W-FEED stream, composed of water at a temperature of 20 $^{\circ}$C and a pressure of 1 bar, is compressed to a pressure of 25 bar. The METHANE stream, composed of purified methane at a temperature of 30 $^{\circ}$C and a pressure of 1 bar, is thereafter mixed with the compressed W-FEED stream. Ensuing this, the mixed feed stream is preheated to a temperature of 1100 $^{\circ}$C so as to adjust the temperature to the appropriate operational condition within the reformer unit. The high temperature and pressure feed stream enters the reformer unit which is set to consider all necessary components, and compute phase and chemical equilibriums at a temperature of 1100 $^{\circ}$C and a pressure of 25 bar. The reformer unit is modeled as an RGIBBS reactor in operation. Subsequently, the product stream attained is cooled down to a temperature of 30 $^{\circ}$C before it is further dehydrated in the water removal drum. In the water removal drum, 95% of the water present within the incoming product stream is removed. Thereafter, the SYNGAS stream is compressed to a pressure of 78 bar within the CP2 unit. Lastly, the stream SYNGAS-3, exits the SMR section at a temperature of 167 $^{\circ}$C and a pressure of 76.98 bar. SYNGAS-3 is then further utilized as a feed to the subsequent MeOH production flowsheet.

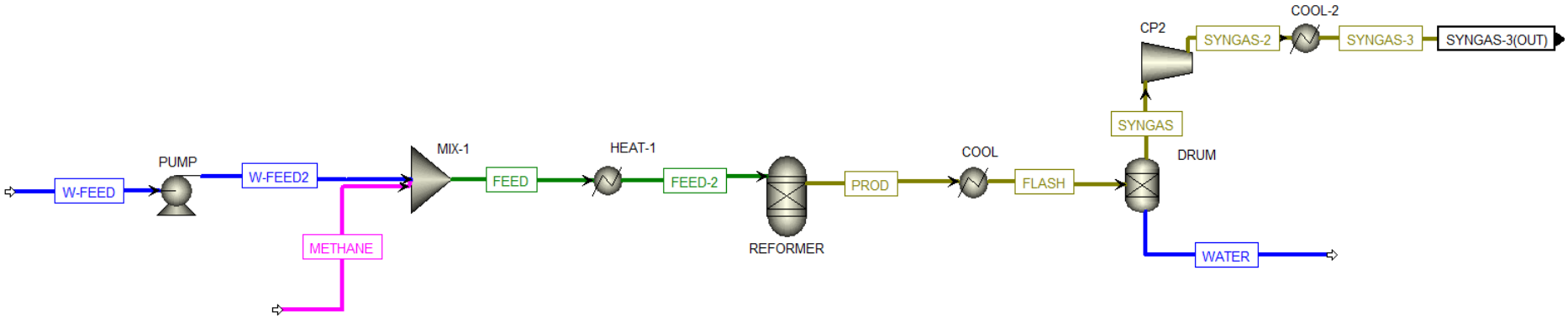

Figure 3.10 Conventional SMR flowsheet for MeOH production

Figure 3.11 vividly portrays the flowsheet employed for the MeOH production process. Reactions 3.1, 3.2, and 3.3 occur within the MeOH reactor. As mentioned previously, these reactions consist of the hydrogenation of CO, hydrogenation of CO_2, and the RWGS reaction. Both reactions, hydrogenation of CO and hydrogenation of CO_2, are exothermic in nature. Whereas, the RWGS reaction is endothermic in nature and necessitates some energy to proceed.

Hydrogenation of CO	$CO + 2H_2 \leftrightarrow CH_3OH$	(R3.1)
Hydrogenation of CO_2	$CO_2 + 3H_2 \leftrightarrow CH_3OH + H_2O$	(R3.2)
RWGS	$CO_2 + H_2 \leftrightarrow CO + H_2O$	(R3.3)

The syngas obtained within the preceding SMR section enters a flash unit which further dehydrates the syngas stream by purging 94 % of the water present. Exiting the FLASH unit at a temperature of 40 °C, the stream SYNGAS-4 is preheated to a temperature of 197.8 °C and a pressure of 70.93 bar within a multistage compressor unit. In addition, the stream SYNGAS-5 is mixed alongside an incoming recycle stream (RECYCLE-3) to yield SYNGAS-6. Thereafter, SYNGAS-6 enters a rigorous METHREAC unit which is modeled as an RPLUG reactor in operation. METHREAC is set as a reactor with constant thermal fluid temperature at 250.9 °C. Reactions 3.1, 3.2, and 3.3 are defined to be active and reversible within the METHREAC unit. The reactor is also selected to be a multitube reactor utilizing 1,634 tubes in operation. Furthermore, the tube dimensions are selected to have a length of 7 m with a chosen diameter of 38 mm. The heat transfer coefficient is set to be 280 $\frac{btu}{hr*ft^2*F}$. Lastly, the catalyst was chosen to have a bed voidage of 0.39 and a particle density of 1,770 $\frac{kg}{m^3}$ (Van-Dal & Bouallou, 2013). Exiting the METHREAC unit, the product stream obtained is cooled down to a temperature of 40 °C before entering FLASH-1. In FLASH-1, the top product is first sent to a RECSPLIT unit which purges 7 % of the recycle stream. Thereafter, the remaining 93 % of the recycle stream is heated to a temperature of 231 °C before being recycled back to the METHREAC unit. On the other hand, the

bottom product of the FLASH-1 unit is sent to a series of flash columns. This configuration retains a crucial aspect of the flowsheet as it enhances the final purity of the desired MeOH product.

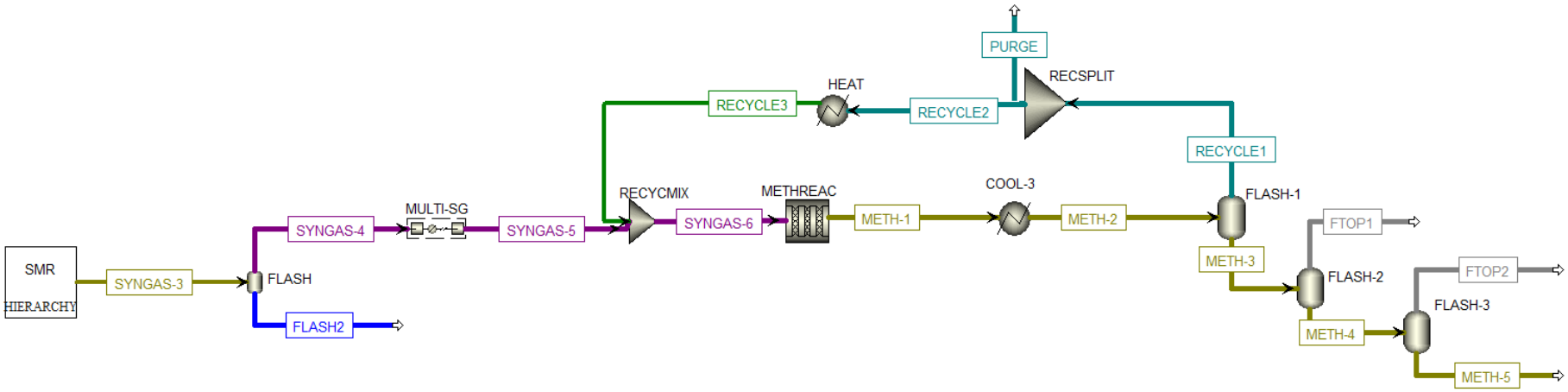

Figure 3.11 MeOH production flowsheet

3.5 CO_2 Utilization Approach for MeOH Production in Aspen Plus

Identical to the conventional approach of manufacturing MeOH, the CO_2 utilization flowsheet was simulated through the use of Aspen Plus™ V10 (Aspen Plus™, 2017). However, the CCU MeOH approach involves an additional stream of CO_2 located within the initial SMR section. Similarly, the numerical values, related to temperature and pressure, present within the SMR section are also attained from the simulation by Milani et al. (2015). Adding to that, the flowsheet employs the use of a heater model as opposed to the Heat-X model selected by Milani et al. (2015).

Essentially, the majority of the SMR flowsheet employed for the utilization scenario will resemble that of the flowsheet utilized in the conventional scenario. Nevertheless, the primary difference exists in the addition of a CO_2 stream that is fed at a mass flowrate of 3,946 $\frac{kg}{hr}$. In this work, the CO_2 feed stream is assumed to encompass negligible amounts of impurities. Moreover, this CO_2 stream is fed to the SMR flowsheet at a temperature of 116 $^{\circ}$C and a pressure of 74.6 bar. Subsequently, the stream is compressed to a pressure of 78 bar and heated to a temperature of 120 $^{\circ}$C before it is mixed alongside the incoming SYNGAS-3 stream. Principally, all other inputs and feed streams are identical to that of the conventional MeOH production scenario. Figure 3.12 portrays the SMR flowsheet employed so as to incorporate CO_2 utilization to the MeOH production process. Similarly, the flowsheet employed in the utilization scenario for MeOH production will resemble that of the flowsheet utilized in the conventional scenario. Notably, all inputs to the process units are identical to that of the conventional scenario. Figure 3.13 vividly illustrates the flowsheet utilized in the MeOH production process.

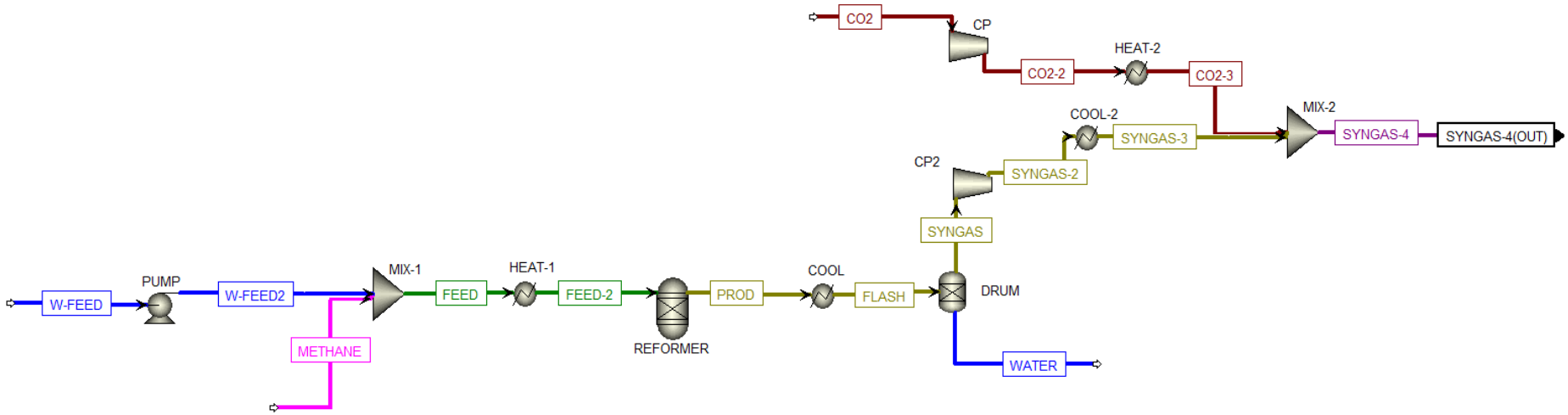

Figure 3.12 Conventional SMR flowsheet incorporating CO_2 utilization for MeOH production

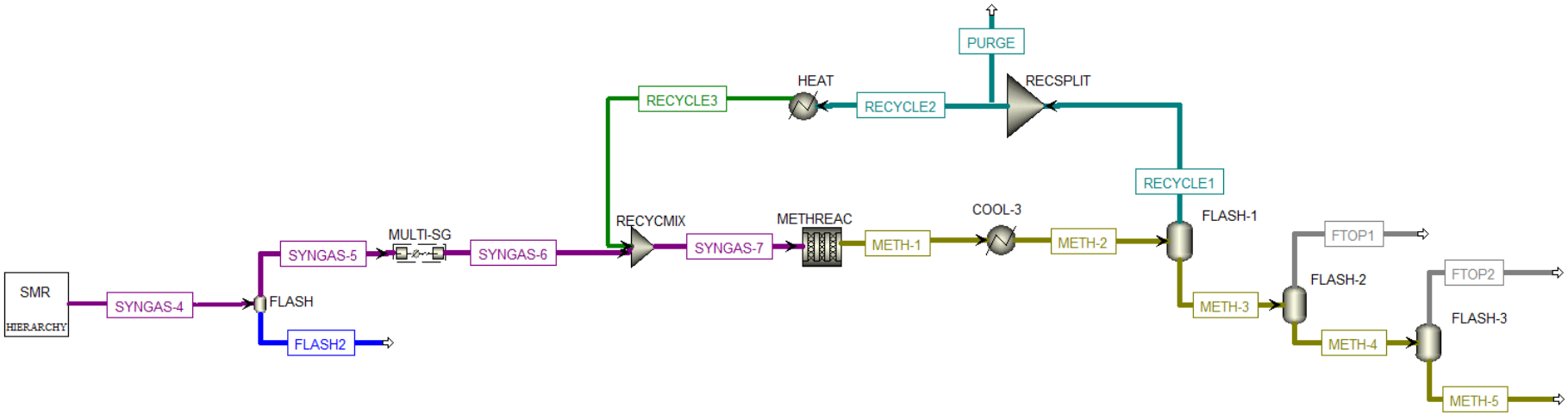

Figure 3.13 MeOH production flowsheet

Chapter 4: Model Implementation and Dynamic LCA Results

Succeeding the model development, the intrinsic model equations, previously developed within Chapter 3, will now be utilized in conjunction with the dynamic LCA framework to assess various CCU processes and products. Chapter 4 entails an in-depth environmental analysis providing a justifiable assessment to CCU processes and products. The products examined within the ensuing section are MeOH and DMC. Adding to that, a comparison between the conventional and utilization approaches of manufacturing these products is also implemented within this section.

Previously discussed within Chapter 3, NGCC PPs are renowned for emitting immense quantities of CO_2 to the atmosphere. Consequently, the implementation of the avoided burden methodology, as explicated by the updated standards from the ISO 14040 and 14044, is undertaken (International Organization for Standardization, 2006a, 2006b). Notably, this approach hinders the underlying environmental effect attributed to the size of the PP unit. For example, selecting a larger PP unit will inherently result in a larger environmental impact. Moreover, the primary scope of this thesis is to explore the environmental impact of various CCU processes and products irrespective of the given size of the PP unit. Therefore, it is integral that this underlying effect is omitted from the ensuing analysis. Figure 4.1 illustrates the avoided burden approach for both a 100 MW natural gas combustion turbine (NGCT) and 300 MW NGCC PP unit integrated with identical DMC utilization processes:

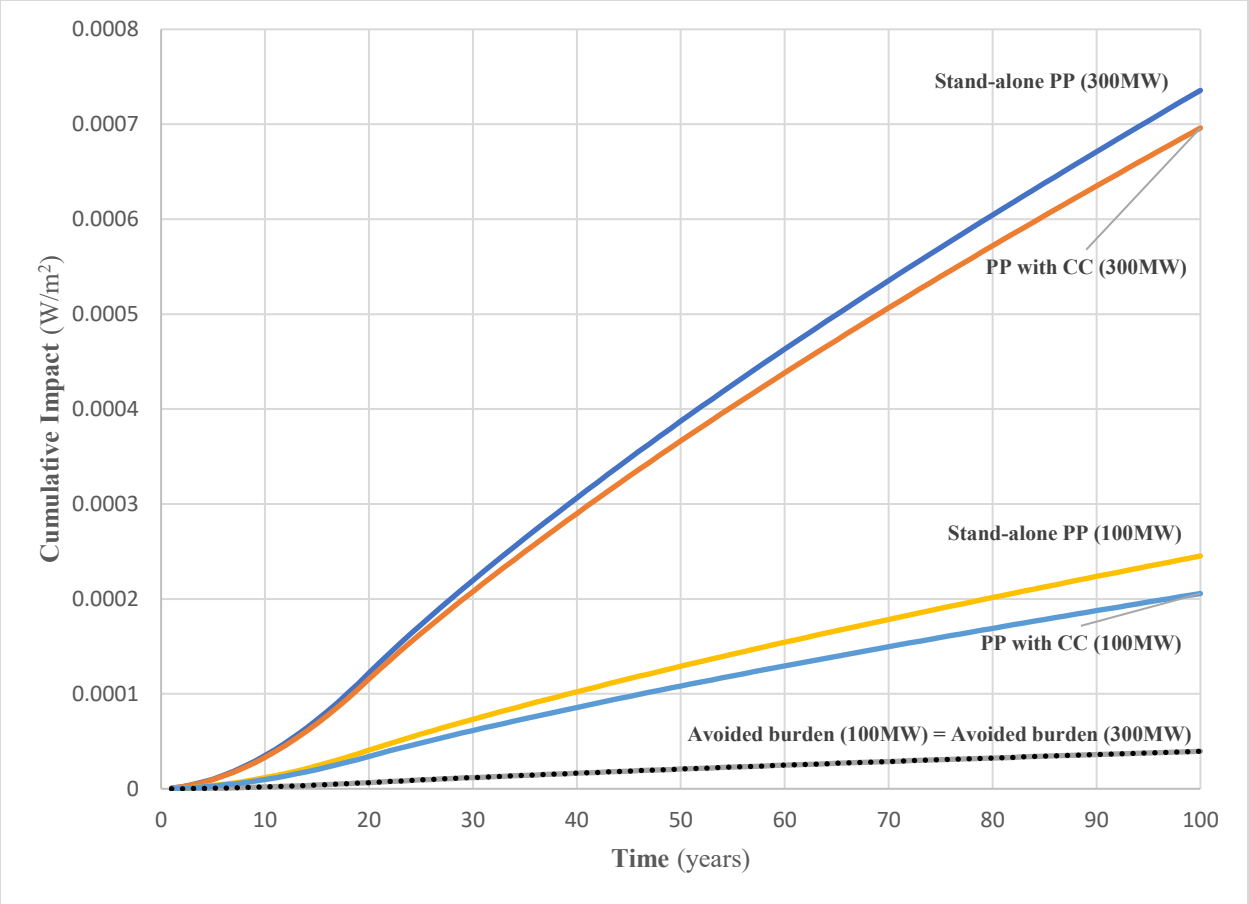

Figure 4.1 Avoided burden for both a 100 MW NGCT and 300 MW NGCC PP unit

As depicted within Figure 4.1, the cumulative impact on radiative forcing, computed for the avoided burden at year 100, is identical for both PP units. The cumulative impact on radiative forcing was attained to be $3.952 * 10^{-5} \frac{W}{m^2}$ for both the 100 MW NGCT and 300 MW NGCC PP units at year 100. Therefore, the avoided burden methodology is implemented so as to obstruct the underlying environmental effect attributed to the size of the PP unit.

4.1 Results for MeOH Production

As previously mentioned, the production of commercial MeOH spans the whole globe encompassing various ultimate chemicals and energy products. Formaldehyde's production, the largest solitary market for MeOH, is associated with one third of the total demand for MeOH (Methanol Institute, 2015). Furthermore, MeOH is the focal component within which the production of formaldehyde, attaining approximately 10 million metric tons, is contingent upon (Andersson, Hernelind, & Augustsson, 2006; Methanol Institute, 2015). Remarkably, formaldehyde, as a final chemical product, possess the ability to be utilized in a varying range of applications. These consist of being utilized in renovation projects, new building activity, automobile production, panelboard substitution for solid wood, changing wood panel mix, and growth in high technology chemicals (Methanol Institute, 2015). Given formaldehyde's large market and accounting for its exceptional ability in delaying CO_2 emissions, the generated MeOH will be utilized to further manufacture formaldehyde. Furthermore, the CO_2 storage duration, within the commercial formaldehyde product, is assumed to be 5 years and the formaldehyde product will be further utilized in the automotive industry. Following the 5-year storage duration, the formaldehyde product will be consumed and the sequestered CO_2 is re-emitted back into the atmosphere.

The ensuing analysis depicts two diverse procedures of manufacturing the commercial MeOH product. The conventional approach, analyzes a stand-alone NG-based MeOH synthesis plant, which operates discretely to the PP unit, in Aspen Plus V10 (Aspen Plus™, 2017). Furthermore, the utilization approach, which employs the integration and implementation of a CO_2 stream to the MeOH synthesis process, is also simulated in Aspen Plus V10 (Aspen Plus™, 2017). Particularly, all the intrinsic data, for systems 2 and 5, utilized within the ensuing calculations are obtained from the Aspen Plus simulations. Furthermore, all plants intrinsic to the conventional and utilization systems are assumed to operate for 333 days per annum. Within Systems 2 and 5, the employed cradle-to-grave analysis will aim to assess all the CO_2 emissions from their initial source, NG, so as to embody a justifiable environmental assessment. Successive to the obligatory computations, the values attained will be utilized as an input to the dynamic LCA framework so as to acquire the cumulative impact on radiative forcing for the two routes being analyzed.

Furthermore, a sensitivity analysis will be conducted so as to comprehend the benefits accompanied by increasing the CO_2 storage duration within the MeOH product.

Before proceeding to analyze the environmental results, it is essential to critically assess the Aspen Plus simulation results for both the conventional and utilization approaches of manufacturing the MeOH product. Within the conventional approach, the final MeOH stream was attained at a mass flowrate of 8,282.85 $\frac{kg}{hr}$ with a purity of 97.6 % MeOH. Moreover, the value attained is deemed reasonable for the conventional approach. In the utilization scenario, the final MeOH stream produced a mass flowrate of 9,476.65 $\frac{kg}{hr}$ with a purity of 88.2 % MeOH. Correspondingly, the amount of MeOH produced within the utilization approach is also deemed reasonable. Given the aforementioned production amounts, the corresponding amount of CO_2 emitted within both scenarios is computed. Notably, the majority of CO_2 emitted, within both scenarios, can be significantly attributed to allocating the necessary resources to account for the processes' immense thermal duties. Therefore, it is compulsory that these duties are accounted for within the domain of these flowsheets so as to compute the resultant net CO_2 emissions in both scenarios. Table 4.1 illustrates a detailed summary for all the intrinsic thermal and electrical duties within both the conventional and utilization scenarios. The values in Table 4.1 have all been converted and presented in units of $\frac{GJ}{hr}$ so as to facilitate the ensuing computations.

Table 4.1 Detailed summary of the thermal and electrical duties

	Conventional		**CO_2 Utilization**	
Units	**Thermal** $(\frac{GJ}{hr})_{th}$	**Electrical** $(\frac{GJ}{hr})_{el}$	**Thermal** $(\frac{GJ}{hr})_{th}$	**Electrical** $(\frac{GJ}{hr})_{el}$
HEAT + HEAT-1	72.52	-	63.48	-
COOL + COOL-2 + COOL-3	83.23	-	77.12	-
REFORMER	60.97	-	60.97	-
DRUM	4.108E-06	-	4.108E-06	-
FLASH	4.289	-	4.684	-
METHREAC	21.67	-	24.74	-
DIST-1 + DIST-2 + DIST-3	8.766E-15	-	2.287E-14	-
MULTI-SG	5.593	-	6.250	-
PUMP	-	0.041	-	0.041
CP	-	-	-	0.014
CP2	-	5.067	-	5.067

In order to maintain a justifiable comparison, the amount of MeOH produced within the vicinity of the conventional route is said to be equal to the amount of MeOH produced within the utilization approach. Initially, the amount of MeOH produced within the conventional approach is normalized to 1 $\frac{tonne\ MeOH}{hr}$. Adding to that, all the other values within the conventional approach maintain the same ratio as they did before this alteration. In order to compute the CO_2 emissions attributed to the thermal duties, it will be necessary to assume that the CO_2 emissions from utility production and operation based on NG combustion is equal to 62.3 $\frac{kg_{CO2}}{GJ}$ including the CO_2 emissions from process fuel production (Van-Dal & Bouallou, 2013). Depending on the exact province within Canada, the GHG intensity related to electricity generation may vary significantly. Assuming the operation of the MeOH process occurs within Ontario, the GHG intensity related to electricity generation is given as 40 $\frac{g_{CO2}}{kwh}$ (National Energy Board, 2017). Significantly, the choice of the province plays a pivotal role when computing the net CO_2 emissions attributed to the electrical duties within the MeOH production process. For example, the GHG intensity related to electricity generation within the province of Alberta is given as 790 $\frac{g_{CO2}}{kwh}$ (National Energy Board, 2017). Within Ontario, the amount of CO_2 emitted, when accounting for electrical duties within the conventional and utilization approaches of manufacturing MeOH, is $6.852 * 10^{-3}\ \frac{tonne\ CO_2}{hr}$ and $6.004 * 10^{-3}\ \frac{tonne\ CO_2}{hr}$ respectively. However, the amount of CO_2 emitted when accounting for electrical duties, in the province of Alberta, for both the conventional and utilization approaches is computed as 0.135 $\frac{tonne\ CO_2}{hr}$ and 0.119 $\frac{tonne\ CO_2}{hr}$ respectively. Therefore, an inordinate amount of caution should be placed when assessing the electrical duties within the MeOH production process. In this work, the province of choice, that will be further utilized in the ensuing computations, will be Ontario.

As previously aforementioned, the majority of CO_2 emitted within the vicinity of the MeOH production process is attributed to allocating the necessary resources to account for the processes' immense thermal duties. However, only a small fraction of CO_2 is actually vented within the production process. Similarly, a minor amount of CO_2 is also emitted when accounting for the necessary electrical duties. Nevertheless, it is essential to account for all these CO_2 emissions when undertaking the subsequent environmental comparison.

Within the conventional MeOH production route, the amount of CO_2 emitted when accounting for thermal and electrical duties is 1.867 $\frac{tonne\ CO_2}{hr}$ and $6.852 * 10^{-3}\frac{tonne\ CO_2}{hr}$ respectively. Moreover, the amount of CO_2 vented within the production process is $4.216 * 10^{-3}\frac{tonne\ CO_2}{hr}$. Therefore, the cumulative amount of CO_2 emitted within the domain of the conventional approach is $1.878\frac{tonne\ CO_2}{hr}$. In the utilization route, the amount of CO_2 emitted when accounting for thermal and electrical duties is 1.520 $\frac{tonne\ CO_2}{hr}$ and $6.004 * 10^{-3}\frac{tonne\ CO_2}{hr}$ respectively. Furthermore, the amount of CO_2 vented within the production process is 0.177 $\frac{tonne\ CO_2}{hr}$. Consequently, this results in a net amount of 1.703 $\frac{tonne\ CO_2}{hr}$ emitted within the utilization approach. Table 4.2 provides a summary of the CO_2 emissions within both the conventional and utilization approaches. Thereafter, the cumulative amounts of CO_2 emissions will be incorporated within systems 2 and 5. Given these values, it is now plausible to proceed with the obligatory computations, utilizing the equations developed in Chapter 3, to calculate the emissions within the other systems.

Table 4.2 Summary of CO_2 emissions for MeOH production

CO_2 Emissions	**Conventional ($\frac{tonne\ CO_2}{hr}$)**	**CO_2 Utilization ($\frac{tonne\ CO_2}{hr}$)**
Thermal Duties	1.867	1.520
Electrical Duties	$6.852 * 10^{-3}$	$6.004 * 10^{-3}$
Vent	$4.216 * 10^{-3}$	0.177
Total	1.878	1.703

Initially, the overall CO_2 emissions within systems 1 and 4 is calculated via the equations developed in Chapter 3. Thereafter, the avoided burden methodology is implemented so as to obscure the underlying environmental effect associated with the size of the PP unit. As a result, the cumulative impact on radiative forcing is computed for both systems 1 and 4 inclusive to their relative difference. The cumulative impact on radiative forcing was obtained as $4.765 * 10^{-6}\frac{W}{m^2}$ for the avoided burden at year 100 attributed to the 620 MW NGCC PP unit. Moreover, this result signifies that $4.765 * 10^{-6}\frac{W}{m^2}$ of radiative forcing is avoided at year 100 through the implementation and integration of the CC unit to the stand-alone 620 MW NGCC PP unit.

Typically, the benefit of CC integration is omitted when comparing a utilization process to the conventional approach of manufacturing a product. However, it is essential to incorporate this benefit so as to obtain a reliable and justifiable comparison within the MeOH scenario.

Subsequently, the effect of delaying CO_2 emissions, through its utilization within the MeOH product, is tested. For a 5-year storage duration, the overall CO_2 emissions, within the domain of system 6, are computed via the equations generated in Chapter 3. Thereafter, the cumulative impact on radiative forcing is calculated for systems 5 and 6 as depicted within Figure 4.2. At year 100, the cumulative impact on radiative forcing related to consuming the MeOH product is obtained as $1.782 * 10^{-5} \frac{W}{m^2}$. Whereas, the cumulative impact on radiative forcing, at year 100, related to the utilization process is computed as $2.308 * 10^{-5} \frac{W}{m^2}$. The result obtained, for MeOH consumption, indicates a relatively large cumulative impact on radiative forcing at year 100. Frequently, the utilization process is only considered within the literature domain, for the environmental analysis, whilst product consumption is omitted. However, the environmental effect attributed to product consumption must be considered within the analysis due to its evidently large environmental impact. Consequently, the resultant incorporation of system 6 to the underlying analysis is undertaken and the combination of systems 5 and 6 is utilized within the ensuing comparison yielding $4.090 * 10^{-5} \frac{W}{m^2}$ for the cumulative impact on radiative forcing at year 100. Notably, this value represents the gate-to-grave impact associated with the utilization approach of manufacturing MeOH. The gate-to-grave impact is defined as the environmental impact considering all pertinent CO_2 emissions from the factory gate until its end-of-life treatment.

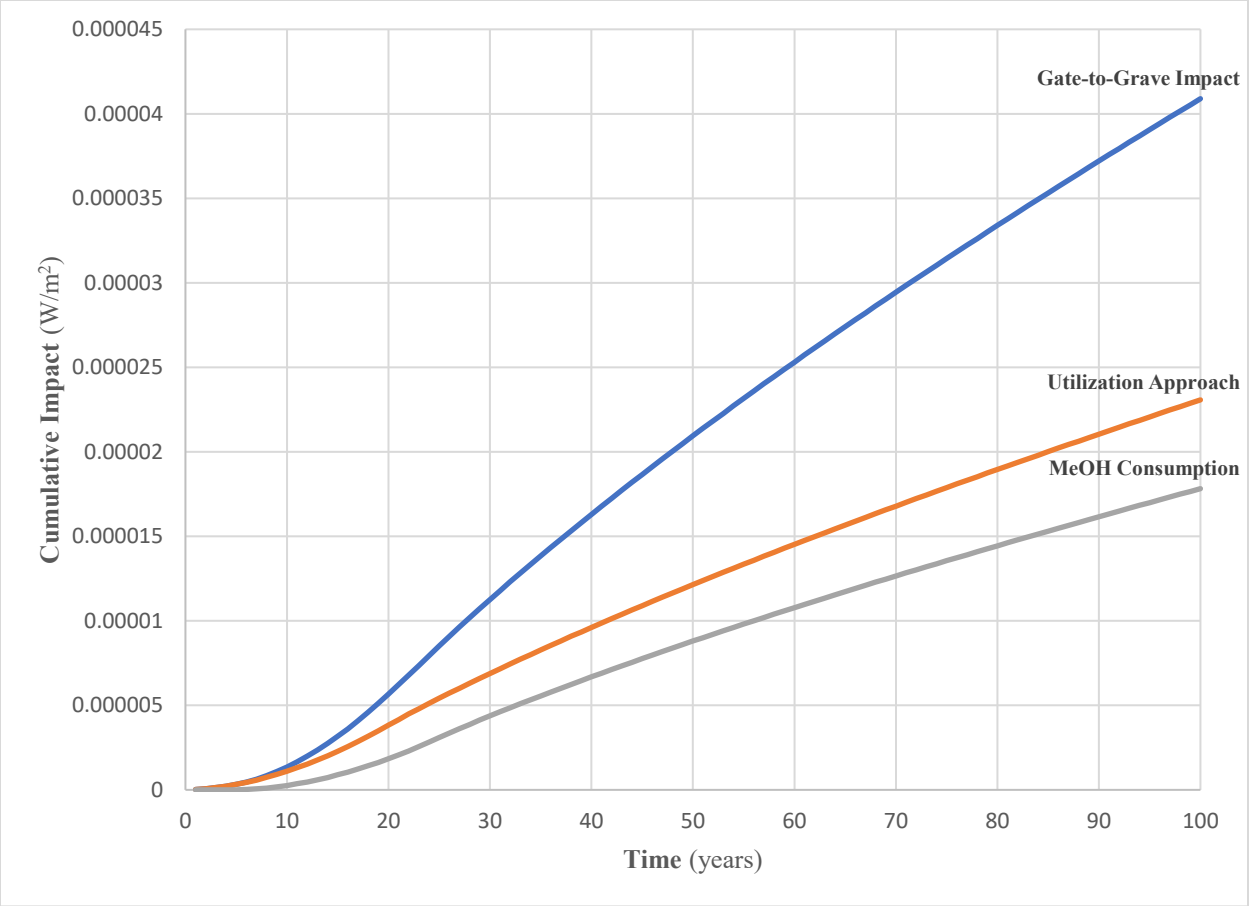

Figure 4.2 Gate-to-grave impact for the MeOH utilization approach

In order to maintain consistency, the consumption of the final MeOH product also occurs after a 5-year storage duration. The overall CO_2 emissions, within the vicinity of system 3, are computed via the equations developed in Chapter 3. Hence, the cumulative impact on radiative forcing is computed and graphed as depicted within Figure 4.3. At year 100, the cumulative impact on radiative forcing related to consuming the MeOH product is obtained as $1.782 * 10^{-5} \frac{W}{m^2}$. Whereas, the cumulative impact on radiative forcing, at year 100, related to the conventional route is computed as $2.546 * 10^{-5} \frac{W}{m^2}$. As a result of the large environmental impact associated with MeOH consumption, the combination of systems 2 and 3 is utilized within the ensuing comparison yielding $4.328 * 10^{-5} \frac{W}{m^2}$ for the cumulative impact on radiative forcing at year 100. Remarkably,

this value represents the gate-to-grave impact associated with the conventional approach of manufacturing MeOH.

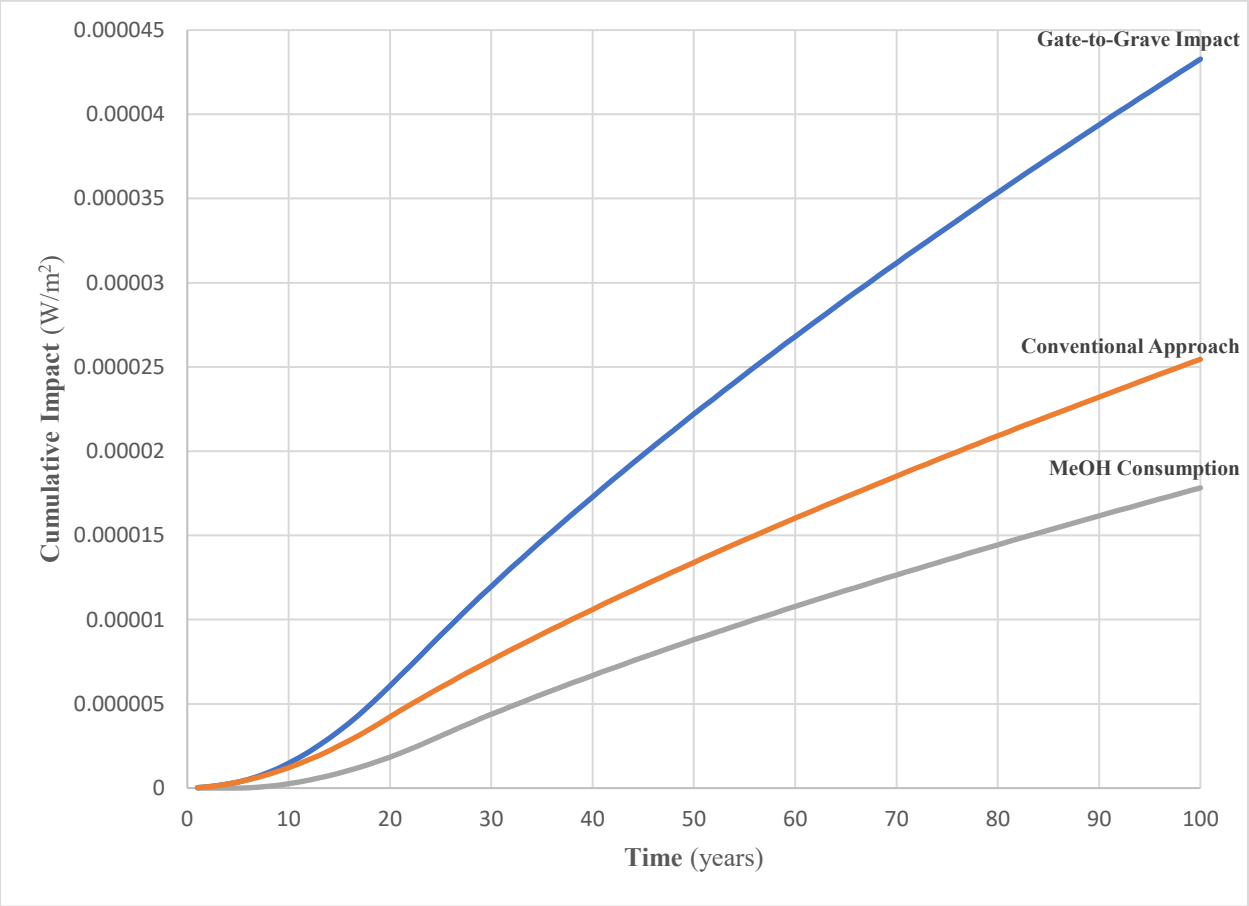

Figure 4.3 Gate-to-grave impact for the MeOH conventional approach

In order to produce a justifiable and reliable environmental assessment, various crucial aspects within the comparison-based analysis have to be accounted for. As such, the avoided burden approach has been implemented alongside the addition of the environmental impact associated with the final consumption of the MeOH product. Moreover, the analysis does not assume a free source of CO_2 and considers the energy required to capture it. As mentioned previously, cradle-to-grave encompasses everything from raw material extraction, including all processes, until its end-of-life treatment. Taking into account these essential factors, Figure 4.4

represents the culmination of the comparison-based assessment. The conventional approach of manufacturing MeOH results in a higher cumulative impact on radiative forcing, at year 100, when compared to the utilization approach. This is evident within Figure 4.4 where the conventional approach yields $4.328 * 10^{-5} \frac{W}{m^2}$ as opposed to the utilization approach which yields $3.613 * 10^{-5} \frac{W}{m^2}$. Moreover, the amount of radiative forcing that can be evaded through the implementation of the utilization approach is also portrayed. Essentially, $7.147 * 10^{-6} \frac{W}{m^2}$ is circumvented when undertaking the utilization route. Consequently, from an environmental standpoint, the utilization route is a better alternative to the conventional approach of manufacturing commercial MeOH. In addition, the percent reduction in the cumulative impact of radiative forcing, at year 100, is also computed as 16.51 %. Notably, a decrease in the percent reduction is evident over the 100-year analysis period.

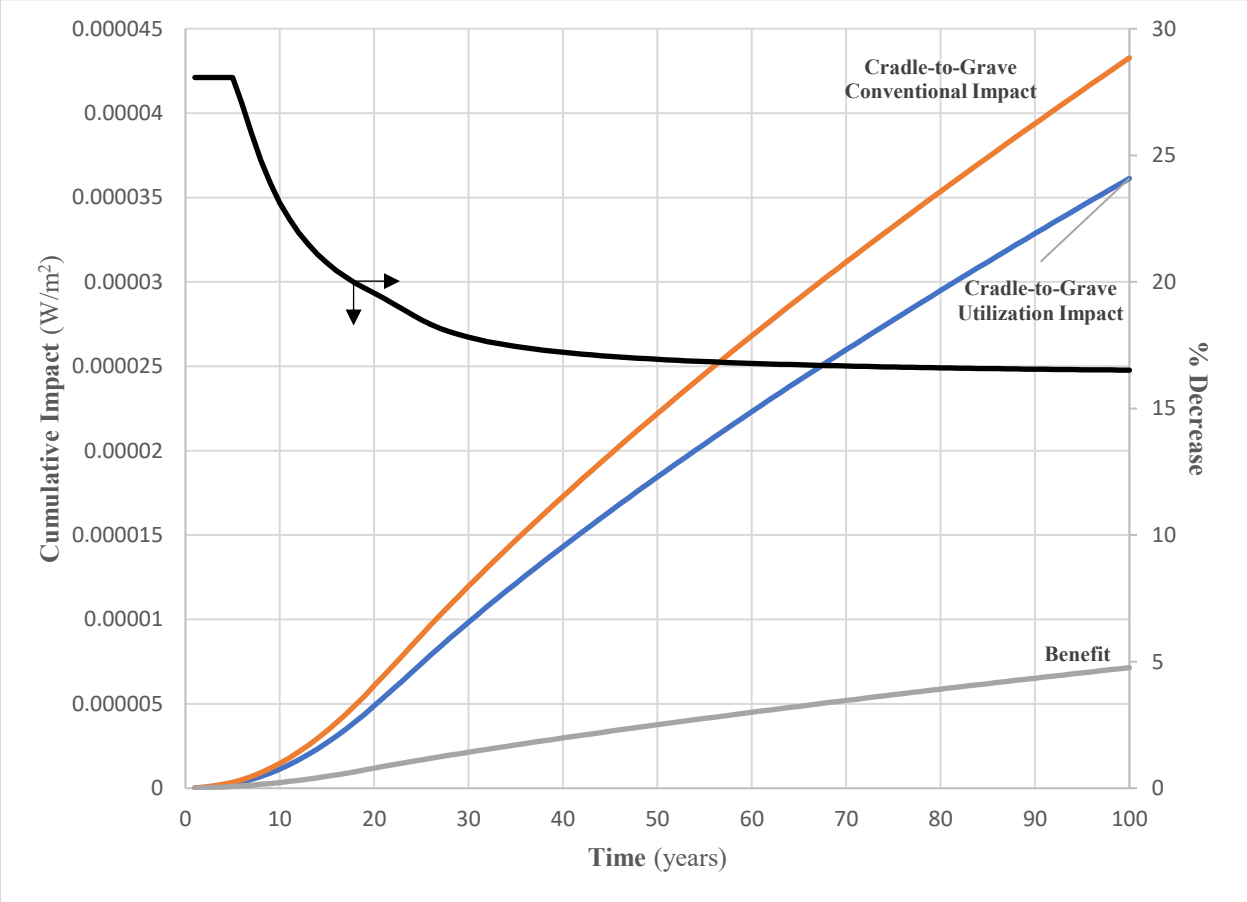

Figure 4.4 Cradle-to-grave impacts for MeOH production

4.2 Results for DMC Production

Exhibiting a growing range of applications within the industrial field, the demand for DMC has been increasing annually (Tan et al., 2018). Pc, one of the promising large-scale applications within which DMC plays a vital role, is primarily synthesized by utilizing DMC as a raw material. As mentioned previously, Pc is widely used in the automotive, building, and electronics industries (Cao et al., 2012). Furthermore, the Pc consumption rate has approximately attained 5.15 million tons globally in 2015 (Tan et al., 2018). Given Pcs large market and its potential to delay CO_2 emissions through its usage in the aforementioned industries, the manufactured DMC will be further utilized to produce commercial Pc. Moreover, the CO_2 storage duration, within commercial Pc, is assumed to be 5 years and the Pc product will be further utilized within the automotive industry. Ensuing the 5-year storage duration period, the Pc product is finally consumed and the sequestered CO_2 is re-emitted back into the atmosphere.

The previously specified two-section scheme, involving the integration of the aforementioned urea alcoholysis route with the conventional approach of utilizing CO_2 to synthesize urea, serves as the base case within which Kongpanna et al. (2016) conducted a comparative simulation of several process alternatives. The principal goal was to attain a viable and optimized alternative that would further enhance the results obtained within the base case. The approach undertaken consisted of three stages termed the synthesis, design, and innovation stages. Overall, sustainability metrics, economic indicators, LCA indicators, and operational feasibility were assessed for various process alternatives. The flowsheets were simulated in Aspen Plus^{TM} in order to obtain the preliminary results necessary for each alternative. Notably, the variations in the process flowsheets occurred primarily within the domain of the DMC synthesis section. Thus, further enhancements were introduced in each successive alternative so as to optimize the parameters required to produce DMC. This meant that within each successive alternative the energy consumption, net profit, and net CO_2 emissions per kg of product were enhanced. Process alternative 1 utilized a pervapouration unit in downstream separation while process alternative 2 utilized a membrane reactor for NH_3 removal. On the other hand, process alternative 3 utilized reactive distillation to incorporate the reaction and separation systems into an individual unit. Thereafter, a detailed comparison between all the process alternatives and the base case ensued resulting in reactive distillation being the optimal process alternative.

The following analysis entails two different approaches of manufacturing the commercial DMC product. The conventional approach, employing the Partial Carbonylation route (BAYER process), is simulated using Aspen Plus^{TM} software (Kongpanna et al., 2015). Moreover, the utilization approach, implementing the urea route through reactive distillation, is also simulated utilizing Aspen Plus^{TM} software (Kongpanna et al., 2016). The model utilized to employ our environmental assessment will incorporate a comparison between the two aforementioned routes. Notably, all the intrinsic data, for the DMC production process, utilized within the ensuing calculations are obtained from the Aspen Plus^{TM} simulations conducted by the aforementioned authors (Kongpanna et al., 2016, 2015). Furthermore, all plants, within the conventional and utilization approaches, are assumed to operate for 333 days annually. Subsequent to the obligatory computations, the values attained will be utilized as an input to the dynamic LCA framework so as to obtain the cumulative impact on radiative forcing for the two routes being analyzed. Lastly, a sensitivity analysis is conducted so as to comprehend the benefits accompanied by increasing the CO_2 storage duration within the DMC product.

Since a cradle-to-grave environmental assessment is employed, it is essential to account for all pertinent CO_2 emissions starting from NG. A schematic is presented within Figures 4.5 and 4.6 illustrating the analysis undertaken for both the conventional and utilization approaches of manufacturing DMC. The developed conventional approach of manufacturing MeOH is utilized to generate both the CO and MeOH inputs to the conventional DMC production process. Adding to that, a conventional cryogenic air separation unit (ASU) is also utilized to produce the O_2 input to the conventional DMC process (Aneke & Wang, 2015). Within the utilization approach, the NH_3 feed is initially analyzed from its basis of H_2 and nitrogen (N_2). Furthermore, the conventional production of H_2 from NG is adopted from the simulation by Tarun et al. (2007). Similarly, a conventional cryogenic ASU is employed to produce the N_2 input to the NH_3 production process (Aneke & Wang, 2015). Thereafter, both the H_2 and N_2 feeds are inputted to the NH_3 production process so as to manufacture the NH_3 required for DMC production. The NH_3 production results are adopted from the simulation conducted by Araújo & Skogestad (2008). Identical to the conventional DMC approach, the utilization approach utilizes the simulation results obtained from the conventional MeOH approach. As such, these results are utilized to generate the MeOH input

to the DMC production process. All CO_2 emissions within the vicinity of these processes are accounted for within the ensuing computations.

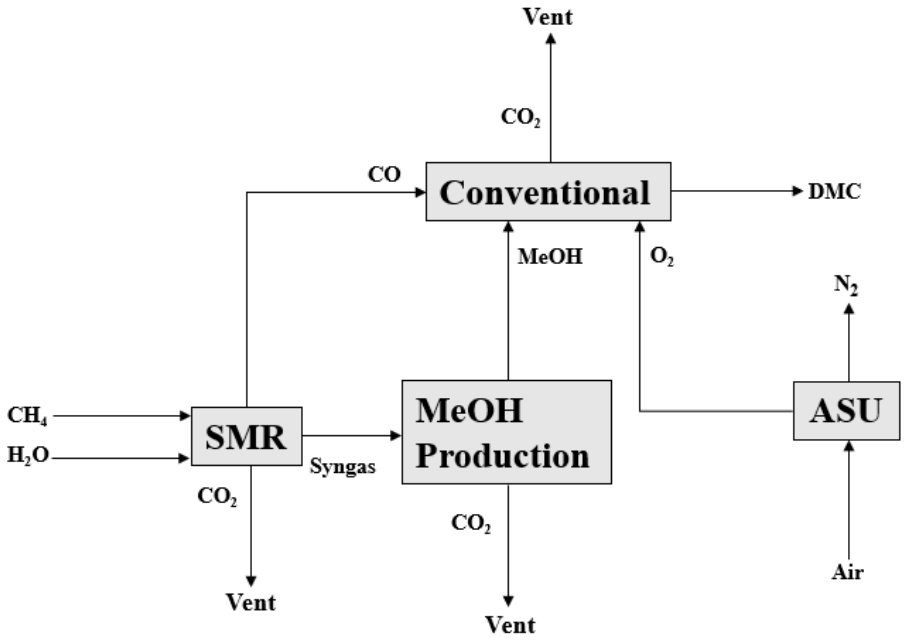

Figure 4.5 Cradle-to-grave assessment for the conventional approach

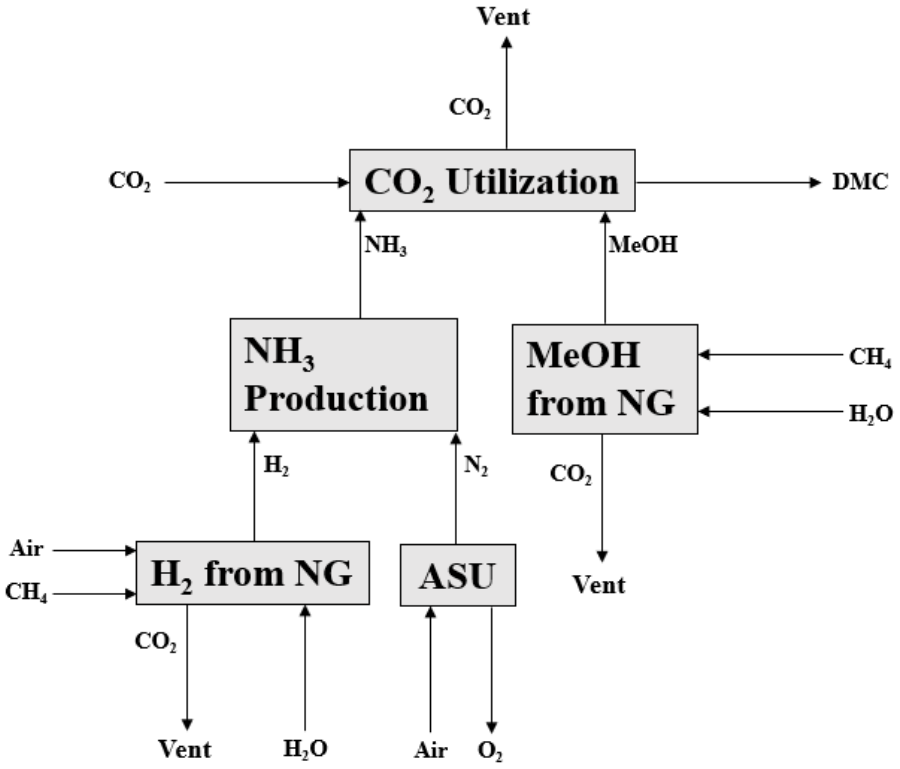

Figure 4.6 Cradle-to-grave assessment for the utilization approach

Initially, the amount of DMC generated within the conventional approach is normalized to 1 $\frac{tonne\ DMC}{hr}$. Furthermore, the amount of DMC generated in both the conventional and utilization approaches is said to be equal. Adding to that, all other values, within both approaches, maintain the same ratio as they did before the normalization. Identical to the preceding MeOH analysis, the CO_2 emissions attributed to thermal duties will be computed by assuming the CO_2 emissions from utility production and operation based on NG combustion is equal to 62.3 $\frac{kg_{CO2}}{GJ}$ including the CO_2 emissions from process fuel production (Van-Dal & Bouallou, 2013). Additionally, the operation of both DMC approaches is said to occur within Ontario yielding 40 $\frac{g_{CO2}}{kwh}$ for the GHG intensity related to electricity generation (National Energy Board, 2017). The GHG intensity related to electricity generation within the province of Alberta is given as 790 $\frac{g_{CO2}}{kwh}$ (National Energy Board, 2017). Taking this into account, a comparison based on the province of choice is further

undertaken. Within the province of Ontario, the amount of CO_2 emitted, when accounting for electrical duties within the conventional and utilization approaches of manufacturing DMC, is $0.010\,\frac{tonne\ CO_2}{hr}$ and $0.019\ \frac{tonne\ CO_2}{hr}$ respectively. Whereas, the amount of CO_2 emitted when accounting for electrical duties, in the province of Alberta, for both the conventional and utilization approaches is computed as $0.202\ \frac{tonne\ CO_2}{hr}$ and $0.375\ \frac{tonne\ CO_2}{hr}$ respectively. This illustrates a significant difference in the CO_2 emissions attributed to electrical duties within these two provinces.

In the conventional approach of manufacturing DMC, several sections were analyzed in-depth so as to compute the net CO_2 emissions. Within the SMR section, the amount of CO_2 emitted when accounting for thermal and electrical duties is $0.417\ \frac{tonne\ CO_2}{hr}$ and $2.507 * 10^{-3}\ \frac{tonne\ CO_2}{hr}$ respectively. In the conventional MeOH section, the amount of CO_2 emitted when accounting for thermal and electrical duties is $1.421\ \frac{tonne\ CO_2}{hr}$ and $5.215 * 10^{-3}\ \frac{tonne\ CO_2}{hr}$ respectively. Moreover, the amount of CO_2 vented within both the DMC and MeOH production processes is $0.522\ \frac{tonne\ CO_2}{hr}$ and $3.209 * 10^{-3}\ \frac{tonne\ CO_2}{hr}$ respectively. Accounting for the electrical duties necessary to produce the pure O_2 feed for DMC production, the specific power consumption was found to be $0.357\ \frac{kwh}{kg\ O_2}$ (Aneke & Wang, 2015). Furthermore, this meant that a total amount of $2.526 * 10^{-3}\ \frac{tonne\ CO_2}{hr}$ was emitted so as to account for the electrical duties necessary to produce the O_2 feed. Overall, a net amount of $2.373\ \frac{tonne\ CO_2}{hr}$ was emitted within the conventional approach of manufacturing DMC.

An identical procedure is implemented within the utilization approach of manufacturing DMC. In the H_2 production section, the amount of CO_2 vented was computed as $1.012\ \frac{tonne\ CO_2}{hr}$. The amount of CO_2 emitted, in the conventional MeOH section, when accounting for thermal and electrical duties is $1.548\ \frac{tonne\ CO_2}{hr}$ and $5.681 * 10^{-3}\ \frac{tonne\ CO_2}{hr}$ respectively. Furthermore, the amount of CO_2 vented within both the DMC and MeOH production processes is $0.809\ \frac{tonne\ CO_2}{hr}$ and $3.496 * 10^{-3}\ \frac{tonne\ CO_2}{hr}$ respectively. Accounting for the electrical duties necessary to produce the pure N_2 feed for DMC production, the specific power consumption was found to be $0.421\ \frac{kwh}{kg\ N_2}$

(Aneke & Wang, 2015). This meant that a total of $6.880 * 10^{-3} \frac{tonne\ CO_2}{hr}$ was emitted so as to account for the electrical duties necessary to generate the N_2 feed. When accounting for the electrical duties within the NH_3 production process, the amount of CO_2 emitted was computed as $6.429 * 10^{-3} \frac{tonne\ CO_2}{hr}$. To sum up, the net CO_2 emitted was computed as 3.391 $\frac{tonne\ CO_2}{hr}$ within the utilization approach of manufacturing DMC. The calculated net CO_2 emissions for the conventional and utilization approaches is further incorporated into systems 2 and 5 respectively. These values, alongside the emissions computed for the remaining systems, will be utilized as an input to the dynamic LCA framework so as to attain the obligatory environmental results.

Table 4.3 Summary of CO_2 emissions for DMC production

CO_2 Emissions	**Conventional ($\frac{tonne\ CO_2}{hr}$)**	**CO_2 Utilization ($\frac{tonne\ CO_2}{hr}$)**
Thermal Duties	1.838	1.548
Electrical Duties	0.010	0.019
Vent	0.525	1.824
Total	2.373	3.391

The procedure implemented to analyze DMC production is identical to the preceding environmental analysis for MeOH production. Firstly, the overall CO_2 emissions within both systems 1 and 4 is calculated. Subsequently, the avoided burden methodology is incorporated into the analysis so as to hinder the underlying environmental effect associated with the size of the PP unit. The cumulative impact on radiative forcing was obtained as $6.385 * 10^{-6} \frac{W}{m^2}$ for the avoided burden at year 100 attributed to the 620 MW NGCC PP unit.

The overall CO_2 emissions within the vicinity of systems 5 and 6 is computed via the equations developed in Chapter 3. For a storage duration of 5 years, the cumulative impact on radiative forcing was computed as depicted within Figure 4.7. Regarding the ultimate consumption of DMC, the cumulative impact on radiative forcing, at year 100, was calculated to be $1.901 * 10^{-5} \frac{W}{m^2}$. Moreover, the cumulative impact on radiative forcing, at year 100, was computed as $4.596 * 10^{-5} \frac{W}{m^2}$ for the utilization approach. This result illustrates the necessity of incorporating the final consumption of the DMC product when assessing the gate-to-grave impact associated

with the utilization approach. Consequently, the ensuing comparison will entail a value of $6.497 * 10^{-5} \frac{W}{m^2}$ for the cumulative impact on radiative forcing at year 100.

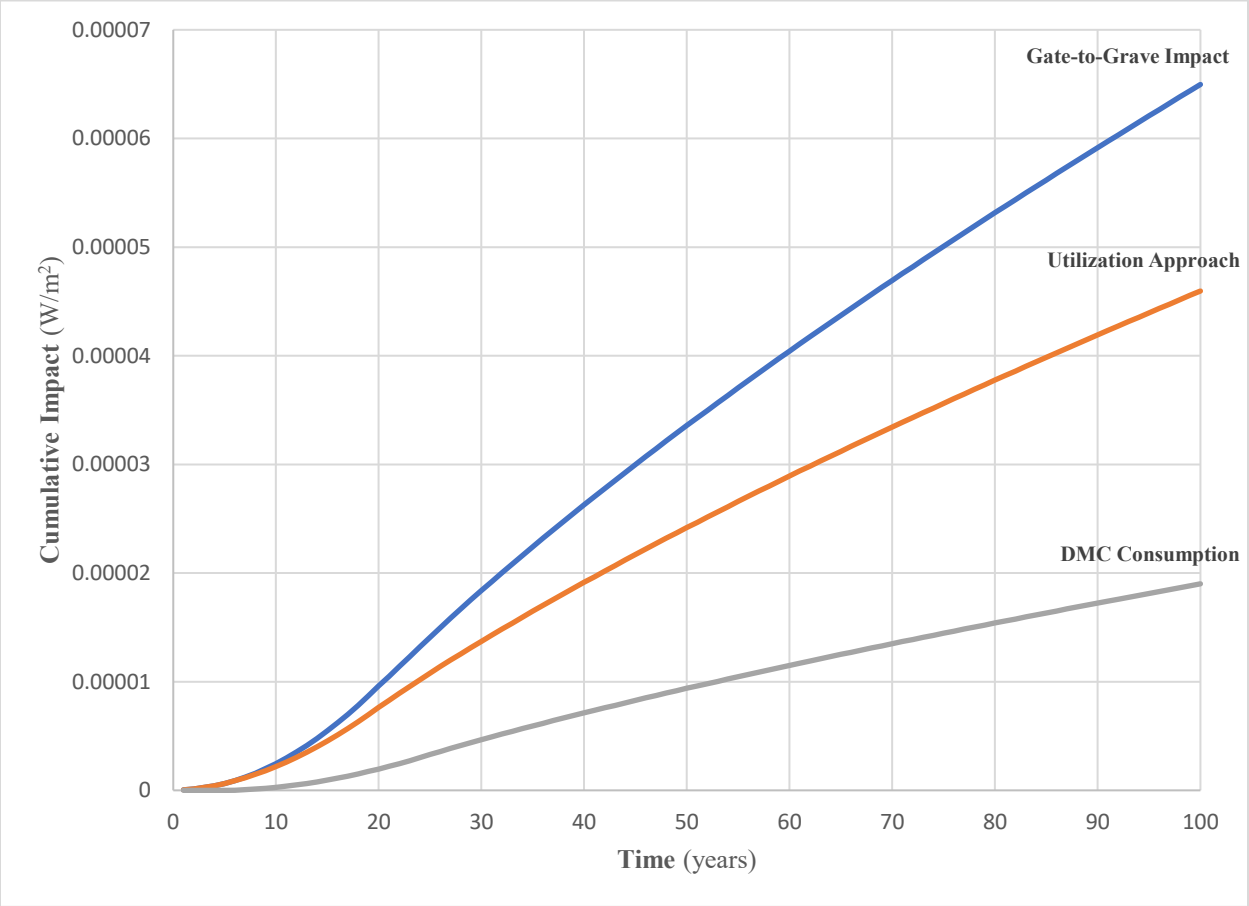

Figure 4.7 Gate-to-grave impact for the DMC utilization approach

The ultimate consumption of the DMC product occurs after storing CO_2 for a 5-year duration period in both the conventional and utilization approaches. This is undertaken so as to maintain consistency within the ensuing comparison-based assessment. Accounting for this, the cumulative impact on radiative forcing is computed and graphed as portrayed within Figure 4.8. At year 100, the cumulative impact on radiative forcing related to consuming the DMC product is obtained as $1.901 * 10^{-5} \frac{W}{m^2}$. Moreover, the cumulative impact on radiative forcing, at year 100, was computed as $3.217 * 10^{-5} \frac{W}{m^2}$ for the conventional approach. When assessing the gate-to-

grave impact related to the conventional approach, the following comparison will entail a value of $5.118 * 10^{-5} \frac{W}{m^2}$ for the cumulative impact on radiative forcing at year 100.

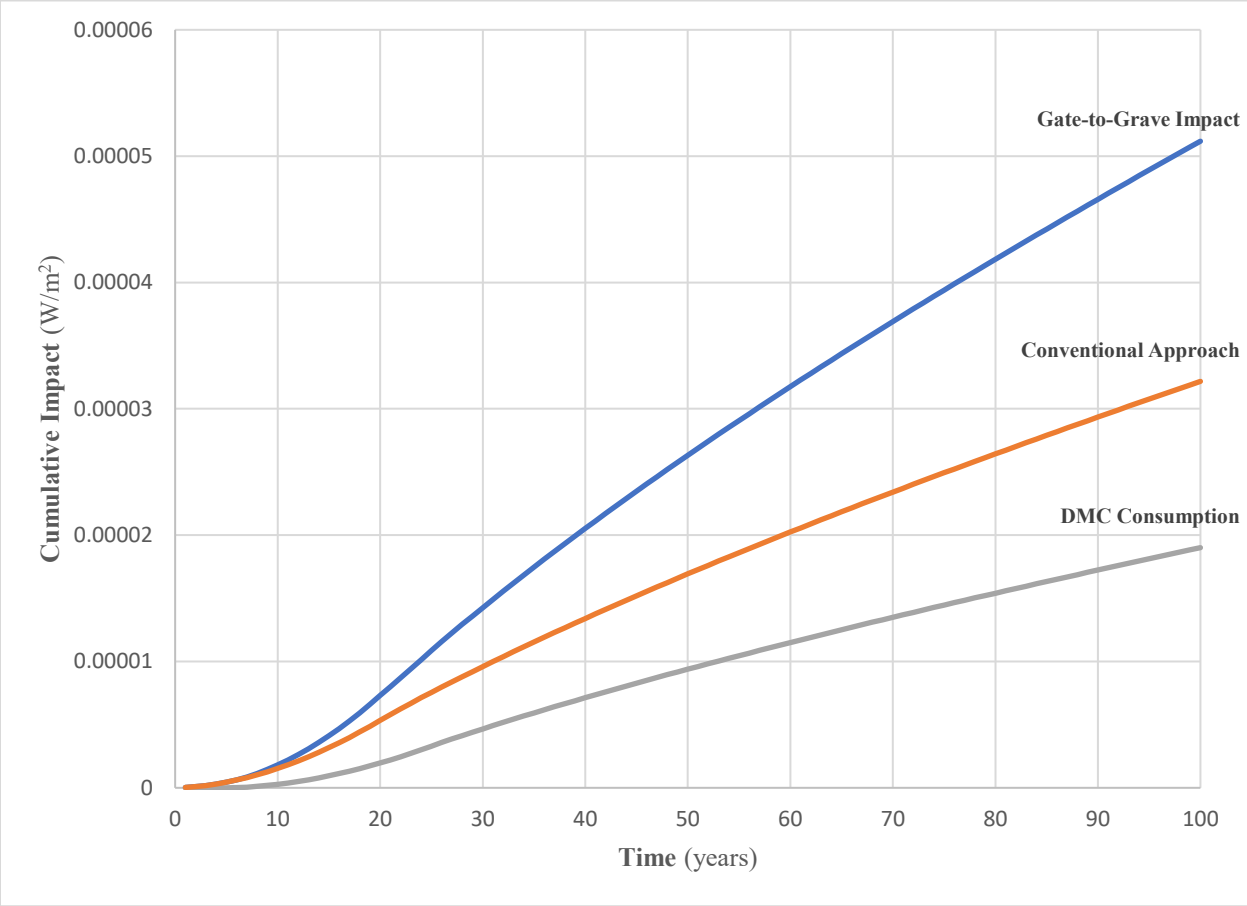

Figure 4.8 Gate-to-grave impact for the DMC conventional approach

As mentioned previously, this approach does not assume a free source of CO_2 and considers the amount of energy required to capture it. Accounting for the crucial factors, Figure 4.9 portrays the cradle-to-grave environmental assessment for both the conventional and utilization approaches of manufacturing DMC. Notably, the utilization approach yields a higher cumulative impact on radiative forcing, at year 100, when contrasted against the conventional approach. This is apparent within Figure 4.9 where the utilization approach is seen to yield $5.859 * 10^{-5} \frac{W}{m^2}$ versus $5.118 * 10^{-5} \frac{W}{m^2}$ which is attained in the conventional approach. Therefore, it is better to employ the

conventional approach of manufacturing DMC as it provides a lower impact. Employing the utilization approach results in $7.401 * 10^{-6} \frac{W}{m^2}$ to be added to the burden of employing the conventional approach. The percent increase in the cumulative impact of radiative forcing, at year 100, is also calculated as 14.46 %. Remarkably, a decreasing trend is apparent for the percent increase in the burden over the 100-year time period.

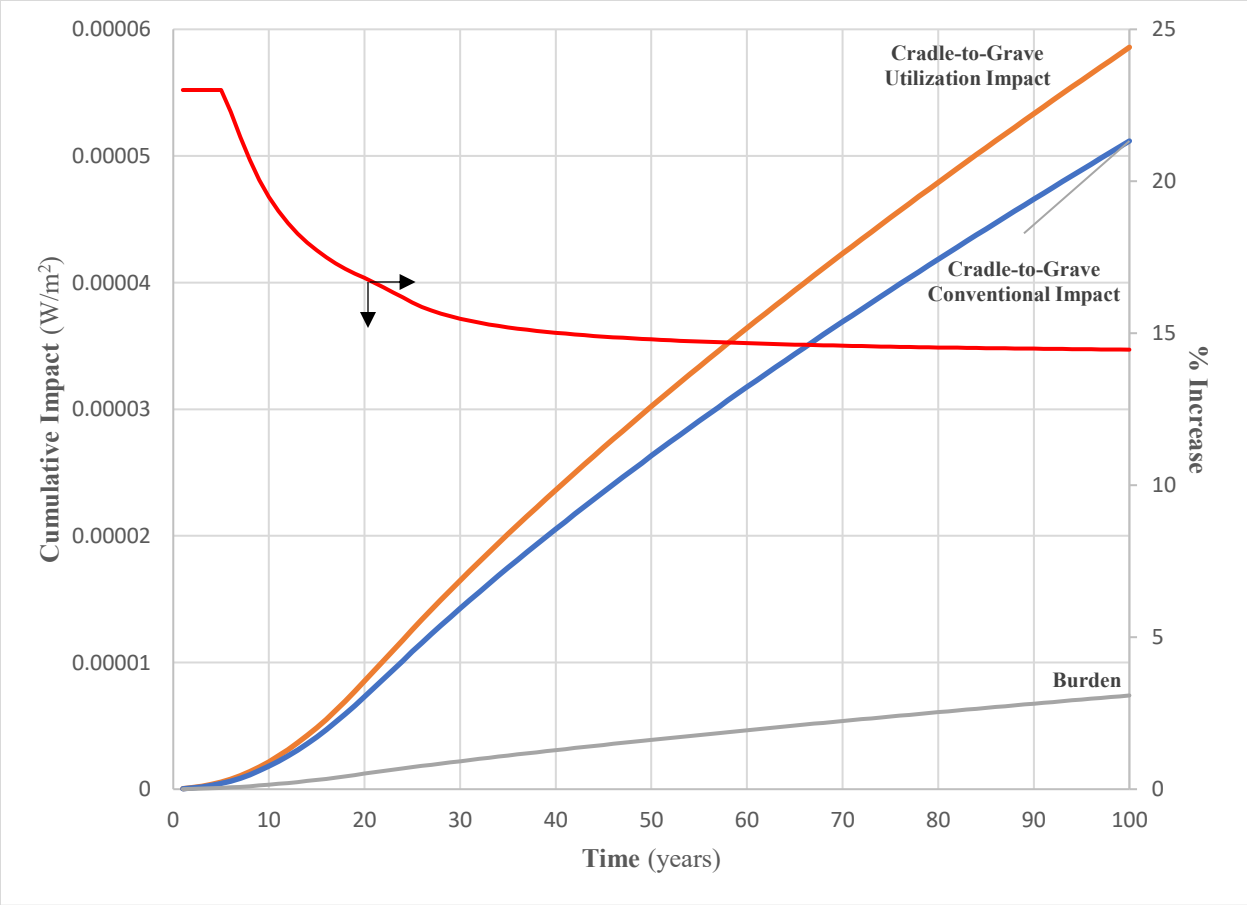

Figure 4.9 Cradle-to-grave impacts for DMC production

4.3 Sensitivity Analysis for MeOH Production

In order to comprehend the environmental benefits associated with the CO_2 storage duration in the MeOH product, a sensitivity analysis was conducted. The time, in years, within which the CO_2 is stored within the MeOH product is increased and this is represented as td. Thereafter, the utilization scenario was tested by increasing the CO_2 storage duration within the MeOH product. Figure 4.10 illustrates the sensitivity analysis conducted for the utilization route. Evidently, increasing the CO_2 storage duration within the commercial MeOH product has a beneficial impact on the environment. This can be seen in the utilization scenario where an increase in the CO_2 storage duration yields a relative decrease in the cumulative impact on radiative forcing at year 200.

In this study, the MeOH product is assumed to be further utilized in the manufacture of formaldehyde. As previously aforementioned, the CO_2 storage duration, within the commercial formaldehyde product, is assumed to be 5 years and the formaldehyde product will be further utilized in the automotive industry. If the final product could store CO_2 for 20 years the cumulative impact on radiative forcing, at year 200, would decrease from $6.547 * 10^{-5} \frac{W}{m^2}$ to $6.338 * 10^{-5} \frac{W}{m^2}$. This signifies a 3.192 % decrease relative to the utilization scenario. Although this is a slight decrease, this is feasible for the formaldehyde product as it has various applications in building activities. However, if the final product could store CO_2 for 100 years the cumulative impact on radiative forcing, at year 200, would decrease from $6.547 * 10^{-5} \frac{W}{m^2}$ to $5.143 * 10^{-5} \frac{W}{m^2}$. This signifies a 21.44 % decrease relative to the utilization scenario. While this decrease is significant, it is very unlikely for the MeOH product to retain CO_2 for a 100-year duration since none of its current applications last that long. Notably, most energy products are typically consumed within a short time frame resulting in a CO_2 storage duration of 0 years. Consequently, if the MeOH product is further converted to an energy product this will increase the cumulative impact on radiative forcing, at year 200, from $6.547 * 10^{-5} \frac{W}{m^2}$ to $6.616 * 10^{-5} \frac{W}{m^2}$. This signifies a 1.043 % increase relative to the utilization approach.

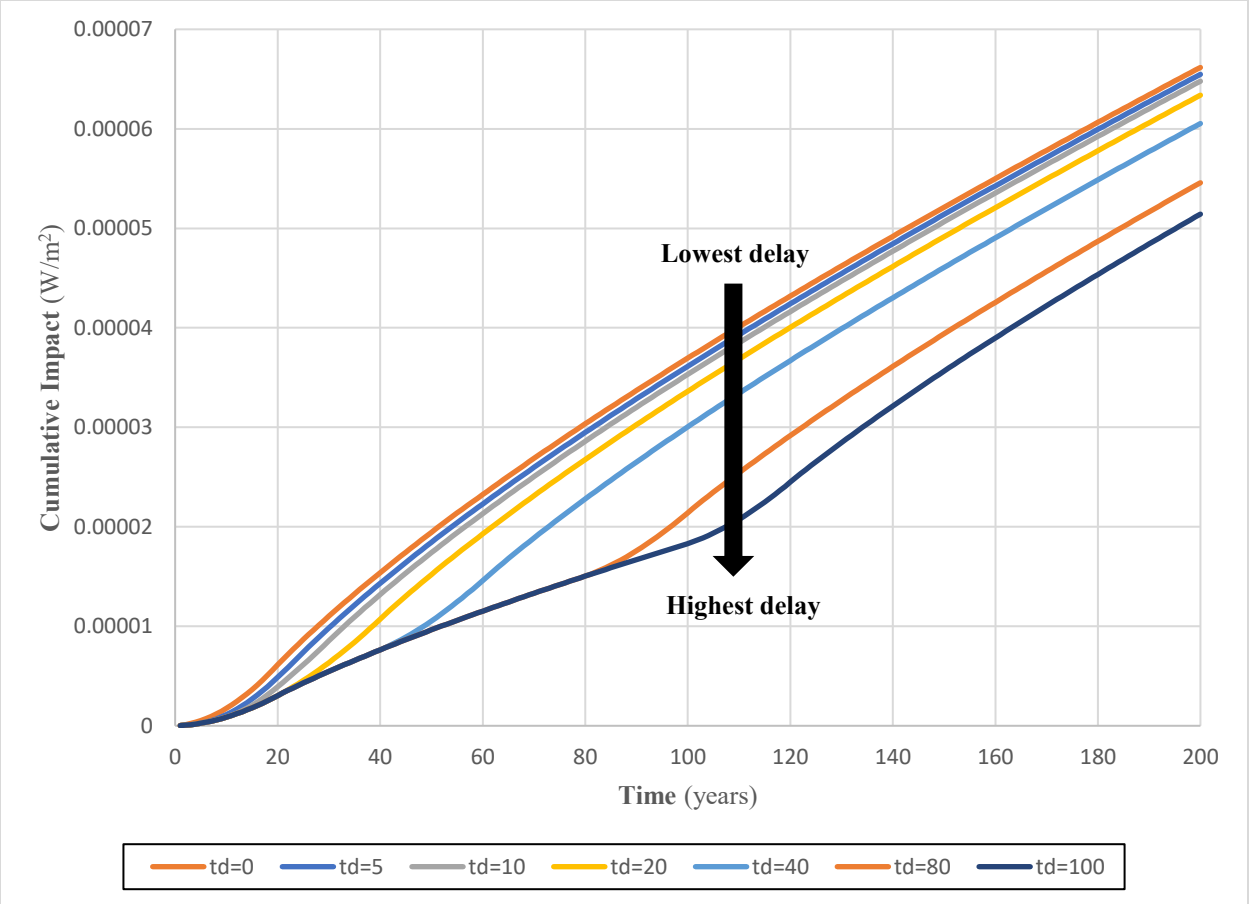

Figure 4.10 Sensitivity analysis for the MeOH utilization approach

4.4 Sensitivity Analysis for DMC Production

Similarly, a sensitivity analysis was undertaken so as to comprehend the environmental benefits associated with the CO_2 storage duration in the DMC product. Furthermore, the utilization approach is tested by incrementally increasing the CO_2 storage duration within the DMC product. Figure 4.11 exemplifies the employed sensitivity analysis for the utilization approach. The time, in years, within which the CO_2 is stored in the DMC product is denoted as td. Consequently, increasing the CO_2 storage duration within the DMC product seems to yield a positive impact on the environment.

In this work, the DMC product is assumed to be further used in the manufacture of Pc. As previously stated, the CO_2 storage duration, within the commercial Pc product, is assumed to be 5 years and the Pc product will be further used in the automotive industry. Increasing the CO_2 storage duration to 20 years results in the cumulative impact on radiative forcing, at year 200, to decrease from $1.057 * 10^{-4} \frac{W}{m^2}$ to $1.035 * 10^{-4} \frac{W}{m^2}$. This illustrates a 2.081 % decrease relative to the utilization scenario. Since Pc has multiple applications in building activities, this slight decrease is feasible in operation. Further increasing the CO_2 storage duration to 100 years results in the cumulative impact on radiative forcing, at year 200, to decrease from $1.057 * 10^{-4} \frac{W}{m^2}$ to $9.075 * 10^{-5} \frac{W}{m^2}$. This signifies a 14.14 % decrease relative to the utilization scenario. This substantial decrease is probable if the Pc product is further utilized in constructing sound walls that last for 100 years. However, if the DMC product is further utilized in conjunction with an energy product this will increase the cumulative impact on radiative forcing, at year 200, from $1.057 * 10^{-4} \frac{W}{m^2}$ to $1.065 * 10^{-4} \frac{W}{m^2}$. This signifies a 0.757 % increase relative to the utilization approach.

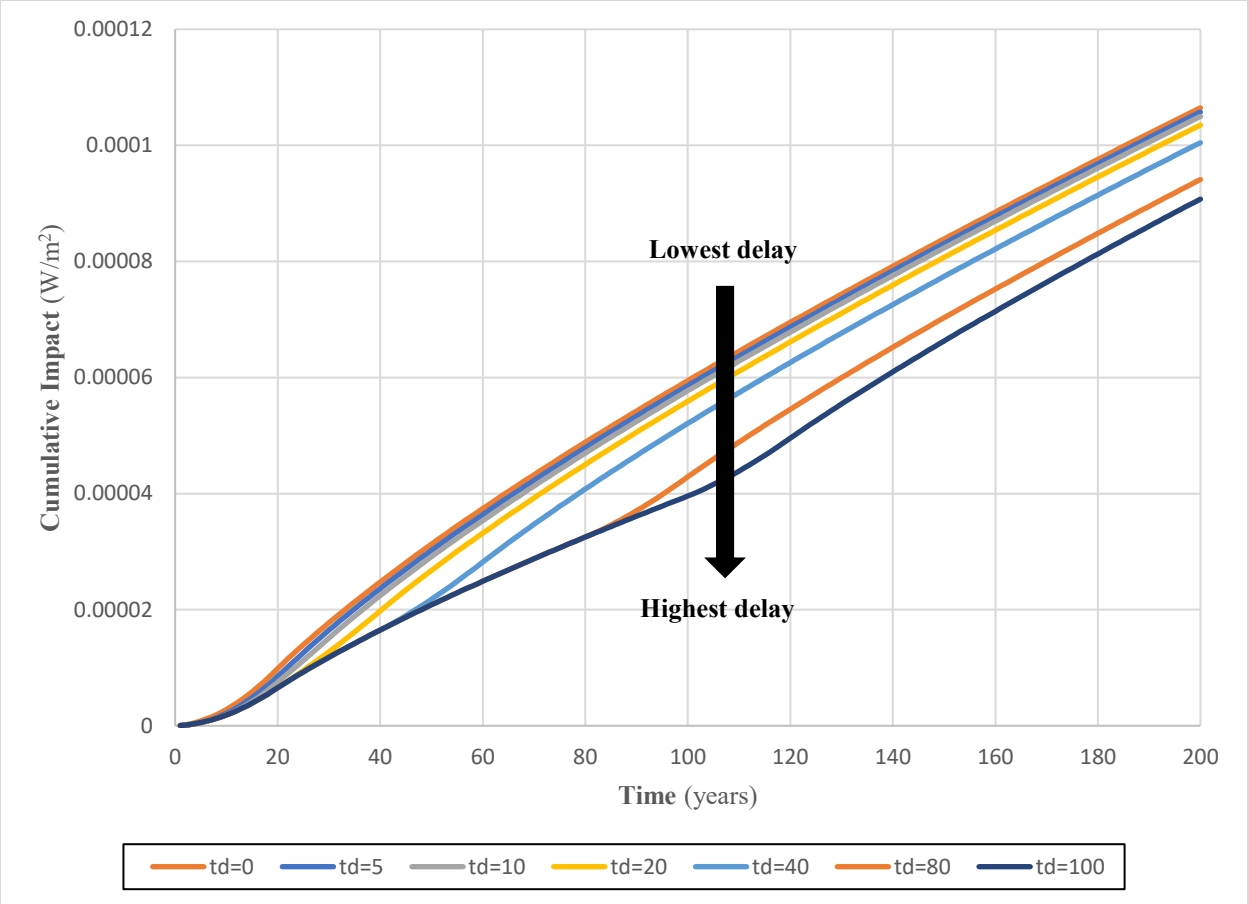

Figure 4.11 Sensitivity analysis for the DMC utilization approach

Chapter 5: Conclusions and Recommendations

5.1 Conclusions

This thesis primarily revolved around the environmental analysis of CCU processes and products through the use of the dynamic LCA methodology. The dynamic LCA approach addresses crucial limitations present within the static LCA and enhances the accuracy of the LCA methodology by implementing a temporal-based framework. As a result, this allowed for a justifiable and reliable environmental assessment to be conducted. Moreover, the scope of the assessment was focused on the analysis of both commercial MeOH and DMC. Two approaches, the conventional and the CO_2 utilization route, were considered and contrasted so as to verify the environmental benefits of employing CCU. Summing up, the dynamic LCA framework was essential in accounting for time varying emissions. Moreover, the inherent flexibility within the tool, permitting a sensitivity analysis to transpire, proved to be extremely useful in comprehending the effect of increasing the CO_2 storage duration within the products.

To sum up, the utilization approach of manufacturing commercial MeOH proved to be a better alternative, from an environmental standpoint, when contrasted against the conventional approach. Remarkably, $7.147 * 10^{-6} \frac{W}{m^2}$ of radiative forcing, at year 100, was evaded when employing the utilization route. Furthermore, the percent reduction in the cumulative impact of radiative forcing, at year 100, was also computed as 16.51 %. If the final MeOH product could store CO_2 for 100 years, the cumulative impact on radiative forcing, at year 200, would decrease from $6.547 * 10^{-5} \frac{W}{m^2}$ to $5.143 * 10^{-5} \frac{W}{m^2}$. This signifies a 21.44 % decrease relative to the utilization scenario. Consequently, the sensitivity analysis showed that increasing the CO_2 storage duration within the commercial MeOH product results in a substantial decrease in the cumulative impact on radiative forcing. However, inordinate caution must be taken into account when assessing the feasibility of delaying CO_2 emissions over a long-term duration since current MeOH applications do not last that long.

Overall, the conventional approach of manufacturing commercial DMC resulted in an inferior impact when contrasted against the utilization approach. Notably, the resultant effect of

broadening the assessment boundary yielded in a reversal of the final conclusions. Therefore, the employed cradle-to-grave analysis resulted in the conventional approach being superior, from an environmental perspective, to the utilization approach. Whereas, a gate-to-gate assessment concluded that the utilization approach is superior, from an environmental viewpoint, to the conventional approach (Kongpanna et al., 2016). Consequently, the choice of the boundary plays a pivotal role when assessing environmental impacts. When undertaking the utilization route, $7.401 * 10^{-6} \frac{W}{m^2}$ of cumulative radiative forcing, at year 100, was added to the conventional approach of manufacturing DMC. Additionally, the percent increase in the cumulative impact of radiative forcing, at year 100, was also computed as 14.46 %. If the ultimate DMC product could store CO_2 for a duration of 100 years, the cumulative impact on radiative forcing, at year 200, would decrease from $1.057 * 10^{-4} \frac{W}{m^2}$ to $9.075 * 10^{-5} \frac{W}{m^2}$. This signifies a 14.14 % decrease relative to the utilization scenario. Accordingly, the sensitivity analysis showed that increasing the CO_2 storage duration within the DMC product results in a lower cumulative impact on radiative forcing.

5.2 Recommendations

Within the domain of this work, an environmental assessment was utilized to contrast two diverse routes of manufacturing commercial MeOH and DMC. However, the basis within which the comparison-based assessment was conducted places an emphasis solely on an environmental standpoint. Therefore, future work is still necessitated so as to incorporate a techno-economic analysis to the current environmental assessment. Integrating other crucial viewpoints into the current assessment permits for a comprehensive comparison-based assessment. One plausible approach that takes into account a techno, economic, and environmental assessment is termed the 3E triangle model (Pan, Lorente Lafuente, & Chiang, 2016). This methodology allows for a comprehensive assessment to be allocated to the discussed approaches by assessing the processes through three different lenses. Moreover, five zones are utilized to assess the performance, cost, and impact of the analyzed process. Within future work, this procedure could be implemented so as to further provide an inclusive assessment to the conventional and utilization processes discussed within this work. This would further allow for an inclusive validation, from three viewpoints, to the process's relative feasibility in operation.

Regarding the developed conventional and utilization approaches to manufacture MeOH, further optimization could also be allocated to the processes. Heat exchangers implementing heat integration to the model is one plausible methodology of enhancing the MeOH model (Milani et al., 2015). In turn, this diminishes the amount of essential resources required to match the immense thermal duties present within both processes. Within future work, various schemes employing heat integration to the MeOH processes could be explored so as to minimize the large thermal duties. Therefore, it is essential to further explore optimal heat integration schemes in order to reduce the net CO_2 emitted within the aforementioned processes.

References

Albo, J., Luis, P., & Irabien, A. (2010). Carbon Dioxide Capture from Flue Gases Using a Cross-Flow Membrane Contactor and the Ionic Liquid 1-Ethyl-3-methylimidazolium Ethylsulfate. *Industrial & Engineering Chemistry Research*, *49*(21), 11045–11051. https://doi.org/10.1021/ie1014266

Al-Kalbani, H., Xuan, J., García, S., & Wang, H. (2016). Comparative energetic assessment of methanol production from CO2: Chemical versus electrochemical process. *Applied Energy*, *165*, 1–13. https://doi.org/10.1016/j.apenergy.2015.12.027

Andersson, A., Hernelind, M., & Augustsson, O. (2006). A study of the ageing and deactivation phenomena occurring during operation of an iron molybdate catalyst in formaldehyde production. *Catalysis Today*, *112*(1–4), 40–44. https://doi.org/10.1016/j.cattod.2005.11.052

Aneke, M., & Wang, M. (2015). Potential for improving the energy efficiency of cryogenic air separation unit (ASU) using binary heat recovery cycles. *Applied Thermal Engineering*, *81*, 223–231. https://doi.org/10.1016/j.applthermaleng.2015.02.034

Araújo, A., & Skogestad, S. (2008). Control structure design for the ammonia synthesis process. *Computers & Chemical Engineering*, *32*(12), 2920–2932. https://doi.org/10.1016/j.compchemeng.2008.03.001

Aresta, M., Caroppo, A., Dibenedetto, A., & Narracci, M. (2002). *Life Cycle Assessment (LCA) Applied to the Synthesis of Methanol. Comparison of the Use of Syngas with the Use of CO2 and Dihydrogen Produced from Renewables. In Environmental Challenges and Greenhouse Gas Control for Fossil Fuel Utilization in the 21st Century; Maroto-Valer, M. M., Song, C., Soong, Y., Eds.; Springer US: Boston, MA,*. https://doi.org/10.1007/978-1-4615-0773-4

Aresta, M., & Galatola, M. (1999). Life cycle analysis applied to the assessment of the environmental impact of alternative synthetic processes. The dimethylcarbonate case: Part 1. *Journal of Cleaner Production*, *7*(3), 181–193. https://doi.org/10.1016/S0959-6526(98)00074-2

Aspen Plus™. (2017). Aspen Plus Technology, Inc., Bedford, MA, USA. Aspen Plus Version 10.

Babad, H., & Zeiler, A. G. (1973). Chemistry of phosgene. *Chemical Reviews*, *73*(1), 75–91. https://doi.org/10.1021/cr60281a005

Beloin-Saint-Pierre, D., Heijungs, R., & Blanc, I. (2014). The ESPA (Enhanced Structural Path Analysis) method: A solution to an implementation challenge for dynamic life cycle

assessment studies. *The International Journal of Life Cycle Assessment*, *19*(4), 861–871. https://doi.org/10.1007/s11367-014-0710-9

Beloin-Saint-Pierre, D., Levasseur, A., Margni, M., & Blanc, I. (2017). Implementing a Dynamic Life Cycle Assessment Methodology with a Case Study on Domestic Hot Water Production. *Journal of Industrial Ecology*, *21*(5), 1128–1138. https://doi.org/10.1111/jiec.12499

Brandão, M., Levasseur, A., Kirschbaum, M. U. F., Weidema, B. P., Cowie, A. L., Jørgensen, S. V., … Chomkhamsri, K. (2013). Key issues and options in accounting for carbon sequestration and temporary storage in life cycle assessment and carbon footprinting. *The International Journal of Life Cycle Assessment*, *18*(1), 230–240. https://doi.org/10.1007/s11367-012-0451-6

BSI (British Standards Institution). PAS 2050: 2008 Specification for the assessment of the life cycle greenhouse gas emissions of goods and services. London, UK: BSI. (2008).

Cabezas, H., Bare, J. C., & Mallick, S. K. (1999). Pollution prevention with chemical process simulators: The generalized waste reduction (WAR) algorithm—full version. *Computers & Chemical Engineering*, *23*(4–5), 623–634. https://doi.org/10.1016/S0098-1354(98)00298-1

Cao, Y., Cheng, H., Ma, L., Liu, F., & Liu, Z. (2012). Research Progress in the Direct Synthesis of Dimethyl Carbonate from CO2 and Methanol. *Catalysis Surveys from Asia*, *16*(3), 138–147. https://doi.org/10.1007/s10563-012-9140-5

Cetesb. (2009). Retrieved February 9, 2019, from http://www.cetesb.sp.gov.br/arquivos_default/100co2. pdf

Chu, S., & Majumdar, A. (2012). Opportunities and challenges for a sustainable energy future. *Nature*, *488*(7411), 294.

City Environmental Quality Review (CEQR) Technical Manual. New York City Mayor's Office of Environmental Coordination. (2012). Retrieved February 10, 2019, from http://www.nyc.gov/html/oec/downloads/pdf/2012_ceqr_tm.

Cook, J., Oreskes, N., Doran, P. T., Anderegg, W. R. L., Verheggen, B., Maibach, E. W., … Rice, K. (2016). Consensus on consensus: A synthesis of consensus estimates on human-caused global warming. *Environmental Research Letters*, *11*(4), 048002. https://doi.org/10.1088/1748-9326/11/4/048002

Costa, P. M., & Wilson, C. (1999). *AN EQUIVALENCE FACTOR BETWEEN CO2 AVOIDED EMISSIONS AND SEQUESTRATION – DESCRIPTION AND APPLICATIONS IN FORESTRY*. 10.

Curran, M. A. (2012). *Life Cycle Assessment Handbook: A Guide for Environmentally Sustainable Products*. John Wiley & Sons.

Dahl, P. J., Christensen, T. S., Winter-Madsen, S., & King, S. M. (2014). *Proven autothermal reforming technology for modern large-scale methanol plants. In: Nitrogen + Syngas 2014 International Conferences & Exhibition, 24–27 February, Paris, France.* 12.

Dillon, D. M., & Iwamoto, R. Y. (1990). *United States Patent No. US4891049A*.

EIA. (2019). U.S. Energy Information Administration (EIA). Retrieved March 25, 2019, from https://www.eia.gov/tools/faqs/faq.php?id=73&t=11

Environmental Protection Authority of Australia. (2002). Retrieved February 10, 2019, from http://www. epa.wa.gov.au/docs/1522_B1075.pdf

European Commission, Joint Research Centre, Institute for Environment and Sustainability. International reference life cycle data system (ILCD) handbook – General guide for life cycle assessment – Detailed guidance. Luxembourg: Publications Office of the European Union. (2010).

Forster, P., Ramaswamy, V., Artaxo, P., Berntsen, T., Betts, R., Fahey, D. W., … Van Dorland, R. (2007). Changes in Atmospheric Constituents and in Radiative Forcing. In: Climate Change 2007: The Physical Science Basis. Contribution of Working Group I to the Fourth Assessment Report of the Intergovernmental Panel on Climate Change [Solomon, S., D. Qin, M. Manning, Z. Chen, M. Marquis, K.B. Averyt, M.Tignor and H.L. Miller (eds.)]. Cambridge University Press, Cambridge, United Kingdom and New York, NY, USA. Retrieved March 19, 2019, from https://archive.ipcc.ch/publications_and_data/ar4/wg1/en/ch2.html

Garcia-Herrero, I., Alvarez-Guerra, M., & Irabien, A. (2016). Electrosynthesis of dimethyl carbonate from methanol and CO_2 using potassium methoxide and the ionic liquid [bmim][Br] in a filter-press cell: A study of the influence of cell configuration: Electrosynthesis of DMC from methanol and CO_2. *Journal of Chemical Technology & Biotechnology*, *91*(2), 507–513. https://doi.org/10.1002/jctb.4605

Garcia-Herrero, I., Cuéllar-Franca, R. M., Enríquez-Gutiérrez, V. M., Alvarez-Guerra, M., Irabien, A., & Azapagic, A. (2016). Environmental Assessment of Dimethyl Carbonate Production: Comparison of a Novel Electrosynthesis Route Utilizing CO_2 with a Commercial Oxidative Carbonylation Process. *ACS Sustainable Chemistry & Engineering*, *4*(4), 2088–2097. https://doi.org/10.1021/acssuschemeng.5b01515

Giammario, A., Leung, J., MacDonald, L., Hale, H., Carrier, A.-F., Ryan, S., & Pratt, L. (2018, April 13). National Inventory Report 1990-2016: Greenhouse gas sources and sinks in Canada, environment and climate change Canada.

Goedkoop, M., Heijungs, R., Huijbregts, M., De Schryver, A., Struijs, J., & van Zelm, R. (2009, January 6). ReCiPe 2008 A Life Cycle Impact Assessment Method Which Comprises Harmonized Category Indicators at the Midpoint and the Endpoint Level. Ruimte en Milieu.

Harder, W., Merger, F., & Towae, F. (1984). *United States Patent No. US4436668A*.

Heijungs, R., Guinee, J. B., Huppes, G., Lankreijer, R. M., Udo de Haes, H. A., Wegener Sleeswijk, A., … de Goede, H. P. (1992). Environmental life cycle assessment of products—Guide and background. Centre of Environmental Sciences, Leiden University, Leiden.

Huang, C., & Tan, C. S. (2014). A Review: CO2 Utilization. *Aerosol And Air Quality Research*, *14*(2), 480–499. https://doi.org/10.4209/aaqr.2013.10.0326

International Organization for Standardization. (2006a, July 1). ISO 14040—Environmental management—Life cycle assessment—Principles and framework. Management environnemental—Analyse du cycle de vie—Principes et cadre. Switzerland.

International Organization for Standardization. (2006b, July 1). ISO 14044—Environmental management—Life cycle assessment—Requirements and guidelines. Management environnemental—Analyse du cycle de vie—Exigences et lignes directrices. Switzerland.

IPCC, 2013: Climate Change 2013: The Physical Science Basis. Contribution of Working Group I to the Fifth Assessment Report of the Intergovernmental Panel on Climate Change [Stocker, T.F., D. Qin, G.-K. Plattner, M. Tignor, S.K. Allen, J. Boschung, A. Nauels, Y. Xia, V. Bex and P.M. Midgley (eds.)]. Cambridge University Press, Cambridge, United Kingdom and New York, NY, USA, 1535 pp, doi:10.1017/CBO9781107415324. (2013). Retrieved March 23, 2019, from https://archive.ipcc.ch/report/ar5/wg1/

Jagtap, S. R., Bhor, M. D., & Bhanage, B. M. (2008). Synthesis of dimethyl carbonate via transesterification of ethylene carbonate with methanol using poly-4-vinyl pyridine as a novel base catalyst. *Catalysis Communications*, *9*(9), 1928–1931. https://doi.org/10.1016/j.catcom.2008.03.029

Jagtap, S. R., Raje, V. P., Samant, S. D., & Bhanage, B. M. (2007). Silica supported polyvinyl pyridine as a highly active heterogeneous base catalyst for the synthesis of cyclic carbonates from carbon dioxide and epoxides. *Journal of Molecular Catalysis A: Chemical*, *266*(1–2), 69–74. https://doi.org/10.1016/j.molcata.2006.10.033

Jarvis, S. M., & Samsatli, S. (2018). Technologies and infrastructures underpinning future CO2 value chains: A comprehensive review and comparative analysis. *Renewable and Sustainable Energy Reviews*, *85*, 46–68. https://doi.org/10.1016/j.rser.2018.01.007

Jing, F., Tan, H., & Lu, Y. (2017). *China Patent No. CN206418062U*.

Joos, F., Prentice, I. C., Sitch, S., Meyer, R., Hooss, G., Plattner, G.-K., … Hasselmann, K. (2001). Global warming feedbacks on terrestrial carbon uptake under the Intergovernmental Panel on Climate Change (IPCC) Emission Scenarios. *Global Biogeochemical Cycles*, *15*(4), 891–907. https://doi.org/10.1029/2000GB001375

Kalakul, S., Malakul, P., Siemanond, K., & Gani, R. (2014). Integration of life cycle assessment software with tools for economic and sustainability analyses and process simulation for sustainable process design. *Journal of Cleaner Production*, *71*, 98–109. https://doi.org/10.1016/j.jclepro.2014.01.022

Karimi, M., Hillestad, M., & Svendsen, H. F. (2012). Natural Gas Combined Cycle Power Plant Integrated to Capture Plant. *Energy & Fuels*, *26*(3), 1805–1813. https://doi.org/10.1021/ef201921s

Keller, N., Rebmann, G., & Keller, V. (2010). Catalysts, mechanisms and industrial processes for the dimethylcarbonate synthesis. *Journal of Molecular Catalysis A: Chemical*, *317*(1–2), 1–18. https://doi.org/10.1016/j.molcata.2009.10.027

Kendall, A., Chang, B., & Sharpe, B. (2009). Accounting for Time-Dependent Effects in Biofuel Life Cycle Greenhouse Gas Emissions Calculations. *Environmental Science & Technology*, *43*(18), 7142–7147. https://doi.org/10.1021/es900529u

Kim, D.-W., Kim, C.-W., Koh, J.-C., & Park, D.-W. (2010). Synthesis of dimethyl carbonate from ethylene carbonate and methanol using immobilized ionic liquid on amorphous silica. *Journal of Industrial and Engineering Chemistry*, *16*(3), 474–478. https://doi.org/10.1016/j.jiec.2010.01.054

Klöpffer, W. (2006). The Role of SETAC in the Development of LCA. *The International Journal of Life Cycle Assessment*, *11*(S1), 116–122. https://doi.org/10.1065/lca2006.04.019

Knifton, J. F. (1987). *United States Patent No. US4661609A*.

Kondoh, T., Okada, Y., Tanaka, F., Asaoka, S., & Yamamoto, S. (1995). *United States Patent No. US5436362A*.

Kongpanna, P., Babi, D. K., Pavarajarn, V., Assabumrungrat, S., & Gani, R. (2016). *Systematic methods and tools for design of sustainable chemical processes for CO2 utilization*.

Kongpanna, P., Pavarajarn, V., Gani, R., & Assabumrungrat, S. (2015). Techno-economic evaluation of different CO2-based processes for dimethyl carbonate production. *Chemical Engineering Research and Design*, *93*, 496–510. https://doi.org/10.1016/j.cherd.2014.07.013

Kricsfalussy, Z., Waldmann, H., Traenckner, H.-J., Zlokarnik, M., & Schomacker, R. (1993). *United States Patent No. US5233072A*.

Lashof, D., & Hare, B. (1999). The role of biotic carbon stocks in stabilizing greenhouse gas concentrations at safe levels. *Environmental Science & Policy*, *2*(2), 101–109. https://doi.org/10.1016/S1462-9011(98)00045-8

Levasseur, A., Lesage, P., Margni, M., Brandão, M., & Samson, R. (2012). Assessing temporary carbon sequestration and storage projects through land use, land-use change and forestry: Comparison of dynamic life cycle assessment with ton-year approaches. *Climatic Change*, *115*(3–4), 759–776. https://doi.org/10.1007/s10584-012-0473-x

Levasseur, A., Lesage, P., Margni, M., Deschenes, L., & Samson, R. (2010). Considering time in LCA: Dynamic LCA and its application to global warming impact assessments. *Environmental Science & Technology*, *44*(8), 3169–3174.

Levasseur, A., Lesage, P., Margni, M., & Samson, R. (2013). Biogenic carbon and temporary storage addressed with dynamic life cycle assessment. *Journal of Industrial Ecology*, *17*(1), 117–128.

Li, F., Xiao, L., Xia, C., & Hu, B. (2004). Chemical fixation of CO2 with highly efficient ZnCl2/[BMIm]Br catalyst system. *Tetrahedron Letters*, *45*(45), 8307–8310. https://doi.org/10.1016/j.tetlet.2004.09.074

Lin, H., Yang, B., Sun, J., Wang, X., & Wang, D. (2004). Kinetics studies for the synthesis of dimethyl carbonate from urea and methanol. *Chemical Engineering Journal*, *103*(1–3), 21–27. https://doi.org/10.1016/j.cej.2004.07.003

Matzen, M., & Demirel, Y. (2016). Methanol and dimethyl ether from renewable hydrogen and carbon dioxide: Alternative fuels production and life-cycle assessment. *Journal of Cleaner Production*, *139*, 1068–1077. https://doi.org/10.1016/j.jclepro.2016.08.163

Mbuyi, K. G., Scurrell, M. S., Hildebrandt, D., & Glasser, D. (2012). Conversion of Synthesis Gas to Dimethylether Over Gold-based Catalysts. *Topics in Catalysis*, *55*(11–13), 771–781. https://doi.org/10.1007/s11244-012-9865-4

Methanol Institute. (2015). The Methanol Industry. Retrieved June 18, 2019, from https://www.methanol.org/the-methanol-industry/

Meyer, L., De Coninck, H., Loos, M., Davidson, O. R., Metz, B., Intergovernmental Panel on Climate Change, issuing body, & Intergovernmental Panel on Climate Change. Working Group III, author. (2005). *IPCC special report on carbon dioxide capture and storage*. Retrieved from https://libproxy.wlu.ca/login?url=http://books.scholarsportal.info/viewdoc.html?id=/ebooks/ebooks0/gibson_cppc/2014-01-22/1/10785215

Milani, D., Khalilpour, R., Zahedi, G., & Abbas, A. (2015). A model-based analysis of CO2 utilization in methanol synthesis plant. *Journal of CO2 Utilization*, *10*, 12–22. https://doi.org/10.1016/j.jcou.2015.02.003

Monteiro, J. G. M.-S., de Queiroz Fernandes Araújo, O., & de Medeiros, J. L. (2009). Sustainability metrics for eco-technologies assessment, Part II. Life cycle analysis. *Clean Technologies and Environmental Policy*, *11*(4), 459–472. https://doi.org/10.1007/s10098-009-0205-8

Naejus, R., Coudert, R., Willmann, P., & Lemordant, D. (1998). Ion solvation in carbonate-based lithium battery electrolyte solutions. *Electrochimica Acta*, *43*(3–4), 275–284. https://doi.org/10.1016/S0013-4686(97)00073-X

NASA, G. C. (2019). Carbon dioxide concentration | NASA Global Climate Change. Retrieved February 19, 2019, from Climate Change: Vital Signs of the Planet website: https://climate.nasa.gov/vital-signs/carbon-dioxide

National Energy Board. (2017). Canada's Renewable Power Landscape 2017 – Energy Market Analysis.

Oh, T. H. (2010). Carbon capture and storage potential in coal-fired plant in Malaysia—A review. *Renewable and Sustainable Energy Reviews*, *14*(9), 2697–2709. https://doi.org/10.1016/j.rser.2010.06.003

O'Hare, M., Plevin, R. J., Martin, J. I., Jones, A. D., Kendall, A., & Hopson, E. (2009). Proper accounting for time increases crop-based biofuels' greenhouse gas deficit versus petroleum. *Environmental Research Letters*, *4*(2), 024001. https://doi.org/10.1088/1748-9326/4/2/024001

Olah, G. A. (2013). Towards Oil Independence Through Renewable Methanol Chemistry. *Angewandte Chemie International Edition*, *52*(1), 104–107. https://doi.org/10.1002/anie.201204995

Olivier, J. G. J., Schure, K. M., & Peters, J. A. H. W. (2017). *Trends in global CO2 and total greenhouse gas emissions — 2017 Report*. 69.

Ono, H., Fujii, H., Morikawa, H., & Fukui, A. (1982). *United States Patent No. US4321410A*.

Ott, J. rg, Gronemann, V., Pontzen, F., Fiedler, E., Grossmann, G., Burkhard Kersebohm, D., … Claus, W. (2012). Methanol, in: Ullmann's Encyclopedia of Industrial Chemistry.

Pacheco, M. A., & Marshall, C. L. (1997). Review of Dimethyl Carbonate (DMC) Manufacture and Its Characteristics as a Fuel Additive. *Energy & Fuels*, *11*(1), 2–29. https://doi.org/10.1021/ef9600974

Pan, S.-Y., Lorente Lafuente, A. M., & Chiang, P.-C. (2016). Engineering, environmental and economic performance evaluation of high-gravity carbonation process for carbon capture and utilization. *Applied Energy*, *170*, 269–277. https://doi.org/10.1016/j.apenergy.2016.02.103

Park, M.-S., Wang, G.-X., Kang, Y.-M., Wexler, D., Dou, S.-X., & Liu, H.-K. (2007). Preparation and Electrochemical Properties of SnO2 Nanowires for Application in Lithium-Ion Batteries. *Angewandte Chemie International Edition*, *46*(5), 750–753. https://doi.org/10.1002/anie.200603309

Peters, M., Köhler, B., Kuckshinrichs, W., Leitner, W., Markewitz, P., & Müller, T. E. (2011). Chemical Technologies for Exploiting and Recycling Carbon Dioxide into the Value Chain. *ChemSusChem*, *4*(9), 1216–1240. https://doi.org/10.1002/cssc.201000447

Pinsonnault, A., Lesage, P., Levasseur, A., & Samson, R. (2014). Temporal differentiation of background systems in LCA: Relevance of adding temporal information in LCI databases. *The International Journal of Life Cycle Assessment*, *19*(11), 1843–1853. https://doi.org/10.1007/s11367-014-0783-5

PlasticsEurope Eco-profiles. (2013). Retrieved January 27, 2019, from https://www.plasticseurope.org/en/resources/eco-profiles

PRe Product Ecology consultants B. V. The Netherlands—Data base SimaPro SP4. (2000). Retrieved June 22, 2019, from SimaPro website: www.pre.nl

Protocol, K. (1997). United Nations framework convention on climate change. *Kyoto Protocol, Kyoto*, *19*.

Quadrelli, E. A., Centi, G., Duplan, J.-L., & Perathoner, S. (2011). Carbon Dioxide Recycling: Emerging Large-Scale Technologies with Industrial Potential. *ChemSusChem*, *4*(9), 1194–1215. https://doi.org/10.1002/cssc.201100473

Ramaswamy, V., Boucher, O., Haigh, J., Hauglustaine, D., Haywood, J., Myhre, G., … Srinivasan, J. (2001). *Radiative Forcing of Climate Change. In: Climate Change 2001: The Scientific Basis. Contribution of Working Group I to the Third Assessment Report of the Intergovernmental Panel on Climate Change [Houghton, J.T., et al. (Eds.)]. Cambridge University Press, Cambridge, United Kingdom and New York, NY, USA, pp. 349–416*. 68.

Reap, J., Roman, F., Duncan, S., & Bras, B. (2008a). A survey of unresolved problems in life cycle assessment. *The International Journal of Life Cycle Assessment*, 15.

Reap, J., Roman, F., Duncan, S., & Bras, B. (2008b). A survey of unresolved problems in life cycle assessment: Part 1: goal and scope and inventory analysis. *The International Journal of Life Cycle Assessment*, *13*(4), 290–300. https://doi.org/10.1007/s11367-008-0008-x

Rezazadeh, F., Gale, W. F., Hughes, K. J., & Pourkashanian, M. (2015). Performance viability of a natural gas fired combined cycle power plant integrated with post-combustion CO 2 capture at part-load and temporary non-capture operations. *International Journal of Greenhouse Gas Control*, *39*, 397–406. https://doi.org/10.1016/j.ijggc.2015.06.003

Roh, K., Frauzem, R., Nguyen, T. B. H., Gani, R., & Lee, J. H. (2016). A methodology for the sustainable design and implementation strategy of CO2 utilization processes. *Computers and Chemical Engineering*, *91*, 407–421. https://doi.org/10.1016/j.compchemeng.2016.01.019

Roh, K., Lee, J. H., & Gani, R. (2016). A methodological framework for the development of feasible CO2 conversion processes. *International Journal of Greenhouse Gas Control*, *47*, 250–265. https://doi.org/10.1016/j.ijggc.2016.01.028

Romano, U., Tesei, R., Cipriani, G., & Micucci, L. (1980). *United States Patent No. US4218391A*.

Romano, U., Tesel, R., Mauri, M. M., & Rebora, P. (1980). Synthesis of Dimethyl Carbonate from Methanol, Carbon Monoxide, and Oxygen Catalyzed by Copper Compounds. *Industrial & Engineering Chemistry Product Research and Development*, *19*(3), 396–403. https://doi.org/10.1021/i360075a021

Rubin, E. S., Chen, C., & Rao, A. B. (2007). Cost and performance of fossil fuel power plants with CO2 capture and storage. *Energy Policy*, *35*(9), 4444–4454. https://doi.org/10.1016/j.enpol.2007.03.009

Saleh, R. Y., Michaelson, R. C., Suciu, E. N., & Kuhlmann, B. (1995). *World Intellectual Property Organization Patent No. WO199501736 9A1*.

Schwietzke, S., Griffin, W. M., & Matthews, H. S. (2011). Relevance of Emissions Timing in Biofuel Greenhouse Gases and Climate Impacts. *Environmental Science & Technology*, *45*(19), 8197–8203. https://doi.org/10.1021/es2016236

Sheppard, R. O., & Yakobson, D. L. (2003). *United States Patent No. US6632846B2*.

Shine, K. P., Berntsen, T. K., Fuglestvedt, J. S., Skeie, R. B., & Stuber, N. (2007). Comparing the climate effect of emissions of short- and long-lived climate agents. *Philosophical Transactions of the Royal Society A: Mathematical, Physical and Engineering Sciences*, *365*(1856), 1903–1914. https://doi.org/10.1098/rsta.2007.2050

Shukla, K., & Srivastava, V. C. (2017). Alkaline Earth (Ca, Mg) and Transition (La, Y) Metals Promotional Effects on Zn–Al Catalysts During Diethyl Carbonate Synthesis from Ethyl Carbamate and Ethanol. *Catalysis Letters*, *147*(8), 1891–1902. https://doi.org/10.1007/s10562-017-2097-2

Song, H., Jin, R., Kang, M., & Chen, J. (2013). Progress in synthesis of ethylene glycol through C1 chemical industry routes. *Chinese Journal of Catalysis*, *34*(6), 1035–1050. https://doi.org/10.1016/S1872-2067(12)60529-4

Souza, L. F. S., Ferreira, P. R. R., de Medeiros, J. L., Alves, R. M. B., & Araújo, O. Q. F. (2014). Production of DMC from CO_2 via Indirect Route: Technical–Economical–Environmental Assessment and Analysis. *ACS Sustainable Chemistry & Engineering*, *2*(1), 62–69. https://doi.org/10.1021/sc400279n

Sun, J., Yang, B., Wang, X., Wang, D., & Lin, H. (2005). Synthesis of dimethyl carbonate from urea and methanol using polyphosphoric acid as catalyst. *Journal of Molecular Catalysis A: Chemical*, *239*(1–2), 82–86. https://doi.org/10.1016/j.molcata.2005.06.001

Swiss Centre for Life Cycle Inventories. (2013). Ecoinvent Version 3.5. Retrieved January 27, 2019, from https://www.ecoinvent.org/

Tan, H.-Z., Wang, Z.-Q., Xu, Z.-N., Sun, J., Xu, Y.-P., Chen, Q.-S., … Guo, G.-C. (2018). Review on the synthesis of dimethyl carbonate. *Catalysis Today*, *316*, 2–12. https://doi.org/10.1016/j.cattod.2018.02.021

Tarun, C. B., Croiset, E., Douglas, P. L., Gupta, M., & Chowdhury, M. H. M. (2007). Techno-economic study of CO2 capture from natural gas based hydrogen plants. *International Journal of Greenhouse Gas Control*, *1*(1), 55–61. https://doi.org/10.1016/S1750-5836(07)00036-9

Thambimuthu, K., Gupta, M., & Davison, J. (2003). *CO2 capture and reuse*.

Tundo, P., & Selva, M. (2002). The Chemistry of Dimethyl Carbonate. *Accounts of Chemical Research*, *35*(9), 706–716. https://doi.org/10.1021/ar010076f

Udo de Haes, H. (2006). How to approach land use in LCIA or, how to avoid the Cinderella effect? *The International Journal of Life Cycle Assessment*, *11*(4), 219–221. https://doi.org/10.1065/lca2006.07.257

UNFCCC (United Nations Framework Convention on Climate Change), C. of the P. (COP). (1998). Report of the conference of the parties on its third session, held at Kyoto from 1 to 11 December 1997, addendum, FCCC/CP/1997/7/Add.1, United Nations Framework Convention on Climate Change. Retrieved March 12, 2019, from http://unfccc.int/cop5/resource/docs/cop3/07a01.pdf.

U.S. Environmental Protection Agency. Draft Regulatory Impact Analysis: Changes to Renewable Fuel Standard Program; EPA- 420-D-09-001; EPA: Washington, DC. (2009, May). Retrieved February 12, 2019, from https://19january2017snapshot.epa.gov/sites/production/files/2015-08/documents/420d09001.pdf

Van-Dal, É. S., & Bouallou, C. (2013). Design and simulation of a methanol production plant from CO2 hydrogenation. *Journal of Cleaner Production*, *57*, 38–45. https://doi.org/10.1016/j.jclepro.2013.06.008

Von Der Assen, N., Jung, J., & Bardow, A. (2013). Life-cycle assessment of carbon dioxide capture and utilization: Avoiding the pitfalls. *Energy & Environmental Science*, *6*(9), 2721–2734. https://doi.org/10.1039/c3ee41151f

Von der Assen, N. V., Lafuente, A. M. L., Peters, M., & Bardow, A. (2015). Chapter 4 — Environmental Assessment of CO2 Capture and Utilisation. In P. Styring, E. A. Quadrelli, & K. Armstrong (Eds.), *Carbon Dioxide Utilisation* (pp. 45–56). https://doi.org/10.1016/B978-0-444-62746-9.00004-9

Von der Assen, N., Voll, P., Peters, M., & Bardow, A. (2014). Life cycle assessment of CO 2 capture and utilization: A tutorial review. *Chem. Soc. Rev.*, *43*(23), 7982–7994. https://doi.org/10.1039/C3CS60373C

Wang, J.-Q., Sun, J., Cheng, W.-G., Shi, C.-Y., Dong, K., Zhang, X.-P., & Zhang, S.-J. (2012). Synthesis of dimethyl carbonate catalyzed by carboxylic functionalized imidazolium salt via transesterification reaction. *Catal. Sci. Technol.*, *2*(3), 600–605. https://doi.org/10.1039/C1CY00342A

Wang, M., Wu, M., & Huo, H. (2007). Life-cycle energy and greenhouse gas emission impacts of different corn ethanol plant types. *Environmental Research Letters*, *2*(2), 024001. https://doi.org/10.1088/1748-9326/2/2/024001

Watile, R. A., Deshmukh, K. M., Dhake, K. P., & Bhanage, B. M. (2012). Efficient synthesis of cyclic carbonate from carbon dioxide using polymer anchored diol functionalized ionic liquids as a highly active heterogeneous catalyst. *Catalysis Science & Technology*, *2*(5), 1051. https://doi.org/10.1039/c2cy00458e

Wells, P. (2013). *Updated Capital Cost Estimates for Utility Scale Electricity Generating Plants*. 201.

Wu, J. (2017). *China Patent No. CN106957283A*.

Yang, Z.-Z., He, L.-N., Dou, X.-Y., & Chanfreau, S. (2010). Dimethyl carbonate synthesis catalyzed by DABCO-derived basic ionic liquids via transesterification of ethylene carbonate with methanol. *Tetrahedron Letters*, *51*(21), 2931–2934. https://doi.org/10.1016/j.tetlet.2010.03.114

Yue, H., Zhao, Y., Ma, X., & Gong, J. (2012). Ethylene glycol: Properties, synthesis, and applications. *Chemical Society Reviews*, *41*(11), 4218. https://doi.org/10.1039/c2cs15359a

Appendix A: Stream Results for Conventional Approach (MeOH Production)

Table A.1 Stream summary for SMR section

Streams	**FEED**	**FEED-2**	**FLASH**	**METHANE**	**PROD**	**SYNGAS**	**SYNGAS-2**	**SYNGAS-3**
Temperature (°C)	23.5	1100.0	30.0	30.0	1100.0	30.0	180.4	167.0
Pressure (bar)	25.0	25.0	25.0	25.0	25.0	25.0	78.0	78.0
Total Molar Flowrate ($\frac{\text{kmol}}{\text{hr}}$)	623.6	623.6	1160.9	311.7	1160.9	1125.3	1125.3	1125.3
Total Mass Flowrate ($\frac{\text{kg}}{\text{hr}}$)	10620.0	10620.0	10620.0	5000.0	10620.0	9977.9	9977.9	9977.9
Mole Fraction								
H2	0.000	0.000	0.699	0.000	0.699	0.721	0.721	0.721
CH4	0.500	0.500	0.037	1.000	0.037	0.038	0.038	0.038
H2O	0.500	0.500	0.032	0.000	0.032	0.002	0.002	0.002
CO	0.000	0.000	0.226	0.000	0.226	0.234	0.234	0.234
CO2	0.000	0.000	0.005	0.000	0.005	0.005	0.005	0.005
CH4O	0.000	0.000	0.000	0.000	0.000	0.000	0.000	0.000
C2H6	0.000	0.000	0.000	0.000	0.000	0.000	0.000	0.000
C2H4	0.000	0.000	0.000	0.000	0.000	0.000	0.000	0.000

Table A.1 Stream summary for SMR section (cont'd)

Streams	**W-FEED**	**W-FEED2**	**WATER**
Temperature (°C)	20.0	21.1	30.0
Pressure (bar)	1.0	25.0	25.0
Total Molar Flowrate ($\frac{\text{kmol}}{\text{hr}}$)	312.0	312.0	35.6
Total Mass Flowrate ($\frac{\text{kg}}{\text{hr}}$)	5620.0	5620.0	642.1
Mole Fractions			
H2	0.000	0.000	0.000
CH4	0.000	0.000	0.000
H2O	1.000	1.000	1.000
CO	0.000	0.000	0.000
CO2	0.000	0.000	0.000
CH4O	0.000	0.000	0.000
C2H6	0.000	0.000	0.000
C2H4	0.000	0.000	0.000

Table A.2 Stream summary for MeOH section

Streams	**FTOP1**	**FTOP2**	**METH-1**	**METH-2**	**METH-3**	**METH-4**	**METH-5**	**RECYCLE1**
Temperature (°C)	36.0		251.0	40.0	40.0	36.0	36.0	40.0
Pressure (bar)	1.5	1.5	70.9	70.9	70.9	1.5	1.5	70.9
Total Molar Flowrate ($\frac{\text{kmol}}{\text{hr}}$)	18.0	0.0	4706.2	4706.2	288.1	270.0	270.0	4418.1
Total Mass Flowrate ($\frac{\text{kg}}{\text{hr}}$)	355.8		24919.1	24919.1	8841.3	8485.5	8485.5	16077.8
Mole Fractions								
H2	3.53E-06		0.849	0.849	2.21E-07	1.88E-14	1.88E-14	0.904
CH4	0.778		0.076	0.076	0.067	0.019	0.019	0.077
H2O	0.001		0.001	0.001	0.021	0.023	0.023	2.71E-05
CO	0.015		0.011	0.011	0.001	3.38E-05	3.38E-05	0.012
CO2	0.019		0.001	0.001	0.002	0.001	0.001	0.001
CH4O	0.187		0.061	0.061	0.909	0.957	0.957	0.006
C2H6	9.56E-05		6.62E-06	6.62E-06	1.10E-05	5.36E-06	5.36E-06	6.33E-06
C2H4	0.000		1.57E-05	1.57E-05	2.15E-05	9.33E-06	9.33E-06	1.53E-05

Table A.2 Stream summary for MeOH section (cont'd)

Streams	**RECYCLE2**	**RECYCLE3**	**SYNGAS-4**	**SYNGAS-5**	**SYNGAS-6**
Temperature (°C)	40.0	231.0	40.0	197.8	224.0
Pressure (bar)	70.9	70.9	78.0	70.9	70.9
Total Molar Flowrate ($\frac{\text{kmol}}{\text{hr}}$)	4108.9	4108.8	1124.7	1124.7	5233.5
Total Mass Flowrate ($\frac{\text{kg}}{\text{hr}}$)	14952.4	14952.2	9966.9	9966.9	24919.1
Mole Fractions					
H2	0.904	0.904	0.722	0.722	0.865
CH4	0.077	0.077	0.038	0.038	0.068
H2O	2.71E-05	2.71E-05	0.001	0.001	0.000
CO	0.012	0.012	0.234	0.234	0.060
CO2	0.001	0.001	0.005	0.005	0.002
CH4O	0.006	0.006	6.36E-08	6.36E-08	0.005
C2H6	6.33E-06	6.33E-06	4.56E-06	4.56E-06	5.95E-06
C2H4	1.53E-05	1.53E-05	9.71E-06	9.71E-06	1.41E-05

Appendix B: Stream Results for CO_2 Utilization Approach (MeOH Production)

Table B.1 Stream summary for SMR section

Streams	**CO2**	**CO2-2**	**CO2-3**	**FEED**	**FEED-2**	**FLASH**	**METHANE**	**PROD**
Temperature (°C)	116.0	120.5	166.0	23.5	1100.0	30.0	30.0	1100.0
Pressure (bar)	74.9	78.0	78.0	25.0	25.0	25.0	25.0	25.0
Total Molar Flowrate ($\frac{\text{kmol}}{\text{hr}}$)	89.7	89.7	89.7	623.6	623.6	1160.9	311.7	1160.9
Total Mass Flowrate ($\frac{\text{kg}}{\text{hr}}$)	3946.0	3946.0	3946.0	10620.0	10620.0	10620.0	5000.0	10620.0
Mole Fractions								
H2	0.000	0.000	0.000	0.000	0.000	0.699	0.000	0.699
CH4	0.000	0.000	0.000	0.500	0.500	0.037	1.000	0.037
H2O	0.000	0.000	0.000	0.500	0.500	0.032	0.000	0.032
CO	0.000	0.000	0.000	0.000	0.000	0.226	0.000	0.226
CO2	1.000	1.000	1.000	0.000	0.000	0.005	0.000	0.005
CH4O	0.000	0.000	0.000	0.000	0.000	0.000	0.000	0.000
C2H6	0.000	0.000	0.000	0.000	0.000	0.000	0.000	0.000
C2H4	0.000	0.000	0.000	0.000	0.000	0.000	0.000	0.000

Table B.1 Stream summary for SMR section (cont'd)

Streams	**SYNGAS**	**SYNGAS-2**	**SYNGAS-3**	**SYNGAS-4**	**W-FEED**	**W-FEED2**	**WATER**
Temperature (°C)	30.0	180.4	167.0	164.4	20.0	21.1	30.0
Pressure (bar)	25.0	78.0	78.0	78.0	1.0	25.0	25.0
Total Molar Flowrate ($\frac{\text{kmol}}{\text{hr}}$)	1125.3	1125.3	1125.3	1214.9	312.0	312.0	35.6
Total Mass Flowrate ($\frac{\text{kg}}{\text{hr}}$)	9977.9	9977.9	9977.9	13923.9	5620.0	5620.0	642.1
Mole Fractions							
H2	0.721	0.721	0.721	0.668	0.000	0.000	0.000
CH4	0.038	0.038	0.038	0.035	0.000	0.000	0.000
H2O	0.002	0.002	0.002	0.002	1.000	1.000	1.000
CO	0.234	0.234	0.234	0.216	0.000	0.000	0.000
CO2	0.005	0.005	0.005	0.079	0.000	0.000	0.000
CH4O	6.89E-08	6.89E-08	6.89E-08	6.38E-08	0.000	0.000	0.000
C2H6	4.56E-06	4.56E-06	4.56E-06	4.23E-06	0.000	0.000	0.000
C2H4	9.71E-06	9.71E-06	9.71E-06	8.99E-06	0.000	0.000	0.000

Table B.2 Stream summary for MeOH section

Streams	**FTOP1**	**FTOP2**	**METH-1**	**METH-2**	**METH-3**	**METH-4**	**METH-5**	**RECYCLE1**
Temperature (°C)	32.3		251.7	40.0	40.0	32.3	32.3	40.0
Pressure (bar)	1.5	1.5	70.9	70.9	70.9	1.5	1.5	70.9
Total Molar Flowrate ($\frac{\text{kmol}}{\text{hr}}$)	61.0	0.0	3070.1	3070.1	418.8	357.9	357.9	2651.3
Total Mass Flowrate ($\frac{\text{kg}}{\text{hr}}$)	1865.2		31265.7	31265.7	12604.9	10739.7	10739.7	18660.8
Mole Fractions								
H2	1.37E-06		0.699	0.699	1.99E-07	6.47E-15	6.47E-15	0.810
CH4	0.404		0.078	0.078	0.068	0.010	0.010	0.079
H2O	0.005		0.017	0.017	0.126	0.147	0.147	0.000
CO	0.023		0.038	0.038	0.003	5.74E-05	5.74E-05	0.044
CO2	0.433		0.065	0.064	0.077	0.016	0.016	0.063
CH4O	0.135		0.103	0.103	0.726	0.826	0.826	0.005
C2H6	4.97E-05		6.35E-06	6.35E-06	9.67E-06	2.84E-06	2.84E-06	5.82E-06
C2H4	0.000		1.52E-05	1.52E-05	1.96E-05	4.99E-06	4.99E-06	1.45E-05

Table B.2 Stream summary for MeOH section (cont'd)

Streams	**RECYCLE2**	**RECYCLE3**	**SYNGAS-4**	**SYNGAS-5**	**SYNGAS-6**	**SYNGAS-7**
Temperature (°C)	40.0	231.0	164.4	40.0	197.8	220.2
Pressure (bar)	70.9	70.9	78.0	78.0	70.9	70.9
Total Molar Flowrate ($\frac{\text{kmol}}{\text{hr}}$)	2465.7	2465.6	1214.9	1214.3	1214.3	3679.9
Total Mass Flowrate ($\frac{\text{kg}}{\text{hr}}$)	17354.5	17354.5	13923.9	13911.2	13911.2	31265.7
Mole Fractions						
H2	0.810	0.810	0.668	0.668	0.668	0.763
CH4	0.079	0.079	0.035	0.035	0.035	0.065
H2O	0.000	0.000	0.002	0.001	0.001	0.000
CO	0.044	0.044	0.216	0.216	0.216	0.101
CO2	0.063	0.063	0.079	0.079	0.079	0.068
CH4O	0.005	0.005	6.38E-08	5.94E-08	5.94E-08	0.003
C2H6	5.82E-06	5.82E-06	4.23E-06	4.22E-06	4.22E-06	5.30E-06
C2H4	1.45E-05	1.45E-05	8.99E-06	8.99E-06	8.99E-06	1.27E-05